Drug Loading onto Polymeric Contrast Agents for Ultrasound Drug Delivery

A Thesis

Submitted to the Faculty

of

Drexel University

by

Odelia Mualem-Burstein

in partial fulfillment of the

requirements of the degree

of

Doctor of Philosophy

May 2008

Acknowledgments

I would like to thank:

Dr. Margaret Wheatley for her endless support in my work, her advice, enlightening guidance and patience, without which this PhD would not have been possible.

My committee members, Drs. Fred Allen, Kenneth Barbee, Chang Chang and Flemming Forsberg for their guidance and advice.

The Thomas Jefferson University team, especially Dr. Flemming Forsberg, for their help with all in vivo studies of this research.

My graduate student colleagues, especially Seunglee Kwon, John Eisenbrey and Kelleny Oum for their support, help and pleasant company.

My husband Dr. Pablo Burstein for his constant support, patience, insightful advice, encouragement and love.

My parents, Yosef Mualem and Yehudit Mualem for planting the seeds of ambition and aspiration and for their endless support and encouragement to go achieve my goals and to my sisters, Yael Mualem and Meirav Mualem for being there for me all along.

Table of Contents

List of Tables

List of Figures

Abstract
Drug Loaded Polymeric Contrast Agents for Ultrasound Drug Delivery
Odelia Mualem-Burstein
Margaret A. Wheatley, Ph.D.

Conventional, systemic chemotherapy has proved to be generally inefficient in the treatment of solid tumors, bearing harmful, toxic side effects. Targeted drug delivery systems can mitigate this. We develop methods to load drugs onto polymeric microbubbles, serving both as ultrasound contrast agents (CA) and drug carriers. These drug-loaded CA have the ability to release their payload in the vicinity of the tumor site. Our CA are fabricated using an adaptation of double emulsion method developed in our lab. Bovine serum albumin (BSA), sudan black (SB), 5-fluorouracil (5-FU) and doxorubicin (DOX) are individually loaded onto our CA, using three different loading methods, namely, incorporation, dry, and wet adsorption. The effects of different preparation parameters on drug yield and echogenicity, for each drug/loading method combination, are studied. Temperature, pH, drug concentration and incubation time, are found to affect BSA loading through dry adsorption. The highest loading efficiency (50.5%) was found for incubating BSA at pH 4.2 at 4°C but compromised its echogenicity, 19.0 dB. In contrast, by incorporation, only 21.9% BSA is loaded still maintaining an echogenicity of 20.9 dB. SB, as a hydrophobic material, is most suitably shell incorporated, yielding 100% loading efficiency while maintaining 21.9 dB echogenicity. Wet adsorption is found to be most suitable for loading 5-FU and DOX; 5-FU loading efficiency is 27.6% while echogenicity is 15.7 dB, and DOX loading efficiency is 79.1% while echogenicity is 15.8 dB. There is a clear trade-off between drug loading efficiency and CA echogenicity; we strive to load as much drug as possible while maintaining acoustic properties.

In vivo feasibility studies show the stability and echogenicity of our drug-loaded CA in cancerous and healthy animal models. In addition, SB-loaded CA are shown to be suitable candidates for lymph channels and sentinel lymph nodes visualization, both through staining

and US. Summarizing, complex relationships are found to exist among drugs, loading methods and CA shell polymers, i.e., specific loading methods should be used for specific drugs and CA. This work demonstrates that our CA are able to carry anticancer drugs, already in clinical use with proven therapeutic effects, while maintaining echogenicity and stability.

1. Introduction

This work was carried out to explore possibilities of loading drugs onto polymeric microbubbles. Those microbubbles serve as contrast agents (CA) and their capacity to carry drugs opens a door to the next generation of CA applications in the therapeutic field. This work is an integral part of a larger project that includes targeting of drug loaded CA to solid cancer tumors, and nano-sized CA development. Combined together, these three aspects can provide a dynamic platform for a variety of drug delivery systems. The role of ultrasound in this project is to provide imaging of the target site, i.e., tumor, and to trigger drug release in a local fashion. This could be a good solution for efficient and effective drug administration when using toxic drugs such as in cancer chemotherapy.

1.1 *Long Term Goals*

The main long term goal is to develop a targeted drug delivery system, based on previously developed polymeric CA that is ultrasound activated. Ultrasound will be used for both imaging and drug release activation. Achievement of these goals can be sub-divided into 4 main research fields:

1. CA acoustic properties: the basic requirements from a good CA are:
    a. narrow size distribution and average size of not more than 8μm to safely pass through the capillary bed,
    b. biocompatibility and biodegradability to safely clear from the body,
    c. stability through injection and for the imaging time period.
2. Drug loading capabilities:
    a. CA should be able to carry a sufficient amount of hydrophilic/hydrophobic drug to its activation site, in a timely fashion.
    b. CA should demonstrate good acoustic properties while loaded.
    c. Drug release should be sensitive to ultrasound energy.

d. The delivered drug should be active at the target site.

3. Targeting: CA should be efficiently accumulating in the target site in a highly selective manner. Targeting process includes: CA surface modification, attachment of high-specificity targeting agent, CA accumulation through cell attachment within a few minutes in the target site, maintaining CA acoustic properties and carried drug capacity.
4. Nano sizing: development of a nano-sized CA, with the above characteristics to enable delivery of drugs through gaps in the leaky neo-vasculature of tumors.

1.2 *Thesis Aims and Objectives*

The objectives of this work are to study drug loading onto polymeric CA, in respect to drug characteristics and CA properties. For this purpose, this work explores 2 model drugs, 2 anti-cancer drugs, and 3 loading methods. The specific aims are:

- Specific aim 1: To develop, optimize and characterize methods of drug loading onto biodegradable polymer contrast agents that have been developed in our laboratory using, poly lactic-co-glycolic acid (PLGA) and poly-lactic acid (PLA). The drug-loading method should be validated and optimized to achieve the required drug loading. The methods of interest are: surface adsorption under different conditions (temperature, incubation time, pH, drug concentration) and or incorporation during CA manufacturing. Surface adsorption may be carried out in a dry mode, post fabrication, or in a wet mode, as part of fabrication.
- Specific aim 2: To characterize the effect of drug loading on acoustic properties. In particular, the effects of loading method and drug chemical properties, i.e., polarity compound class (small organic molecule or globular protein), on loaded CA echogenicity and ultrasound signal stability, by constructing dose and time response curves.
- Specific aim 3: To investigate acoustically-triggered drug release capabilities of drug loaded CA. To carry out preliminary experiments to understand the effects of the

ultrasound frequency, and pressure on drug release profile. To carry out preliminary experiments to study the effects of loading method and shell composition on ultrasound triggered drug release. To prove feasibility of using loaded CA in vivo.

2. Background and Literature Review

This chapter presents background and a literature survey on the following topics: ultrasound as an imagining modality and its involvement in therapeutic applications of drug delivery, CA drug loading techniques for adsorption and incorporation of drugs onto polymeric microbubbles, cancer as a target to drug delivery applications, PLA and PLGA microbubbles as a dynamic platform of drug carriers, and model drugs used in this work as well as anti-cancer drugs.

2.1 *Imaging Modalities*

Medical imaging techniques are widely used in diagnosis of numerous pathological conditions and early detection of many cancers. Currently there are six main imagining modalities in use for anatomical and functional imaging (Rembielak, Cullen, Saleem, & Price, 2008; Tilcock, 1999): (1) X-ray, a technique that uses high energy ionizing radiation (including mammography), (2) Computed tomography (CT), based on x-ray and uses a computer to acquire cross-sectional images of the target, (3) Magnetic resonance imaging (MRI) is based on a powerful magnetic field that aligns the magnetization of hydrogen atoms in the body and radio waves are used to systematically alter this alignment causing hydrogen atoms to produce a rotating magnetic field detectable by the scanner, those signals are further manipulated to reconstruct an image, (4) Radionuclide imaging, a technique that involves a gamma camera that detects gamma rays emitted from radio-labeled media that are administered prior to imaging (and is often organ specific), (5) Near infrared optical imaging (NIR) uses visible/near infra-red non ionizing light for diagnostic imaging, and (6) Ultrasound that uses reflected beams of high/low (20-90kHz/ 1-15MHz) frequency sound waves to generate images.

Among these modalities ultrasound demonstrates several advantages: it is the safe, not based on radio-isotope injections and not using harmful high energy radiation, it is portable and available in all medical centers, for a relatively low operational cost. This makes ultrasound a good choice of imaging modality for cancer therapeutic applications.

2.2 *Ultrasound*

Ultrasound is an imaging modality generating images from backscattered sound waves after they encounter an acoustic impedance mismatch boundary. Acoustic impedance, Z, is defined as the product of density, ρ, and the speed of sound, c, in a medium (Kinsler, Frey, Coppens, & Sanders, 2002):

$$\mathbf{Z = \rho \times c} \qquad \text{eq. 2-1}$$

Such boundaries, of acoustic mismatch, can be found between a soft tissue and a bone, a tissue and a liquid filled body, and between a tissue and a gas-containing body. However, in the boundary between two soft tissues, i.e. tissue and a tumor, or between tissue and blood vessels the impedance is similar, making it difficult for discrimination.

Ultrasound has been extensively used as a diagnostic imaging tool for decades in many areas of medical practice. Its availability, low cost, portability and real time capabilities contributed to the ease of use, and motivate further rapid development, in the area of 2D 3D and contrast media (Dalecki, 2004). Ultrasound has been is use for cancer diagnosis as well, especially in lesion detection, characterizing lesion (e.g. cystic or solid), and for estimating the extent and stage of the tumor. Ultrasound is also used to provide real-time imaging for obtaining biopsies, and serves as a tool for assessing response and complications during and after treatments. The use of contrast agents in ultrasound imaging substantially enhances the ability to discriminate between tumor tissue and healthy tissues (Marret et al., 2004). The use of Doppler technique is especially useful in blood flow imaging (Rembielak et al., 2008). Doppler based methods are used to asses both flow direction and velocity, especially for diagnosis of malignancies in the cardio-vascular system (Lindner, 2004).

2.3 *Ultrasound Contrast Agents*

Bubbles were first reported to enhance ultrasound contrast in 1968 when Gramiak and Shah demonstrated the echo-contrast effect by injecting agitated saline containing gas bubbles into the aorta (Garmiak & Shah, 1968). This observation was later reasoned to be due to the presence of bubbles in the insonated field (Kremkau, Shah, & Kramer, 1969). Since this discovery of contrast ultrasound enhancement effect many efforts were made towards development of fabrication techniques for production of stable microbubbles. A variety of agents were developed where air, perfluorocarbon, nitrogen and sulfur hexafluoride were stabilized in a shell made of protein (Albunex® and Optison® (Mallincrodt Medical Inc., St. Luis, MO, USA)), lipid (SonoVue®) (Bracco Inc.), sugar (Echovist® (Schering AG, Berlin, Germany)), surfactant (ST68, (Forsberg et al., 1997)) or polymer (El-Sherif & Wheatley, 2003) (Goldberg, Raichlen, & Forsberg, 2001; Raisinghani & DeMaria, 2002; Wheatley, 2001). The FDA (Food and Drug Administration) approved Optison®, Definity™ (Bristol-Myers, NY, USA), and Imagent® (IMCOR Pharmaceuticals Co., San Diego, CA, USA) for intravenous use in the United States for clinical applications in echocardiography.

CA are injected intravenously prior to imaging and based on their cross sectional area they scatter ultrasound waves to enhance vascular definition and provide more imaging information. CA have to be smaller than 8μm in size to traverse the capillary bed, stable enough in the blood stream to provide enhancement through insonation and biocompatible (Stride & Saffari, 2003).

Backscattering can be described mathematically where the received intensity, I_s, is a function of the incident intensity, I_i, and the bubble cross section, σ, as described by the following equation (Forsberg, 2001):

$$I_s = \frac{I_i \sigma}{4\pi R^2} \qquad \text{eq. 2-2}$$

Where *R* represents the distance between the transducer and the scatterer (i.e.,bubble). This relationship relies on Rayleigh's theory where, the scatterer is minute in comparison to the wavelength λ. The scattering cross section can be described by the scatterer material properties, i.e., compressibility and density, and the surrounding media properties as in the following equation (Forsberg, 2001):

$$\sigma = \frac{4\pi}{9} k^4 r^6 \left[\left(\frac{\kappa_s - \kappa}{\kappa} \right)^2 + \frac{1}{3} \left(\frac{3(\rho_s - \rho)}{2\rho_s + \rho} \right)^2 \right] \quad \text{eq. 2-3}$$

Where κ is the adiabatic compressibility of the medium, ρ denotes density, *k* is the wave number that equals 2π/λ and s scatterer properties are indexed in s. Based on this equation the most significant enhancement of back scattered signals occurs when the scatterer is a gas bubble and the medium is liquid. It has been shown that microbubbles resonate, harmonically oscillate (expand and compress), as a response to an external sound field. Resonance response depends on fluid pressure, P_0, and density ρ_0, shell elasticity, S_e, bubble diameter, *d*, the resonance frequency of a thin elastic bubble shell can be described by the following equation (de Jong, Hoff, Skotland, & Bom, 1992):

$$f_0 \approx \frac{1}{2\pi r} \sqrt{\frac{3\gamma}{\rho_0} \left(P_0 + \frac{\pi}{3} \frac{S_e}{\gamma r r} \right)} \quad \text{eq. 2-4}$$

And shell elasticity, S_e, is defined as:

$$S_e = 8\pi \frac{E(r_0 - r_i)}{1 - \upsilon} \quad \text{eq. 2-5}$$

Where the adiabatic gas constant is represented by γ, elasticity (Young's module) E and Poisson ratio is υ. Under the assumptions of negligible medium damping, no bubble surface tension effect nor thermal conductivity.

The first generation of CA was designed to enhance B-mode and Doppler modes, used in diagnostic imaging, based on the linear resonance response of CA to the external sound field. Later on, CA were used for more advanced methods, such as second harmonic imaging and pulse or phase inversion, based on the non-linear resonance response of CA to ultrasound (Forsberg & Goldberg, 2000; Jakobsen, 2001), flash echo for minimizing bubble destruction (Kamiyama, Moriyasu, Mine, & Goto, 1999) and micro flow streaming (Kamiyama, 2004). Ultrasound enhancement may come from either reflection of the signal or asymmetrical vibration or disruption of the microbubbles (bubbles destruction). Hence, depending on the CA mechanical properties and the choice of destructive or non destructive strategy, a decision of imaging mode and mechanical index to be used must be made. Mechanical index is an expression reflecting the out power of ultrasound beam and is related to mechanical deformation (compression and expansion) of CA under ultrasound. MI is defined mathematically as ratio of power, W, and the square root of frequency, f_0:

$$MI = \frac{W}{\sqrt{f_i}} \qquad \text{eq. 2-6}$$

At low MI (MI<0.1) little microbubbles destruction is provoked by ultrasound. At intermediate MI (0.1<MI<0.5) the microbubble oscillations amplitude increases and for proper frequency and ultrasound intensities microbubbles produce harmonic response. At high MI (MI>0.5) bubbles are disrupted after a series of strong and rapid oscillations (Correas et al., 2001).

After demonstrating the enhancement abilities of CA and following the discovery that CA can be selectively targeted to leukocytes, a whole new concept of CA emerged. Site-targeted

CA were developed for ultrasound diagnostics. This trend was soon followed by the development of CA assisted drug delivery.

There are several ways where CA and ultrasound can be involved in medical applications and assist in drug delivery. We discuss several of them in the next sections. Despite the rapid development of CA, and the therapeutic promise they hold, the FDA approved very few of them for diagnostic use, and currently no CA is approved for drug delivery of chemotherapeutic agents as treatment for solid cancer tumors.

2.4 *Therapeutic Ultrasound*

Ultrasound is best known for its diagnostic applications, however, a variety of medical therapies are being developed based on its ability to focus within tissues and induce therapeutic bioeffects non-invasively (Dalecki, 2004). Such procedures include, lithotripsy, the fragmentation of kidney stones using high-amplitude focused acoustic shock waves (Delius, Ueberle, & Gambihler, 1994; Eassa et al., 2008; Ikeda et al., 2006) and thrombolysis. Thrombolysis can be carried out in one of two modes. The first is based on ultrasound alone, where a catheterized transducer causes mechanical fragmentation through direct mechanical contact. The other mode is using ultrasound to accelerate enzymatic thrombolysis without mechanical disruption of the thrombus (Daffertshofer & Fatar, 2002; Jonathan R. Lindner, 2004; Pieters, Hekkenberg, Barrett-Bergshoeff, & Rijken, 2004; Z. Wang, Moehring, Voie, & Furuhata, 2008). Effective thrombolysis can also be achieved with the assistance microbubbles, resonating and mechanically break the clot, with or without thrombolitic agents (Culp, Erdem, Roberson, & Husain, 2003; E. C. Unger et al., 2004). Applications of therapeutic ultrasound with assistance of microbubbles are discussed separately below. The use of an injectable thrombolitic agent and assisted delivery with ultrasound for dissolving brain blood clots was under clinical trials (phase II) was reported by Alexandrov (Alexandrov, 2006). He showed that ultrasound enhances the thrombolitic activity of a drug in humans, and there was a 25% increase

in recovery 2 hours after treatment in tested group compared to 8% in control group. Moreover the ultrasound treated group showed a trend of 13% more patients achieving favorable outcome after 3 months from the treatment. At the proximity of the occlusion the blood flow is stagnant and the pressure waves that ultrasound generates propagate through tissues, induce fluid motion and help the drug to reach the binding sites.

Ultrasound is also widely investigated for its use for a variety of drug delivery applications, among them gene therapy, drug therapy (including chemotherapy) and protein delivery. Those applications are reviewed in the following sections.

2.4.1 *Transdermal and Intracellular Drug Delivery*

The phenomenon of enhancing transdermal drug transport by application of different combinations of ultrasound parameters, such as, frequency, intensity and time is defined as sonophoresis (Wang, Siahaan, & Soltero, 2005). The propagation of an ultrasonic wave through the skin results in cavitation and heating. The overall effect is an increase in skin permeability due to increased fluidity of intercellular lipids by heating or mechanical stress and/or by enlarging intercellular space, or by creating permanent or transient holes. This increase in skin permeability to drugs may not persist after the end of sonication (Liu, Lewis, & Prausnitz, 1998; Machet & Boucaud, 2002). Most of the recent work is focused on promotion of proteins' transport using low-frequency ultrasound (20 kHz) (Tang, Wang, Blankschtein, & Langer, 2002). Mitragotri et al. found a correlation between ultrasound intensity and transported protein dose when using low frequency and low intensity (mW/cm^2 range) for proteins in the range of 6,000-48,000Da size (Mitragotri, Blankschtein, & Langer, 1995).

It has also been demonstrated that ultrasound can facilitate uptake of drugs in the cellular level, using cell cultures. Keyhani et al. showed that cancer cell cultures that were sonicated internalized molecules at a level approaching thermodynamic equilibrium, they found that there

was an optimal pressure (peak positive pressure 2.7 atm) and optimal exposure time (0.2-0.5 s) that maximized cell uptake and that pulse length did not have a significant effect on cell uptake (Keyhani et al., 2001). Zderic et al showed that ultrasound can increase transcorneal drug uptake by tenfold when applyng low frequency (20 kHz) ultrasound (Zderic et al., 2004). They also found a linear correlation between the permeability increase and the ultrasound energy (range 0.19-0.56 W/cm^2). Sonoporation was also used to deliver BH3 peptide (having a pro-apoptotic activity) into cancer cell cultures, resulting in a 35% increase in cell death. Moreover, the use of ultrasound did not compromise protein activity inside the cells (Kinoshita & Hynynen, 2005).

2.4.2 *Gene Delivery*

There are over 4000 human inherited diseases that are associated with dysfunctional, nonfunctional and missing gene-coded proteins. A replacement of a defective gene with a normal one, namely "Gene therapy", is a concept that had been developed to address these genetic disorders (Bekeredjian, Grayburn, & Shohet, 2005; Wang et al., 2005). The delivery of nucleic acid into cells can be made either via virus vector or by physical and chemical methods or via plasmid DNA (Wei et al., 2004). There are several ways by which ultrasound can enhance gene transfection and delivery to cells. One way is by sonoporation, created by ultrasound shock waves. This method might result in extensive cell lysis due to the high ultrasound intensity. For this reason low-intensity (1MHz, 0.4-0.5 W/cm^2) ultrasound was a good alternative and produce better results of cell survival and successful gene transfection (Lawrie et al., 1999; E. C. Unger, McCreery, & Sweitzer, 1997). The main mechanism by which ultrasound enhances gene transfection is cavitation, creating nonlethal membrane perforations. The presence of CA lowers the energy level needed for cavitation, hence DNA loaded microbubbles are coupled with this method (Deng, Sieling, Pan, & Cui, 2004; Ferrara, Pollard, & Borden, 2007).

2.4.3 *Ultrasound Assisted Drug Delivery*

There are several ways to assist drug delivery using ultrasound and CA. One approach is to co-inject free drug with microbubbles to the blood stream and apply ultrasound at the target site. Under the influence of ultrasound microbubbles will oscillate and cavitate. Ultrasonic cavitation in liquid-solid systems produces high energy effects such as intense local heating and high pressure which have short lifetime. Thos effects on liquids generate large shear and strain gradients that may improve mass transport, generate surface damage at solid liquid interface and fragmentation of solids. These phenomenon can be used towards drug delivery enhancement (Suslick & Price, 1999). Being pushed towards the vessel wall by radiation force, microbubbles alter the blood vessel wall to allow passage of the drug by extravasation (Larina et al., 2005b; Price & Kaul, 2002; Price, Skyba, Kaul, & Skalak, 1998). Dayton et al. investigated the displacement of microbubbles in the blood stream using radiation force (Dayton et al., 1999). They showed that radiation force can displace CA from the center of the streamline to the wall of 50μm blood vessel in mouse cremaster muscle. Moreover, radiation force was found to reduce the velocity of flowing CA and produce CA aggregation by the wall. This is especially relevant for releasing drug payload at a close vicinity to the target cells. This was later re-confirmed by a detailed study in vitro showing the direct effect of radiation force on targeted CA accumulation in the target area (Rychack et al., 2005). Model drugs were also used to demonstrate the potential of using CA to lower cavitation threshold and facilitate free drug delivery, locally at the cavitation site (Larina et al., 2005a). In this study the effects of duty cycle, insonation duration, frequency, intensity and CA volume on adsorption of different molecular weight (MW) drugs by target cells and cell death were tested. Results show that drug penetration into cancer cells depends on the drug molecular weight. Using 1MHz frequency resulted in twice the quantity of cells death than at 3MHz.

A second approach is to incorporate the drug in the CA and rupture them in the target vasculature. The CA payload will be released locally. There is evidence that using radiation

force to push microbubbles in close proximity to the vessel wall and rupturing them there, increases drug delivery in comparison to ultrasound alone. Having the drug incorporated into or adsorbed onto the CA may offer protection to the drug from inactivation or removal from the blood stream. Focal destruction of CA offers local delivery and hence a means to decrease the systemic exposure to the drug toxicity (Lindner, 2002). Liposomes and micelles carrying drugs were reported to deliver their payload in the target vicinity using ultrasound as a burst driving force (Huang & MacDonald, 2004; Rapoport, Pitt, Sun, & Nelson, 2003).

The third method is more specific and applies to incorporation of ligands on the microbubbles surface, designated to adhere to markers presented on the target cells. Microbubbles were shown to adhere to target cells and application of ultrasound in the target area results in a selective delivery of the drug to the target (Lanza & Wickline, 2003; Takalkar, Klibanov, Rychak, Lindner, & Ley, 2004; Tsutsui, Xie, & Porter, 2004).

2.5 *Cancer and Chemotherapy*

More than 560,000 deaths occur annually in the USA due to cancer malignancies, and about 1.44 million new cases are diagnosed, making cancer a major public health problem (Jemal et al., 2007). Although remarkable progress has been achieved in development of new anti cancer agents in the past two decades, success in solid tumor therapy had been limited. Solid tumors are developed in 85% cases of cancer and unfortunately their treatment efficacy is challenged by several factors: the blood flow inside the tumor is tortuous, the interstitial pressure is high, and the drug needs to pass through the cancer cell membrane (Ruoslahti, 2002). Diffusion is not fast enough to deliver anti cancer drugs to cancer cells before they reach their half-lives (Baxter & Jain, 1991). To improve efficacy and limit toxicity of chemotherapy it is necessary to provide carrying mechanism and enhance the delivery of anticancer drugs locally.

When solid tumors evolve they create and expand their own new vasculature, in a process called angiogenesis (sprouting of new vessels from existing vessel). The tumor vessels

have unique characteristics, they are tortuous and leaky, thin-walled and their diameter is irregular. The abnormal form of neo-vascularization results in poor alignment of endothelial cells with wide fenestrations. The combination of this with the absence of smooth muscle layer and poor lymphatic drainage leads to abnormal molecular and fluid transport dynamics inside the tumor. Resulting in drugs leakage or permeability to tumor tissues. This effect is called "Enhanced permeability and retention" (EPR) and it can be utilized to deliver large molecular size anticancer agents into the tumors (Maeda, Greish, & Fang, 2006). In addition tumor vasculature expresses unique angiogenic endothelial markers and molecules (Ruoslahti, 2002). Those unique markers can be used towards design of therapeutic agents, antibodies, peptides, proteins and targeting ligands. Targeting ligands can be attached to the surface of CA microbubbles and facilitate CA accumulation in tumor for therapeutic purposes, this application is discussed below.

2.5.1 *Anticancer Ultrasound Therapy*

Ultrasound can help fight cancer on two different fronts, diagnostics and therapeutics. In the diagnostic field ultrasound has been found to play a major role in visualization and quantification of tumor microcirculation (Ferrara & Merritt, 2000; Forsberg, Ro et al., 2004; Foster, Burns, Simpson, Wilson, & Christopher, 2000). Ultrasound was also found to enhance chemotoxicity by one or a combination of three non-thermal effects of ultrasound: cavitation (collapsing microbubbles), radiation pressure (pressure peaks in the medium that originate form radiation force and can displace bodies) and acoustic microstreaming (steady circulatory flow that is the result of radiation force acting on a medium near a boundary). Chemotoxicity enhancement of small molecular weight drugs using low (20 kHz) or high (~1.5 MHz) frequency ultrasound was reported (Harrison, Balcer-Kubiczek, & Gutierrez, 1996; Keyhani et al., 2001; Liu et al., 1998).

Rupture of drug loaded liposomes and micelles by ultrasound was reported by several groups (Rapoport, Pitt, Sun, & Nelson, 2003; E. Unger, McCreery, Sweitzer, Caldwell, & Wu, 1998) showing a substantial reduction on free drug toxicity and increase in therapeutic effects.

Polymeric CA that were previously developed in out lab were shown to adhere to cancer cells after being conjugated with GRGDS peptide, which recognizes integrins that are expressed by cancer cells (Lathia, Leodore, & Wheatley, 2004). This demonstrates the potential of developing a new drug loaded polymeric CA that is targeted to solid tumor cellular markers.

2.6 *Drug Delivery and Microcapsules*

Conventional drug administration has many disadvantages such as systemic toxicity, and short half life, lowering treatment efficacy. Drug delivery systems, featuring local drug delivery and controlled release mechanisms, ensure reduced total drug doses and elevated treatment efficacy. Polymeric microspheres were extensively investigated and developed for their role in drug delivery systems in the past 3 decades. Administration of medications and therapeutic agents via such systems is highly advantageous; they offer a dynamic platform for drug loading, they allow attachment of targeting molecules to ensure their accumulation in their destiny, their composition can be tailored to address desired release profiles (Freiberg & Zhu, 2004; Oh, Nam, Lee, & Park, 1999).

There are various traditional methods to produces polymeric microspheres, among them, single and double emulsions, spray drying and coacervation (Jain, 2000; Kawaguchi, 2000). Biodegradable polymers were extensively used for development of drug delivery systems. Polyester-based polymers are the most widely studied group among biodegradable polymers, where PLA and PLGA have been most commonly investigated (De Rosa et al., 2002; Ruan & Feng, 2003; Tamber, Johansen, Merkle, & Gander, 2005; Yang, Chung, & Ping Ng, 2001). Both polymers degrade by a simple hydrolysis of ester bonds producing glycolic and lactic acid, natural metabolites that further go through Krebs cycle and further degrade to CO_2 and water

(Omathanu & Panchagnula, 2001; Tamber et al., 2005). PLGA has an added value since it was approved by the FDA for use in medical sutures.

This work is focused on PLA and PLGA microbubbles made by a double emulsion method (El-Sherif & Wheatley, 2003). The detailed steps on CA preparation process are presented in methods section and appendix A. Our polymeric microbubbles are suitable candidates for drug delivery in addition to their acoustic properties as CA, hence, we found them suitable as a basis for this work.

2.6.1 *Polymers as Shell Materials*

Contrast agents may be fabricated from different shell materials like phospholipids, proteins, surfactants and polymers. The chemical composition of the shell plays a major role in determining the physical properties of CA and their acoustic behavior. For example, microbubble shell elasticity can affect their resonance and harmonic response to ultrasound, some shells are not stable enough in the circulation and may not last at the target for imaging, other shells might be picked up by the reticuloendothelial system (Forsberg, 2001). Shell composition also plays a part in the capabilities of CA to bear targeting molecules and carry drugs, and affects drug release kinetics.

Fabrication of CA from either PLA or PLGA has many advantages, i.e., biocompatibility, biodegradability, stability in the circulation, rigid shell that still allows for resonance and harmonic imaging (El-Sherif, Lathia, Le, & Wheatley, 2003; El-Sherif & Wheatley, 2003; Forsberg, Lathia et al., 2004).

Forsberg et al. studied the effect of different lactic and glycolic acid ratios 50:50, 75:25, 85:15 and 100:0 in CA made of block copolymer PLGA, on their acoustic properties (Forsberg, Lathia et al., 2004). They demonstrated that contrast effect duration increased by an order of magnitude as the shell became more hydrophobic, as lactic acid component in the shell polymer increased. Another effect that could have contributed to this result is based on the fact that

PLGA glass transition temperature (Tg=36°C) is closer to body temperature than PLA's Tg (65°C) (Lewis, 1990).

Based on the information above we found that PLA and PLGA are suitable shell materials for ultrasound CA, with the added potential of carrying drugs and targeting molecules.

2.6.2 *Drug Loading Methods onto Microspheres*

There are several ways to load polymeric microbubbles that were fabricated by a double emulsion process with drugs. Incorporation within the microbubble shell is a straight forward loading method when fabricating microbubbles by a double emulsion process. In this process there are two emulsification steps and the drug, depending on its hydrophobicity can be included in either organic phase (hydrophobic drug) or aqueous phase (hydrophilic drug) (Freiberg & Zhu, 2004; Yang et al., 2001). When drug loading is an integral part of microbubble fabrication, changing process parameters to achieve more loading is very limited, since it can change microbubbles properties. The amount of drug that can be loaded is also limited by drug solubility in the phase it is dissolved in. Drug amount in the microbubble shell can also affect its physical properties, hence, it is limited. Those aspects of drug loading are studied in detail in this work.

Drug may also be adsorbed onto the surface of microbubbles based electrostatic interactions, hydrogen bonding and hydrophobic interactions (Li, Hu, & Liu, 2005). In this case the loading is done post microbubble fabrication and the microbubbles are incubated with the drug solution. The drug solution properties, i.e. pH, ionic strength, play a major role in drug loading. The incubation time of drug and microbubbles and drug concentration also affect loading process and outcome. Those aspects are to be explored in this work. When adsorbing a protein there is an additional factor in play, that is protein conformation that affects its adsorption onto microbubble surface. There is an obvious limitation to loading by surface adsorption, which is

the surface area of the microbubbles available for drug adsorption. In comparison, more drug can be loaded by incorporation.

Drug may also be conjugated or covalently attached to the surface of microbubbles, and in this case it will released due to the polymer backbone hydrolysis, a process that may take weeks (Oh et al., 1999). This method, however, is not applicable for our purposes, since we hope to achieve rapid release that is ultrasonically activated.

2.6.3 *Model Drugs for Current Research*

Two model drugs were chosen to study loading onto polymeric CA in this work, fluorescently labeled bovine serum albumin (FITC-BSA), which is a high molecular weight protein and Sudan Black B (SB) a hydrophobic small molecular weight dye.

2.6.3.1 *Bovine Serum Albumin*

Bovine serum albumin is a popular drug model for drug delivery systems (Hamidi M, Zarei N, Zarrin A, & S, 2007; Kelner & Schacht, 2005; Pareta & Edirisinghe, 2006; Wischke & Borchert, 2006) due to its availability in highly purified form at law cost, easily soluble in water and its lack of effect in many biochemical reactions. Its fluorescently labeled form, FITC-BSA, fluorescein isothiocyanate, is relatively easy to detect and for this reason was chosen for this work.

2.6.3.2 *Sudan Black B*

Administration of lipophilic drugs is challenged by their poor aqueous solubility and limited cell adsorption (O'Driscoll & Griffin, 2008). However many drugs are lipophilic, among them anti-cancer such as taxol family. Hence, there is a need to provide transport means for delivery of hydrophobic drugs to their targets. Over the years many transport system were developed for the transport of hydrophobic drugs, the most popular of them were conjugation with lipids

carriers and encapsulation in liposomes and microspheres. Using ultrasound CA can not only deliver the hydrophobic drugs but also provide extra aid in their cell uptake due to the sonoporation effect it has on cells.

Sudan Black B (SB) is a lipophilic neutral ink, which is mainly used for staining of fats which can also serves as a model drug for lipophilic drugs (Katayama et al., 1995; E. Unger et al., 1998). It expresses an intense dark blue color, which can be easily picked up and quantified by simple absorbance reading. When fabricating microbubbles by double emulsion procedure, SB is most suitable to be encapsulated by incorporation, where it is added to the organic phase, due to its hydrophobic nature. For those reasons, we chose SB to model the incorporation of hydrophobic drug onto PLA microbubbles.

2.6.4 *Anti Cancer Drugs*

2.6.4.1 *Doxorubicin*

Doxorubicin (DOX), is an anti cancer drug having a strong activity against various solid tumors especially breast cancer, and also against leukemia. After entering the cell, DOX binds and intercalates with DNA strands and consequently inhibits cellular functions such as DNA and RNA synthesis (Lin et al., 2005). Sinha and Gregory confirmed their suggestion that once DOX enters the cell it goes under reduction reaction in the presence of microsomal NADPH and becomes active so it alkylates nucleic acids and proteins after covalently attaching to them, leading to the cell's death (Sinha & Lewis, 1981). On the other hand, DOX was found to have high cardio toxicity even when administered in low doses, it acts as a vasodilatant and might also cause necrosis in its injection site. Minding this, and the hydrophilic nature of DOX, traditional drug administration is limited, and there is a need to encapsulate the potent drug (Lin et al., 2005; Tan, Lin, & Wang, 2005). Controlled drug delivery methods where drug is carried to its target and released locally can restore DOX therapeutic power and efficiency.

Many attempts were made trying to conjugate/encapsulate DOX prior to its administration to the body, among them, encapsulated DOX in PLGA microparticles (Lin et al.), entrapped DOX in liposomes (Charrois & Allen, 2004; Yuh et al., 2005) micelles (S. Q. Liu, Tong, & Yang, 2005), peptide-conjugated DOX (Arap, Pasqualini, & Ruoslahti, 1998) and sugar conjugated (Zaman, Tan, Joshi, & Ying, 2006). Tan et al. demonstrated DOX release from double-walled microspheres, where polymer degradation was the release mechanism (Tan et al., 2005). Neither of these approaches was using ultrasound to enhance DOX uptake and therapeutic effects in cancer cells.

Previous research has also suggested a synergy between doxorubicin and ultrasound. Yuh et al investigated the delivery of liposome-encapsulated doxorubicin, to tumors treated with high-intensity focused ultrasound (1-10 MHz, 35W), suggesting delivery mechanisms, such as, cavitation, disruption of tumor vessel endothelial cell barriers, improving vascular permeability and vasodilation of tumor blood vessels due to hyperthermia (Yuh et al., 2005). Huseini et al. also encapsulated DOX in micelles and used low frequency 20-90 kHz) to acoustically trigger its release (Husseini, Christensen, Rapoport, & Pitt, 2002; Husseini, Myrup, Pitt, Christensen, & Rapoport, 2000; Rapoport et al., 2003). The use of micelles and liposomes has limitations, since both carriers are short lived in the blood stream, have a drug release burst effect and do not allow for prolonged imaging sessions. Another feature of micelles carrying DOX is that once the ultrasound insonation is stopped the drug is re-encapsulated in the micelles, and no longer available for cellular uptake (Husseini et al., 2002; Husseini et al., 2000). We hypothesized that incorporating DOX onto our microbubbles, will provide safe carrying mechanism, prolonged ultrasound imaging, use of cavitation, sonoporation and shock waves to enhance DOX release and uptake by cancer cells. For these reasons we chose DOX to be one of the anti cancer drugs to be incorporated in polymeric CA.

2.6.4.2 *5-Fluorouracil (5FU)*

Five-fluorouracil is an important used anti-cancer drug used for treating tumors of several organs such as, breast, colon, stomach, pancreas, ovary and lung (Parikh, Parikh, Dubey, Soni, & Kapadia, 2003). It is a pyrimidine analogue, which acts as antimetabolite and immunosuppressive agent, leading cells to apoptosis after interfering with cell cycle functions. It is water soluble and has a rapid plasma clearance, leading to a short half life of 10-20 minutes. Encapsulation of this drug into microbubbles can prolong its presence in the circulation and facilitate effective administration in the tumor site.

For these reasons carrying alternatives for 5FU delivery were investigated; conjugation with nanoparticles (L. Liu, Jin, Cheng, Zhang, & Zhang, 2006), encapsulation in polymeric micelles (Jie, Venkatraman, Min, Freddy, & Huat, 2005), encapsulation in PLGA microparticles (Faisant, Akiki, Siepmann, Benoit, & J., 2006) and encapsulation in microspheres prepared by a solvent evaporation method (Parikh et al., 2003). None of these applications involved contrast agents nor ultrasound enhanced delivery.

Several studies demonstrated that combination of free 5FU with ultrasound contrast agents improved 5FU effect on cancel cells by cavitation (Larina et al., 2005a; Larina et al., 2005b). Chumakova et al. studied the effect of combining Optison as cavitation agent on cancer cell cultures that were incubated with 5FU media Several studies demonstrated that combination of free 5FU with ultrasound contrast agents improved 5FU effect on cancel cells and (Chumakova, Liopo, Evers, & O., 2006). They found that 5FU effect on cancer cells was synergistic to ultrasound insonation, and was greater than 5FU effect alone. Moreover, they confirmed previous results that Optison itself was responsible for cells death due to enhanced apoptosis that was a result of Optison interactions with cell membrane components leading to cell signaling cascades (van Wamel, Bouakaz, Versluis, & de Jong, 2004). Five-FU was also encapsulated in hydrogel nanoparticles that were injected to the circulation of tumor inoculated

mice, comparison of insonated tumors and non-insonated ones, demonstrated the synergism of 5fU and ultrasound (Myhr & Moan, 2006).

Five-FU is suitable for incorporation in various delivery systems, however, the potential of loading it onto polymeric CA and using ultrasound to enhance its release was not investigated. For these reason it was chosen to be loaded onto our CA.

3. Materials and Methods

3.1 *Materials*

3.1.1 *Polymers*

Poly (D,L-lactic acid) MW=83 kDa and 50:50 Poly (D,L lactic-co-glycolic acid) MW=47kDa (3A) were purchased from Lakeshore Biomaterials Inc. (Birminham, Alabama, USA). Poly (vinyl alcohol), 88% mole hydrolyzed, with a MW of 25 kDa and 6 kDa were from Sigma-Aldrich Inc. (St. Louis, Montana, USA).

3.1.2 *Drug models and drugs*

Bovine serum albumin (FITC-BSA), sudan black B, 5-fluorouracil and doxorubicin were from Sigma-Aldrich Inc. (St. Louis, Montana, USA).

3.1.3 *Other Chemicals*

(1R)-(+)-camphor, Ammonium carbonate and BCA protein kit were from Sigma-Aldrich Inc. (St. Louis, Montana, USA). All other chemicals were reagent grade from Fisher Scientific (Fair Law, NJ, USA).

3.2 *Methods*

3.2.1 *Contrast Agent Fabrication by Double Emulsion*

There are several acceptable methods to produce polymeric microbubbles, among them, solvent evaporation, solvent extraction, coacervation, spray drying and double emulsion. The CA to be discussed in this work are made of PLA or PLGA by an adaptation of a double emulsion process and solvent evaporation, that was previously developed in our lab [(El-Sherif & Wheatley, 2003; Narayan & Wheatley, 1999). The main steps of the double emulsion process are illustrated in Figure 3-1, and the detailed procedure including lot numbers and mnufacturers information is listed in Appendix A. Briefly, camphor (0.05g) and PLA/PLGA (0.50g) were

dissolved in 10mL methylene chloride, and 1mL of ammonium carbonate 4% (w/v) solution was added. The polymer solution was probe sonicated at 110W for 30sec using sonicator (Ultrasonic Processor XL, Misonix Inc., New Highway Farmingdale, NY), to create the first emulsion (W/O). The porogen materials are sublimed out when the microbubbles are lyophilized leaving voids in their place. So that the aqueous phase porogen is expected to leave voids in the microbubble core (later on filled with gas or air) and the organic phase porogen is potentially responsible for shell porosity and brittle. The resulting (W/O) emulsion was then poured into cold (4°C), 5% polyvinyl alcohol solution and homogenized using homogenizer (PT 3100, Polytron Inc., USA, blade: 95/polytron PT-DA 3020/2S, Kinematica, Switzerland), for 5 min at 9000 rpm, to create the second emulsion ((W/O)/O). The double emulsion was then poured into a 2% isopropanol solution and stirred at room temperature for 1 hour (Corning stirrer, multiple position, 300rpm). The capsules were then collected by centrifugation and washed three times with hexane. The capsules were mixed with 3mL DI water and frozen in a -85°C freezer, lyophilized for 48 hours. Camphor and ammonium carbonate sublime in the lypophiliser, leaving a void in their place. The dried samples were stored in a freezer at -20°C until used. This method was used in this work to produce air filled microbubbles, of mean size 1.2μm, with acoustic properties and drug carrying capabilities.

Several process variables can be changed in order to affect the resulting microbubbles properties. Homogenization speed and polymer molecular weight were found to affect microbubbles size, surfactant concentration and molecular weight play a role in microbubbles stability and integrity and polymer choice, polymer molecular weight and concentration affect the sensitivity to hydrolysis . All of those variables have the potential to eventually affect the acoustic properties of the resulting microbubbles and hence they provide a dynamic platform of tailoring the right microbubbles depending on their role. Some of those variables were studied for their contribution to drug release and the preliminary results are presented in Chapter 5.

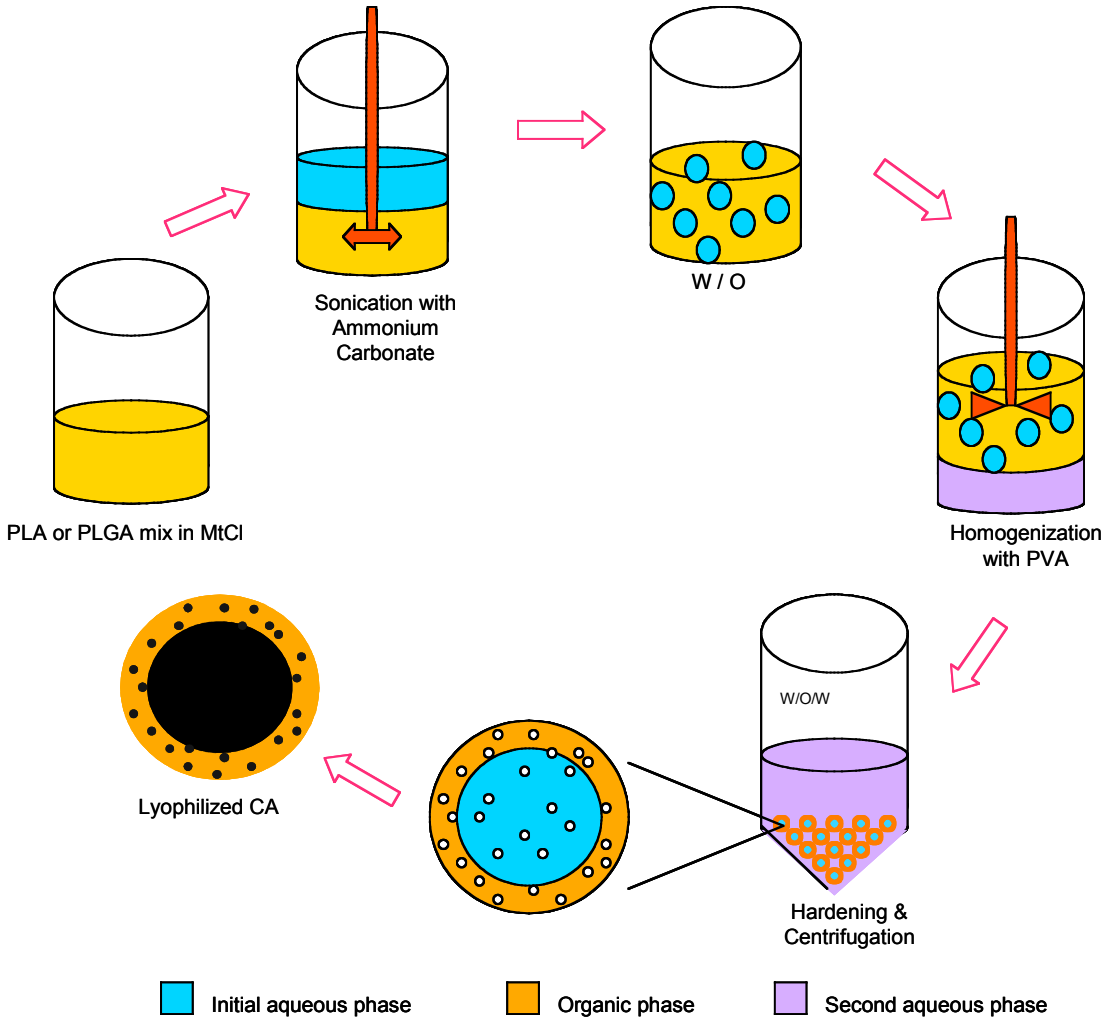

Figure 3-1 Illustration of the main steps of contrast agents fabrication made by a double emulsion process.

3.2.2 *Shell Material*

3.2.2.1 *Polymer of Choice*

PLA and 50:50 PLGA were both used as shell materials in this work. In the case of 50:50 PLGA a double amount of methylene chloride was used to dissolve the polymer in the initial stage of CA fabrication. The polymer used is identified for each experiment.

3.2.2.2 *Porogen Content in the Shell*

Two porogens were used in this work, one, ammonium carbonate was used as a core porogen and the second, camphor was used as a shell porogen.

3.2.3 *Acoustic Studies*

In vitro (attenuation, dose and time response) and in vivo (qualitative) acoustic studies were performed. Section ß3.3.1 describes the in vitro system used for all acoustic studies in our lab, where sections ß3.3.1.1 and ß3.3.1.2 describe the standard acoustic tests, including a detailed experimental description and testing conditions.

3.2.3.1 *In Vitro Acoustic Testing*

All in vitro acoustic studies were done using the pulse-echo US system set up described in Figure 3-2. In this system a one-dimensional pulsed A-mode ultrasound set-up was used with one of five single element broadband, 12.7mm element diameter, 50.8mm spherically focused transducers (Panametrics, Inc., Waltham, MA). Table 3-1 provides a detailed information regarding transducers' center frequency, peak frequency, bandwidth and low/high spectrum range.

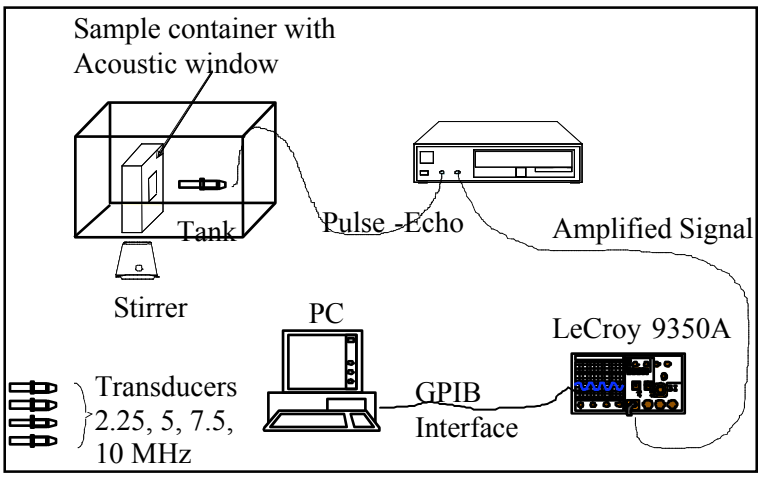

Figure 3-2 In vitro ultrasound experimental system

The transducer was submerged in a 37°C water bath filled with 17.8 MΩ deionized (DI) water (E-Pure D4641, deionization unit, Barnstead, Iowa, USA). The transducer was then focused through an acoustically transparent window (made of 15µm thick plastic tape) in the sample holder at a depth of 14 cm from the top of the water tank cover. The ultrasound transducer was carefully mounted using an x-y positioning system (Edmund Scientific, Barrington, NJ, USA) that was fixed to the tank cover, so that it was aligned perpendicular to the acoustic window in the sample vessel. The transducer was stationed 11cm below fluid level to mimic blood pressure. A pulser/receiver (5072 PR Panamterics Inc.) was used to generate a pulse repetition frequency of 100 Hz. Received signals were then amplified 40 dB and read on an oscilloscope (LeCroy 9350 A, Chestnut Ridge, NY, USA). Table 3-2 details the pressure values that were measured, using a probe hydrophone (Precision Acoustics limited, Dorchester, England), for the 4 energy levels for 5MHz transducers.

Table 3-1 Transducers information for in vitro experiments

Transducer	2.25 MHz	5 MHz	7.5 MHz	10 MHz	15 MHz
Model	V306	V309	V320	V311	V319
Serial number	236834	228153	255112	228185	237135
Center Frequency[MHz]	2.31	5.45	7.60	9.80	14.50
Peak Frequency [MHz]	2.53	6.40	7.65	10.70	14.50
(-6dB) Bandwidth %	89.18	91.74	60.53	65.31	51.03
Spectrum range (low) MHz	1.28	2.95	5.30	6.60	10.80
Spectrum range (high) MHz	3.34	7.95	9.90	10.70	18.20

Table 3-2 Pressure measurements for 5MHz transducer [kPa]

Energy level	5MHz Focused (at focal length)	5MHz Un-focused (mid sample vessel)
1	686	252
2	918	350
3	1236	495
4	1562	671

The pulser/receiver was set with the following parameters:

· Pulse Repetition Frequency = 100Hz

· Energy Level = 1 (~13 Joules)

· Damping Level = 3 (50 Ohms parallel output electrical resistance)

· Gain = 40dB

· Pulse-echo mode

The 2.0ms time-gated rms (root mean square) data was collected and analyzed using Labview 7 Express (National Instruments, Austin, TX, USA). The sample vessel was custom made of high density polyethylene (diameter=4.25mm height=140mm) to allow a total volume of 50mL or more. The sample vessel was mounted in a fixed location in the water tank. The water tank was equipped with 2 submerged titanium heaters (AZOO, AZ60052, Taiwan), to keep a fixed water temperature of 37°C±0.5. The sample was stirred throughout the insonation

period using a magnetic stir bar to keep the contrast agent suspended and uniformly distributed in the vessel (Basude & Wheatley, 2001).

Prior to each experiment a baseline of an average of 60rms measurements was recorded for stirred PBS alone ($mV_{baseline}$). Following baseline acquisition, the CA was inserted using a 1 mL pipette and after allowing a 10 seconds period for CA to properly mix, another average of 60rms measurements was taken, this time (mV_{CA}). Equation 3.1 was used to calculate the backscatter acoustic enhancement of the CA in reference to the baseline (Basude & Wheatley, 2001; Forsberg et al., 1997):

$$BackscatterEnhancement(dB) = 20 \cdot Log(\frac{mV_{baseline}}{mV_{CA}}) \qquad \text{eq. 3-1}$$

3.2.3.2 *In Vitro Dose Response*

Dose response is a protocol built to evaluate the increase in the backscattered US waves enhancement increase as a result of CA dose increase. This procedure provided a means of comparison for the acoustic properties of all CA fabricated in the lab, loaded or not loaded with drugs. This procedure can be done in two different fashions, a more rapid cumulative one and generation by plotting a curve obtained from single-step readings.

In the non-cumulative procedure 3mg of CA were suspended in 800µL of 37°C PBS. After choosing the US transducer and experimental parameters, the sample vessel was filled with 50ml of 37°C PBS the system was ready for alignment of the US beam. Following that, a baseline measurement was acquired. Then a 20µL aliquot ("dose") of CA suspension was added to the sample vessel, stirred for 10 sec followed by data recording. The addition of CA was continued in 20µL steps to reach 10 dose points. All dose response points were obtained using three different samples, each repeated three times. This method was used initially to screen samples and evaluate the preparation method and CA stability in 37°C aqueous solution.

In the more accurate procedure, 3mg of CA are suspended in 800µL of warm, 37°C, PBS. After choosing the US transducer and parameters, the sample vessel was filled with 50ml of 37°C PBS and US beam was aligned. Following that, a baseline measurement was acquired. Then a 20µL aliquot ("dose") of CA suspension was added to the sample vessel, stirred for 10 sec followed by data recording. The sample vessel was then rinsed in DI water and placed again in the water tank ready to be filled with 50ml of 37°C PBS, and the next dose of CA was added. Each individual dose of CA was taken from a fresh suspension of 3mg/800µL CA in PBS. This method prevents degradation of the sample with time affecting late-time readings.

3.2.3.3 *In Vitro Time Response*

Time response is a protocol designed to establish the stability of the contrast agent in a simulated physiological environment, for a chosen dose of CA. This procedure also enables one to evaluate and compare the acoustic properties of fabricated CA. The procedure is similar to the dose response: the same US set up is used. The sample vessel is filled with 50ml 37°C PBS and baseline data are acquired. Based on the plotted results of dose response a single dose is chosen to be tested in this protocol. It is the dose of CA that produced the maximal enhancement on the rise of the dose response curve. This dose is taken out from a fresh CA suspension of 3mgCA/800µL PBS. After allowing 10 sec for CA to properly stir and mix in the sample vessel the recording started, taking a 60rms measurements once a minute for 15 minutes.

3.2.4 *Size Distribution Analysis*

Size distribution was measured using a Malvern Nano ZS Particle Sizer, (Malvern Instruments, Worcestershire, United Kingdom), based on dynamic light scattering (DLS) technique. In short, a suspension of 1mg/mL of dry microbubbles were inserted into a

measuring cuvette and placed in the reading chamber. This was repeated 3 times for each sample. The result was a number/volume distribution of sizes presented in graph and table.

3.2.5 *Morphology by Electron Microscopy*

3.2.5.1 *Sample Preparation*

Samples were mounted and coated with a conductive material to facilitate scanning. In short, a double-sided carbon type is attached to a metal stub, and a small aliquot of the sample to be scanned was sprinkled on top. Agent that did not adhere was removed with a gentle stream of air. The stubs were inserted into a platinum/palladium sputter coater, Cressington, 208 HR, Watford, England, for 30 seconds (stage angle 30°, 0.2mBar, 60mA).

3.2.5.2 *Sample Scanning*

Surface morphology and cross section of prepared microbubbles were scanned using an environmental scanning electron microscope (FEI XL30, Oregon, USA). Some specimens were initially broken with vigorous sonication to reveal their shells and inner surfaces. Starting operation conditions were:

Acceleration voltage: 5kV

Spot size: 3

Filter: 3

Magnifications: x1000, x3000, x6000 and x9000.

Changes in those set up parameters were made according to the quality of scanning, the sample, and the ESEM conditions.

3.2.6 *Microbubbles Loading*

Microbubbles were loaded with drug using four different methods according to the drug properties.

3.2.6.1 *Incorporation*

Using this method the drug is incorporated into the microbubble shell and as a part of the CA fabrication process, thus it is added at the very first stages of fabrication. There are two phases from which drug could be loading during shell incorporation, one is the aqueous phase, suitable for hydrophilic drugs such as FITC-BSA, 5FU and DOX, and the other is the organic phase, suitable for hydrophobic drugs, i.e., SB. Since incorporation is part of microbubbles fabrication process, the parameters that can be investigated are limited to the process conditions, and only drug concentration can be altered.

Hydrophilic drug was weighted (according to the desired final drug concentration) and dissolved in the ammonium carbonate phase. One mL of the ammonium carbonate (0.1M) containing the drug was added to the organic phase which included the dissolved polymer and followed by sonication, to create a first emulsion of W/O. The fabrication process continues without further changes, Figure 3-3.

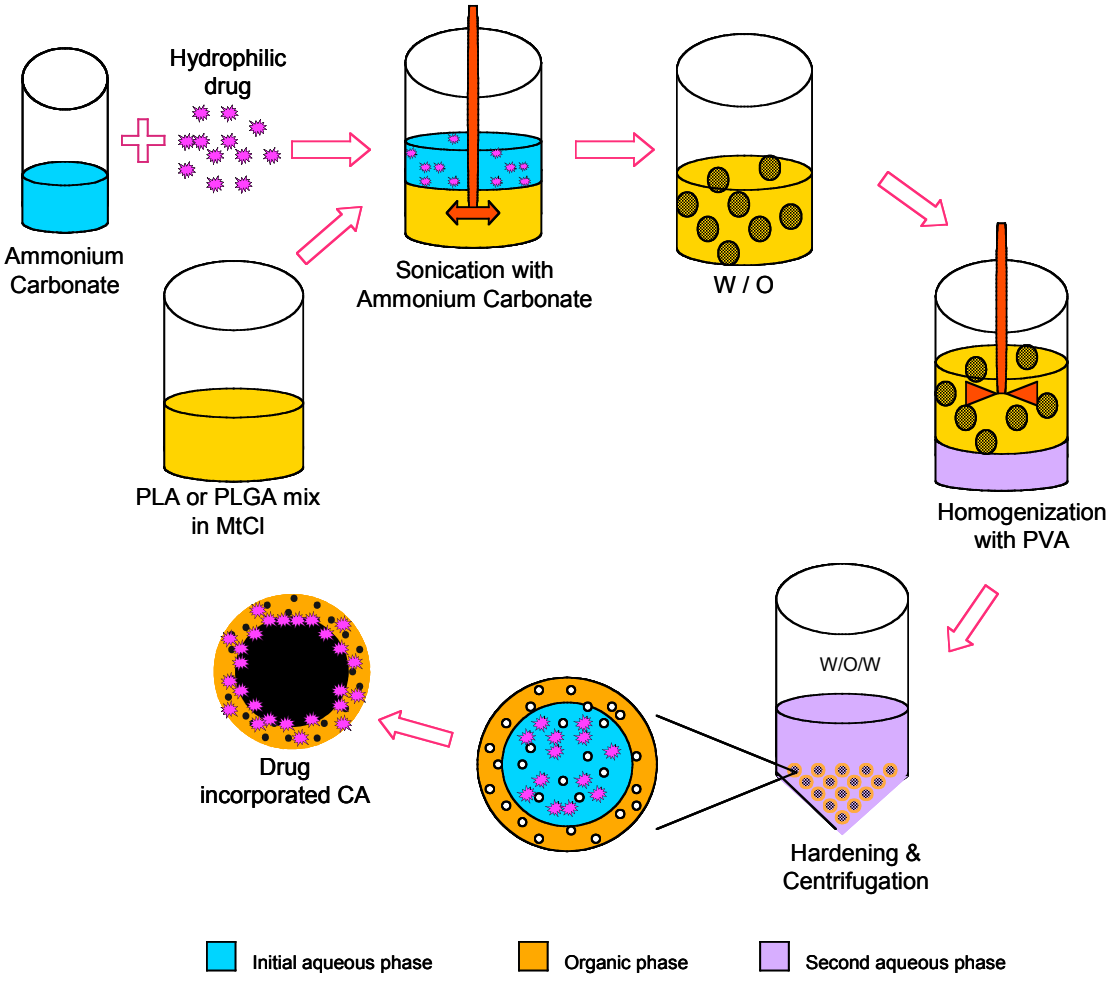

Figure 3-3 Illustration of incorporation loading method for a hydrophilic drug. Drug is added to the primary aqueous phase of ammonium carbonate, and then homogenized with organic phase including the polymer. Ammonium carbonate solution is sublimed out during lyophilization leaving the drug on the inner shell surface.

For hydrophobic drugs, incorporation occurs at the organic phase, as illustrated in Figure 3-4. The hydrophobic drug was weighted (according to the desired final drug concentration) and added to the primary organic phase together with the polymer and camphor. The rest of CA fabrication process continued without any changes. Unencapsulated drug was removed along the fabrication process at various wash steps and centrifugations. A detailed protocol is listed in Appendix F.

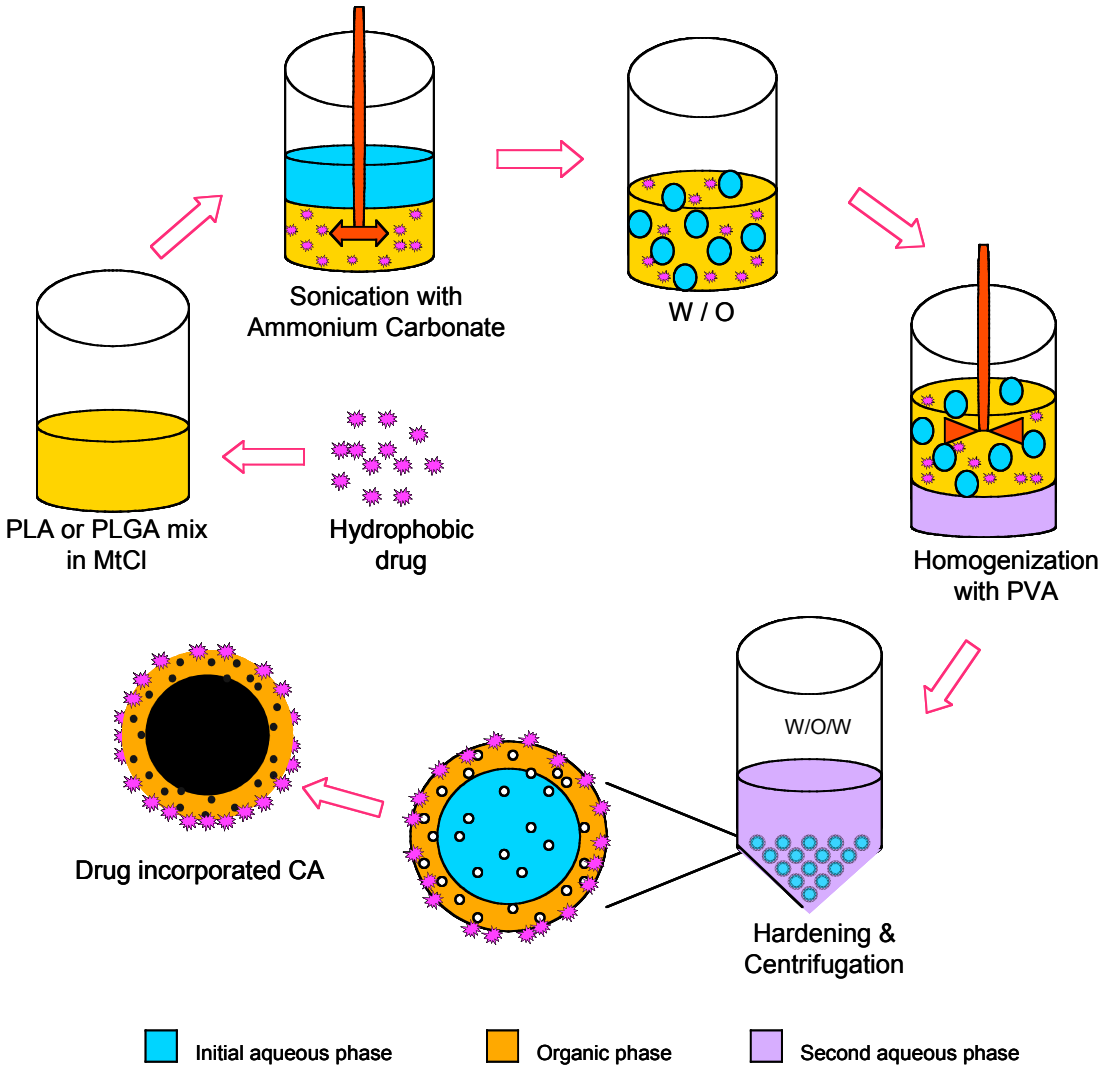

Figure 3-4 Illustration of incorporation loading method for a hydrophobic drug. Drug is added to the primary organic phase, and mixed with the polymer. Drug is mixed in the shell material, and ends up as part of the shell.

3.2.6.2 *Adsorption (Wet, Dry)*

Surface adsorption in the most versatile method demonstrated in their work. It is a method that can be applied post-fabrication onto dry microbubbles (dry adsorption), and allows for a

variety of loading conditions related to incubation temperature, time, pH and drug concentration. Adsorption can also be done before the final CA is formed, during the final fabrication steps, when the microbubbles are still wet, just before they are lyophilized (wet adsorption).

3.2.6.2.1 *Dry Adsorption*

As mentioned above dry adsorption is a dynamic method allowing adjustment of several variables depending on the drug of choice. In this work drug incubation time, temperature and pH were investigated, as well as drug initial concentration. Figure 3-5 shows an illustration of dry adsorption method.

Briefly, 0.1g of dry microbubbles was placed in a vial with 2mL of buffer, and the drug of choice. The buffer was chosen according to the drug and polymer characteristics, mainly between their iso-electric pH points, when they bear opposite charging, to ensure maximal attraction between drug and CA surface. In case of FTIC-BSA one of two buffers was used, NaAc pH=4.2 and PBS pH=7.4, as detailed in the results section 4.2.1.1. The incubation time was tested in the range of 3-27 hours. FITC-BSA dry adsorption was also carried out for 3 different temperatures, 4°C, 22°C and 37°C. The last variable tested for dry adsorbed FITC-BSA was initial drug concentration, ranging from 5%-30% (Wdrug/Wtotal%).

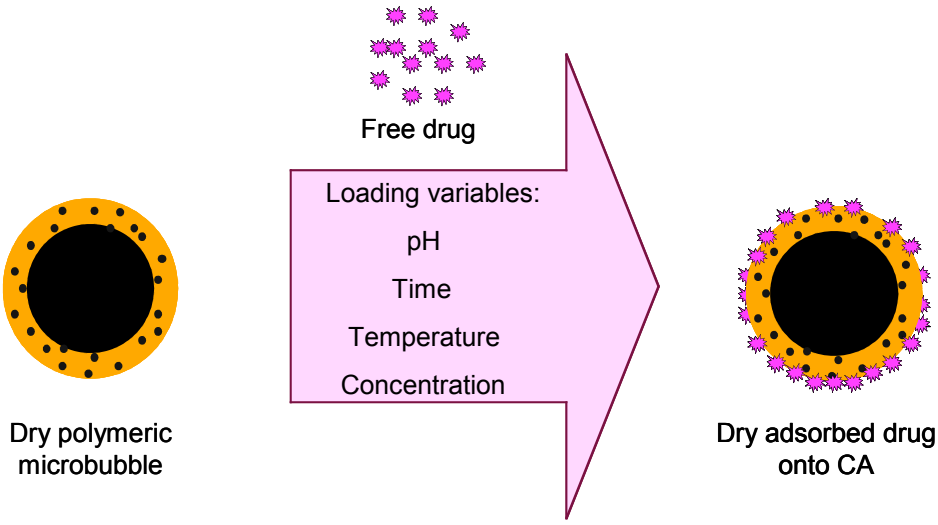

Figure 3-5 Illustration of dry adsorption loading method, dry CA is incubated in a drug solution, post fabrication.

In the case of DOX and 5FU, incubation of drug and microbubbles occurred in DI water, at a pH of 5.5. The time period for each incubation process was ranging between 3-27 hours. All incubation reactions for drug and CA were done at 4°C. Drug concentration varied between 0.1%-4% (W/W%) for both drugs. A detailed description of each loading process is listed in Appendix G. Following incubation, the microbubbles are washed 3 times with 50mL buffer, freeze dried, and ready to use.

3.2.6.2.2 *Wet Adsorption*

In this method dry drug is weighted (according to the desired final drug concentration) and added to the, still wet, microbubbles at the hardening phase, after they have been washed with hexane, Figure 3-6. The drug is expected to adsorb onto the wet thin PVA. The drug is stirred into the microbubbles paste and left for 30minutes in a fume hood. At the end of adsorption time period the bubbles are washed with DI water and centrifuged to separate them from free

unloaded drug and solvents. The microbubbles are then ready to be lyophilized. A detailed protocol is listed in Appendix G.

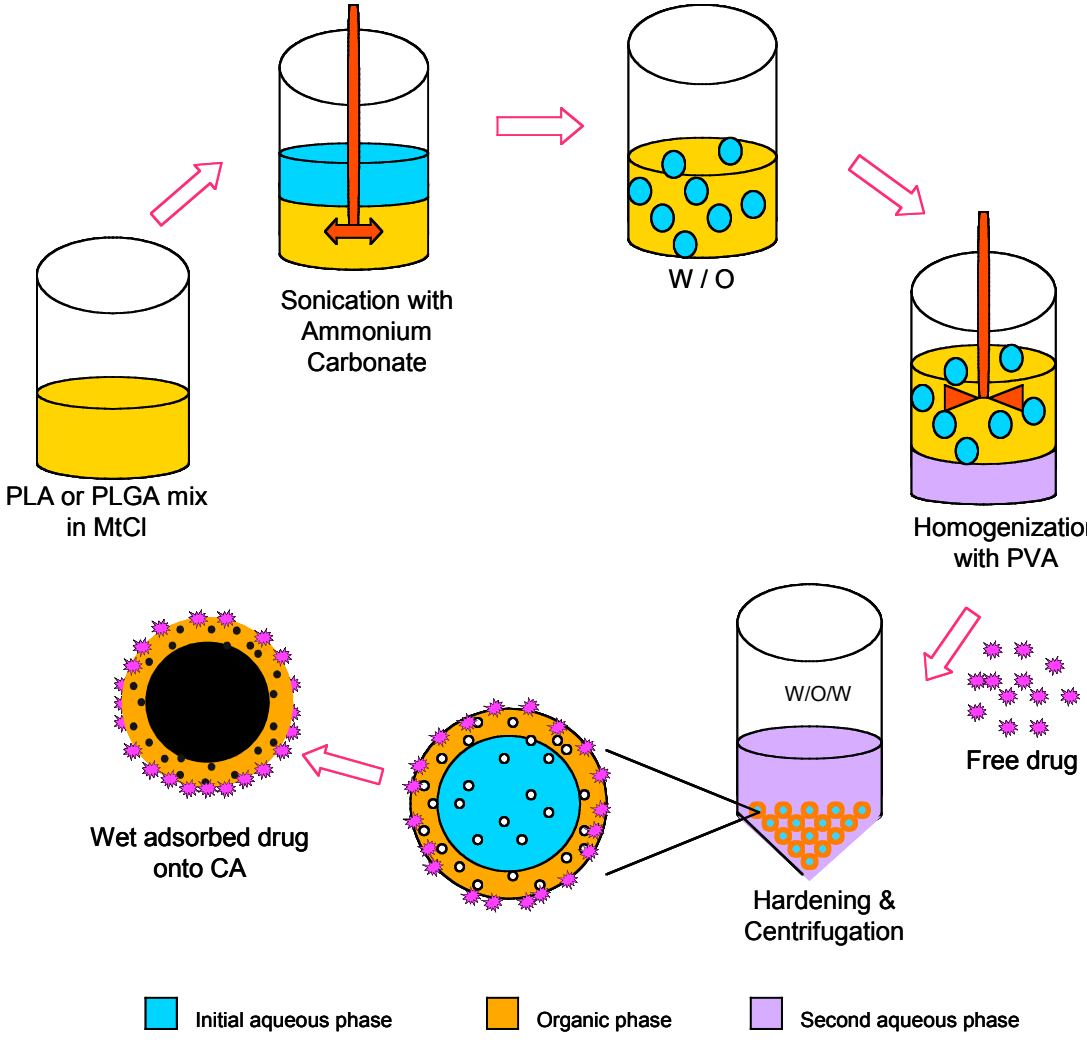

Figure 3-6 Illustration of wet adsorption loading method, powdered drug is added to wet microbubbles after hexane wash, and before final centrifugations and lyophilization.

3.2.7 *Drug Encapsulation Analysis*

Loaded drug amounts were quantified for all drug loaded samples, by dissolving the microbubbles, and determining free drug amount using a plate reader (Faisant, Akiki, Siepmann, Benoit, & Siepmann, 2006). Briefly, 4mg of dry loaded CA were weighted and put in a test tube containing 2mL of DMSO. The tube was vortexed for 10 sec and left for 10 minutes to allow proper dissolution of CA shell. Meanwhile, a calibration curve for the drug in DMSO was prepared, using a series of concentrations ranging between 0.1-1mg/mL. All samples were then plated, 0.2mL per well, in a 96-well plate and the absorbance or fluorescence was read at the respective wave-lengths. A detailed method and equations for calculating drug percent and encapsulation efficiency (EE) are available in Appendix H.

3.2.8 *Drug Release*

Drug release tests were done using the in vitro acoustic set up, Figure 3-2. Briefly, 10mg of loaded CA were weighted and added to warm (37°C) 1mL PBS in a test tube. Ultrasound sample vessel was filled with warm (37°C) PBS, and stirring was turned on. CA suspension was added and immediately followed by removal of first sample, 700µL. Ultrasound was turned on, using the chosen transducer, for a period of 30minutes. Samples were removed every 5 minutes, each of 700µL. Each sample was centrifuged, at 5000rpm for 5minutes using a table top Eppendorf centrifuge, immediately after they were taken. The supernatant was plated, 200µL per well, in a 96-well-plate in triplicates. The control in this experiment was an un-loaded CA. Detailed protocol is presented in Appendix J.

3.2.9 *In Vivo*

All in vivo tests were carried out at Thomas Jefferson University Hospital, Philadelphia, PA, USA.

3.2.9.1 *Ultrasound Enhancement in Rabbit Kidney*

Animal model: Rabbit kidney is a preferred model for a rich vasculature organ and is frequently used as a model for CA enhancement tests. Rabbit used in this experiment were New Zealand white rabbits (of either sex), within the weight range of 2.5-5.0 kg. They were sedated prior to imaging and sacrificed at the end of procedure. The detailed protocol is listed in Appendix C.

Ultrasound Imaging: Power Doppler (PDI) and pulse inversion harmonic (PIHI) imaging of the kidney was performed using an abdominal scan. The ultrasound system in use was HDI 5000 scanner with an L7-4 linear array (Philips Medical Systems, Bothell, WA). Power Doppler imaging was done with a broad bandwidth L12-5 transducer (5-12 MHz), a PRF of 700 kHz and a mechanical index (MI) of 0.33. Pulse inversion harmonic imaging was performed with an L7-4 broad bandwidth transducer and an MI of 0.26. Digital clips were stored for off-line review.

Contrast agents in test: Sudan-PLA microbubbles (4%, loaded by incorporation) were used for all injections in this experiment. Forty mg of CA were weighted and placed in vials ready for use. Just before injection 1mL of saline was added to one CA vial, and the vial was gently shaken to properly suspend the CA. The agent was injected through a catheterized ear vein followed by an immediate port flush with 5mL of saline.

3.2.9.2 *Lymph Nodes and Lymph Channels Dyeing*

Animal model: This study was set to test PLA loaded with 4% Sudan Black by incorporation, for evaluating intra-abdominal organs via intravenous injection. The purpose was to see if these CA can enhance sentinel lymph nodes (SLNs) on ultrasound imaging by subcutaneous injection, and test the ability of drug loaded CA to travel along lymph channel reaching to their lymph nodes. For this purpose Sudan black loaded CA are most suitable since their color is visibly detectable and can be matched with position of ultrasound signal enhancement.

Rabbit experiments were done using the same protocol for in vivo studies, details and animal information including preparation, anesthesia and handling are available in Appendix C. Each injection ranged between 0.5 to 1.0 ml of a PLA-based CA into the right foot pad of the hind leg and same amount of saline was injected as control into the left foot pad. After contrast injection, the area was massaged for up to 5 minutes to stimulate contrast movement into the lymphatic channels (LCs) and SLNs. Soon after contrast administration, contrast lymphosonography was used to identify the location of the draining LCs and ultimately the SLN(s).

Ultrasound imaging: The rabbits were imaged using a Sonoline Elegra scanner (Siemens Medical Solutions, Issaquah, WA) and a 7.5 MHz linear array transducer. Grayscale pulse inversion harmonic imaging (PIHI) with a 3.6/7.2 MHz transmission/reception frequency pair.

Contrast agents in test: Forty mg of CA were weighted and placed in vials ready for use. Just before injection 1mL of saline was added to one CA vial, and the vial was gently shaken to properly suspend the CA. Rabbits were injected with Sudan-PLA (4%, loaded by incorporation). The following equation was used to calculate the CA dose that was injected in each injection, for a 3kg rabbit:

$$0.35\text{mL/kg} * 3\text{kg} * 0.04\text{g/mL} = 0.042\text{ g CA} \qquad \text{eq. 3-2}$$

4. Results and Discussion

The long term goal of this work is to develop a drug delivery system that is using ultrasound for imaging drug target and releasing the drug. Drug release in general is affected by many parameters which can be divided into two main categories; preparation conditions and release conditions. Preparation conditions include, loading method (pH, temperature, time), loaded concentrations. In case of loading onto microbubbles which are prepared by double emulsion, the ratios of volumes of each phase play role in drug loading as well. Release conditions include medium chemical properties (hydrophobocity, osmolarity, buffer concentration, ionic strength, pH), temperature, additional catalizators. In the case of drug release in vivo the release conditions are pre-set, limiting the release to physiological environment properties, hence the best way to affect drug release is by optimizing its loading. This chapter presents the results and discussion for loading study done on CA that were developed in our lab.

Results and discussion are presented in this chapter for two drug models, FITC-BSA and Sudan Black, and two chemotherapeutic anti-cancer drugs, 5-fluorouracil and Doxorubicin, loaded onto polymeric microbubbles. FITC-BSA and Sudan Black were chosen to model PLA loading with hydrophilic and hydrophobic drugs, respectively. 5-fluorouracil and Doxorubicin, both hydrophilic drugs, were chosen as representative chemotherapeutics and loaded onto PLA and PLGA CA platforms, respectively.

This chapter is divided into two main sections presenting microbubble characterization and drug loading results, respectively. Drug loading results are divided into four sub-sections each dedicated to one drug/model-drug. More results and discussions related to US triggered drug release, and nano and micro bubbles mixtures and more in vivo tests are presented in Chapter 5. Adding nanobubbles to microbubbles have the potential to enhance acoustic performance and perhaps even drug delivery having more surface area available for drug loading and being able to leak out from blood vessels into tissues. A brief literature survey is presented alongside preliminary results in Chapter 5.

4.1 *Contrast Agent Characterization*

Each batch of microbubbles that was fabricated was first tested for size distribution, morphology, and echogenicity, prior to drug loading. Morphology was obtained using ESEM pictures. Size distribution was analyzed using a dynamic light scattering technique, where samples were suspended in DI for testing. Characterization of microbubbles prior to loading enables a uniform start point, enabling comparison among the different loading methods studied in the following sub-sections.

4.1.1 *Morphology*

Dry samples were fixed and coated prior to picture taking as detailed in 3.2.5. Pictures were taken at three magnification levels, 3000x, 6000x and 9000x, to reveal aggregates, residues, and free individual microbubbles. Some of the samples were broken down by vigorous sonication, to reveal their cross section and inner surface. Figure 4.1 shows the morphology of PLA microbubbles for a representative sample not loaded with drug. Some of the samples that were fabricated ended in a honey-comb surface, due to inaccuracies in organic and aqueous phase ratio originating from organic solvent evaporation prior to first emulsion formation (Cui et al., 2005). Yang et al. demonstrated that a low organic phase volume results in a more viscous solution, that is more difficult to break up the internal water into smaller droplets during first emulsion sonication. The water droplets entrapped in the core of the microbubbles coalesce with one another leaving a big hole after being lyophilized. In addition, low organic phase results in bigger and more porous microbubbles (Yang et al., 2001). Re-measuring the organic phase volume and compensating for the evaporated a volume yielded smooth surface microbubbles as seen in Figure 4.1. Figure 4.1 shows the morphology of a non-loaded PLGA sample. Some of PLGA samples presented a wrinkled surface, again, as a result of smaller organic phase relative

to aqueous phase, this time the volumes of organic phase was doubled in order to yield the right ratio for smooth surface. PLGA was far more susceptible to this phenomenon than PLA.

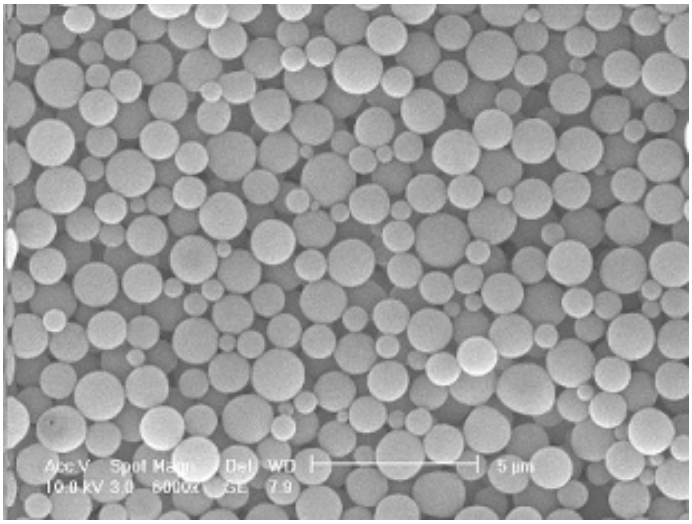

Figure 4-1 Scanning electron micrograph showing the surface morphology of PLA microbubbles fabricated by a double emulsion process, at 6,000X magnification mean size 1.19±0.24 (size bar 5µm). Note the bimodal distribution.

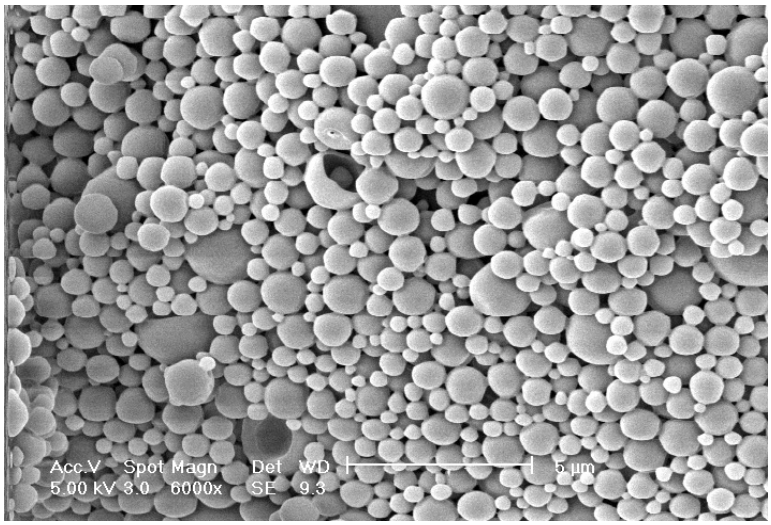

Figure 4-2 Scanning electron micrograph showing the surface morphology of 50/50 PLGA microbubbles fabricated by a double emulsion process, at 6,000X magnification mean size 1.24±0.40 (size bar 5µm). Note the greater size distribution compared to PLA.

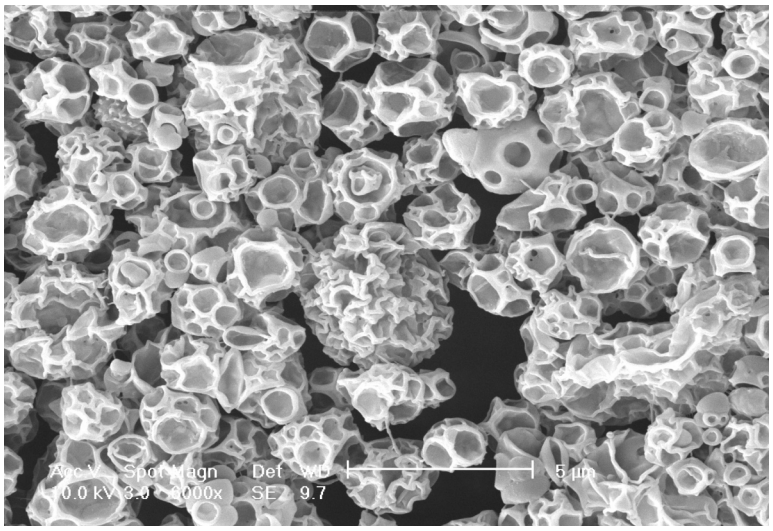

Figure 4-3 Scanning electron micrograph showing the surface morphology of 50/50 PLGA microbubbles, with a wrinkled surface, fabricated by a double emulsion process, at 6,000X magnification (size bar 5 µm). Note the greater size, possible due to capsule fusing.

4.1.2 *Size Distribution Analysis*

Another integral part of microbubbles characterization is the size distribution analysis. We performed this analysis using a dynamic light scattering method. One of the basic requirements from CA is that they do not block the capillary bed, i.e., microbubbles should be smaller than 6µm in diameter. Moreover, mean size and size distribution have a critical effect on microbubbles behavior under ultrasound beam, as inferred from (Forsberg, 2001):

$$I_s = \frac{I_i \sigma}{4\pi R^2} \qquad \text{eq. 4-1}$$

relating the scattering cross section of the microbubble (in m^2), σ, and I_s, the receiving ultrasound intensity. I_i, and, R are the incident intensity and the distance from the transducer, respectively.

Size can be controlled by adjusting the parameters in several steps in CA fabrication process, among them, homogenization speed for creating the second emulsion, polymer molecular weight. Figure 4-4 shows a comparison of size distribution for PLA and PLGA using a DLS technique. The mean diameters are 1.13±0.19µm and 1.24 ±0.40µm for PLA and PLGA respectively. Both agents satisfy the size requirements for intravenous injection. Some samples were showing a bimodal size distribution having part of their microbubbles in the micron range and part in the nano range. This distribution is favorable since there are several advantages of nanobubbles as drug carriers; nanobubbles have more surface area available for targeting molecules attachment and drug loading, their smaller size allows them to reach different destinations in tissues, and outside blood vessels, higher and more efficient intracellular uptake (by mechanism, of endocytosis), they can pass through smaller capillaries and do not bear risk of blockage of capillaries due to aggregation (Panyam et al., 2003).

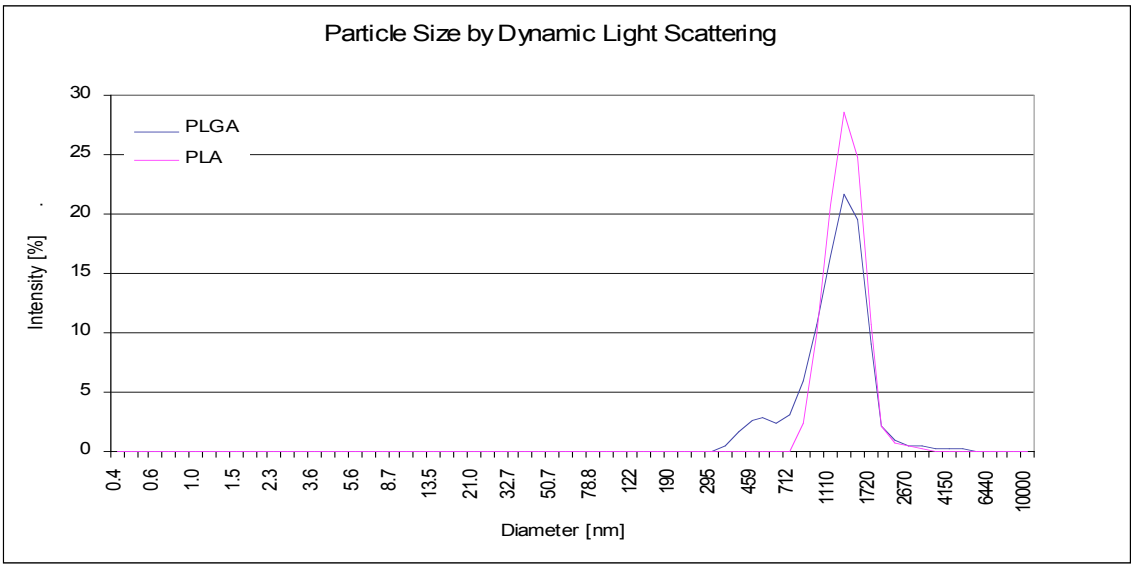

Figure 4-4 Comparison of size distribution for PLA and PLGA using a DLS (Dynamic light scattering) technique. The mean diameters are 1.13±0.19µm and 1.24 ±0.40µm for PLA and PLGA, respectively.

Figure 4-5 shows the shell thickness of PLGA microbubbles. Microbubbles were broken by intense sonication (10 minutes at 130W, over ice bath), and shell thickness measures about 10% of microbubble diameter.

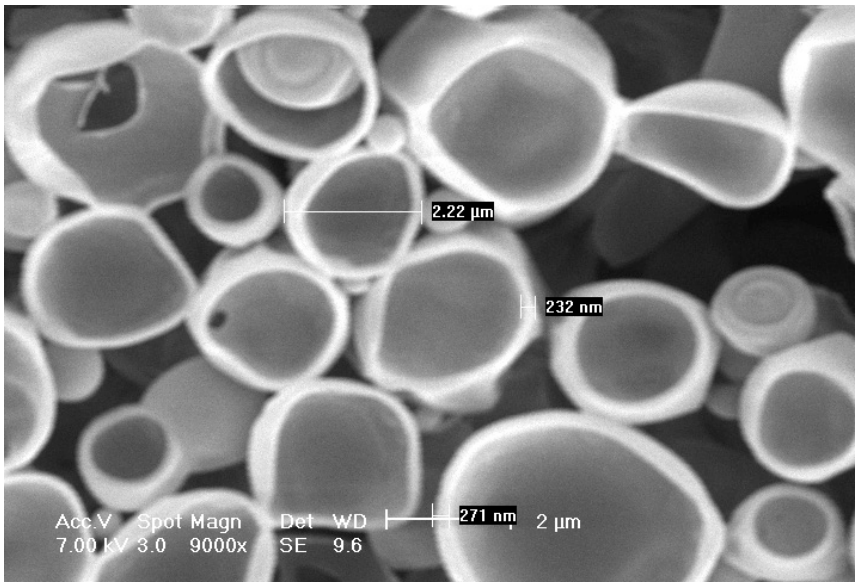

Figure 4-5 Scanning electron micrograph of broken PLGA microbubbles showing their shell thickness. Shell thickness is about 10% of microbubble diameter (9,000X magnification, size bar 2µm).

4.2 *Drug Loading*

Two drug models, BSA and Sudan Black, and two chemotherapeutic drugs, 5FU and DOX were chosen to be investigated in this work. BSA, a large molecular weight (~66 kDa) and hydrophilic protein is readily available in its fluorescently labeled form (FITC-BSA, fluorescein isothiocyanate). Sudan black is a small molecular weight (456.54g/mol) hydrophobic die, readily measured spectrophotometrically, and easily detectable in tissues it is delivered to. Both models present different chemical characteristics that affect their loading capacity onto PLA microbubbles, as described below. 5FU is a hydrophilic anti-cancer drug that is also readily measured spectrophotometrically, and was tested on PLA CA. DOX, is a water soluble,

naturally fluorescent, anti-cancer drug, also available in radiolabeled form, which can be used for tissue culture and in vivo experiments. DOX was loaded onto PLGA microbubbles due to their higher loading capacity in comparison to PLA CA, ¶4.2.4.1. This section is organized into four sub-sections, one for each drug/model drug.

4.2.1 *Bovine Serum Albumin (BSA)*

Bovine serum albumin is a popular drug model for drug delivery systems (Hamidi M et al., 2007; Pareta & Edirisinghe, 2006; Wischke & Borchert, 2006) due to its availability in highly purified form at relatively low cost, and its ease of dissolution in water. Its fluorescently labeled form, FITC-BSA, fluorescein isothiocyanate, is relatively easy to detect and for this reason was chosen for this work. We hypothesized that loading method conditions would have effects on loading percent and efficiency as well as echogenicity of the loaded CA. In dry adsorption, for example, incubation of drug and CA is necessary, during this step, several variables were thought to play role: temperature, time, pH and drug concentration. In order to study these effects we chose FITC-BSA as a model. Results pertaining loading conditions and acoustic performances are presented below in the following subsections.

4.2.1.1 *Loading Methodology*

In this section, we compare the effects of loading FITC-BSA onto PLA microbubbles, on their echogenicity and drug loading capacity, for two different methods:

Dry surface adsorption, a post-fabrication method

Shell incorporation, as an integral part of the fabrication process

The loading process steps and quantities are detailed in section 3.2.6¶. It is important to notice that there are two optional phases for drug incorporation, while fabricating CA. The aqueous phase favors incorporation of hydrophilic drugs, such as FITC-BSA, while the organic phase, favors incorporation of hydrophobic drugs. Since drug incorporation is part of the

microbubbles fabrication process, which is pre-defined robust (see 3.2.6.1), there is no room for altering loading variables to affect loading efficiency. For this reason drug concentration available for loading was the only variable studied for incorporation method. On the other hand dry surface adsorption loading is done post-fabrication and enables exploration of different loading conditions, such as incubation time, incubation pH, incubation temperature and drug concentration. Results for drug encapsulation and acoustic performances for dry adsorption of FITC-BSA for the above-mentioned variables are presented and discussed below.

4.2.1.2 *Dry Surface Adsorption for Protein-Drug*

The dry surface adsorption method is thoroughly described in 3.2.6.2.1. In this method an already prepared and dry CA is incubated in a drug solution for a pre-determined period of time, under specific pH and temperature conditions. At the end of incubation the drug was attached by cause of electrostatic attraction originating form opposite charges to the outer CA shell.

4.2.1.2.1 *pH and Incubation Time Effects on Encapsulation*

Since surface adsorption is a process that mainly relies on electrostatic attraction between opposite charged groups, the pH of incubation solution plays a significant role in drug adsorption onto the microbubble surface. In the case of FITC-BSA, a sodium-acetate buffer (NaAc), pH 4.2, was chosen as incubation solution to warranty that FITC-BSA is predominantly positively charged (iso-electric point at pH 4.7) while PLA is predominantly negatively charged (pKa at pH 3.85). Moreover, Li et. al. (Li et al., 2005) showed that at pH 4.3, the amount of adsorbed BSA onto poly-methyl-methacrylate (PMMA) microspheres reaches its maximum, with a significant decrease at lower and higher pH values, 2.2 and 7.4, respectively. They related those results to BSA spatial conformation, which tends to be more folded at the pI than in other pH values, and combination of opposite charging and conformation yielded the best surface adsorption of BSA onto PMMA.

We hypothesized the incubation of our CA in acidic pH of 4.2 might compromise the acoustic properties of our CA and lower its stability in aqueous solution. Since these features are key in CA, we adsorbed FITC-BSA also at a higher pH of 7.4, which is close to neutral. Although this pH was not expected to yield high drug loading percents, we hoped it would maintain acoustic properties.

Incubation time plays a critical role in the drug encapsulation efficiency. On one hand more time may allow for more drug to adsorb but on the other hand, exposing CA microbubbles to the drug solution has the effect of degrading the CA integrity, and at some point this has unacceptable effect on the echogenicity. Figure 4-6 shows the results of encapsulation percentage for FITC-BSA loaded PLA, for increasing incubation time periods at pH 4.2, 4°C, and initial FITC-BSA concentration of 10% percents (W/W%). The means for 3 to 14 hours of incubation were not significantly different ($n=5$, $p>0.05$) from one another suggesting that after 3 hours there is saturation of the adsorption sites. This trend is supported by encapsulation efficiencies as seen in Figure 4-8. For increasing incubation time, up to 3 hours, there is and increase in loaded BSA, and starting at 8 hours more incubation time results in similar loading. Since adsorption depends on available surface area, it is possible that for 10% BSA that surface area is taken by the protein within 3 hours, so that further adsorption is not possible.

However, as it will be discussed later on, these incubation conditions (at pH 4.2) are responsible for a decrease in acoustic performances, 4.2.1.3.1.

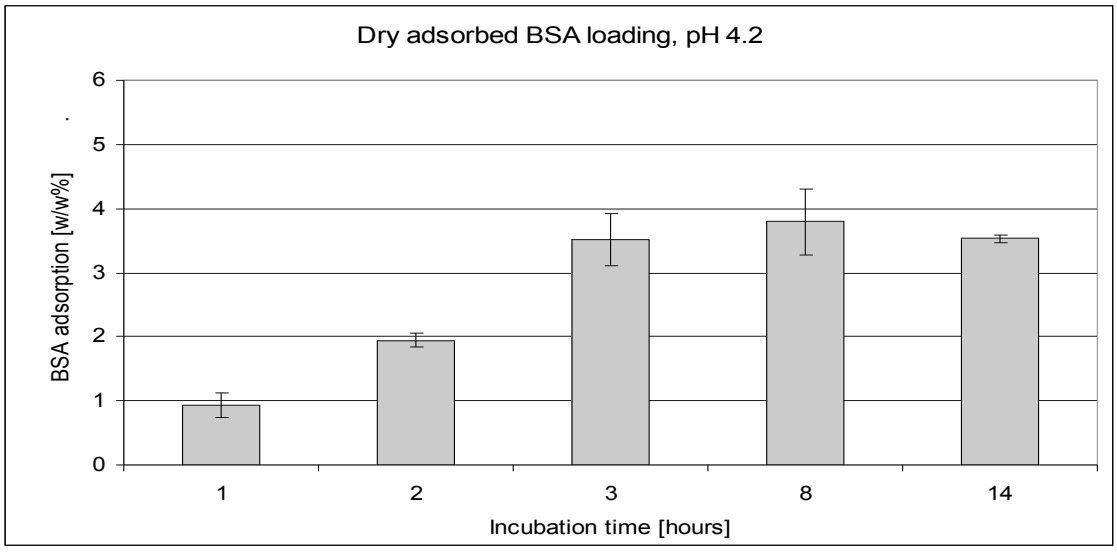

Figure 4-6 Incubation time study. FITC-BSA loaded onto PLA microbubbles, at pH 4.2 environment (4°C, for 10% initial concentration). Means are significantly different, for $P<0.01$, by one way ANOVA test (n=5, ± standard error from the mean)

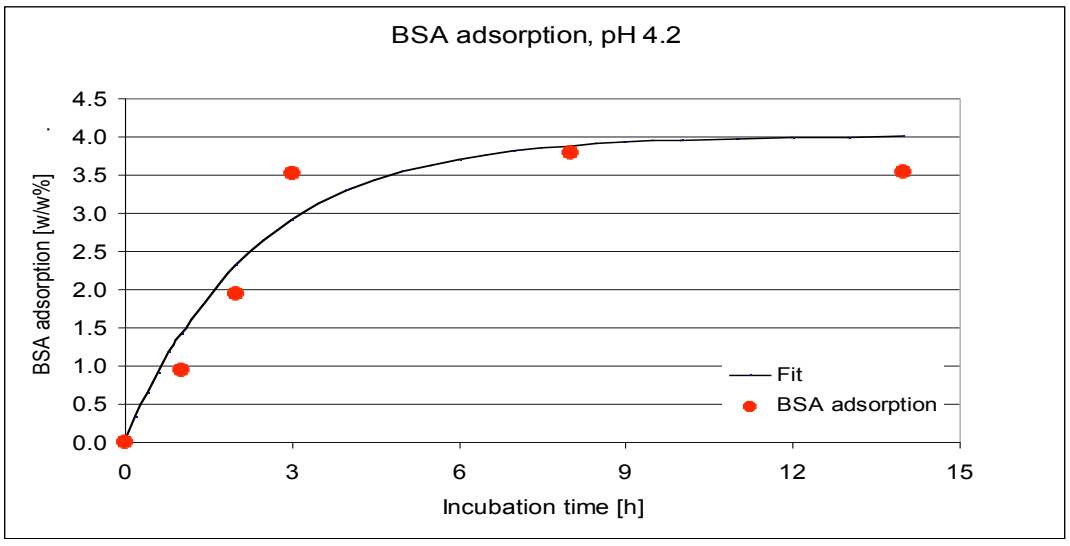

Figure 4-7 FITC-BSA loaded-PLA microbubbles, at pH 4.2 environment (4°C, for 10% initial concentration).

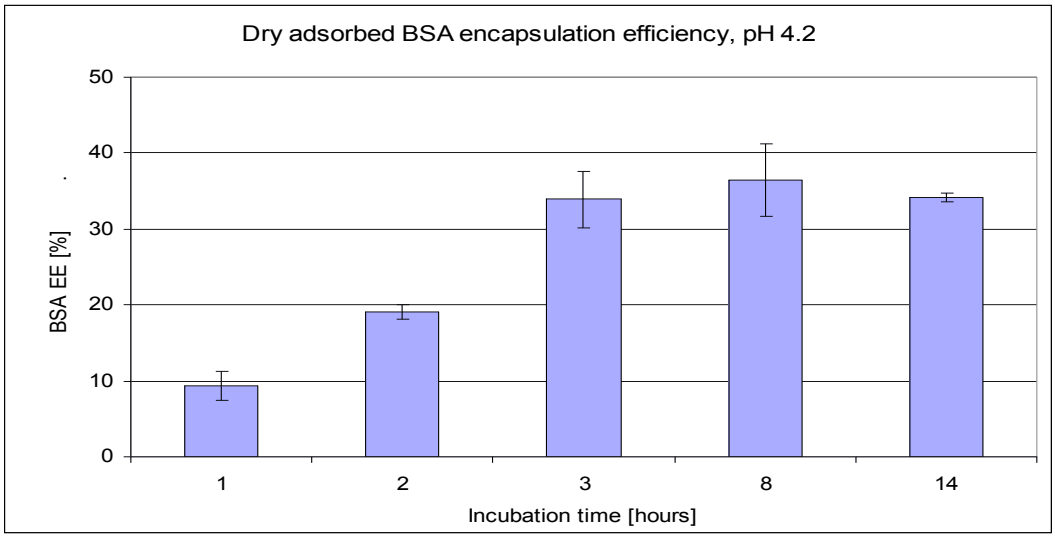

Figure 4-8 EE (EE) for FITC-BSA loaded onto PLA microbubbles, at pH 4.2 environment (4°C, for 10% initial concentration). Means are significantly different, for $P<0.05$, by one way ANOVA test (n=5, ± standard error from the mean)

In a second experiment, a phosphate buffer saline (PBS), with a pH of 7.4 was used to incubate the microbubbles. Loading FITC-BSA onto PLA in a pH 7.4 environment, with an initial loading concentration of 10% FITC-BSA, yielded less than 1% encapsulated protein, for all tested incubation time periods, Figure 4-9. This result was expected since, at such a pH, the polymer and the protein have similar charging and, as a consequence, their affinity is compromised. Moreover, there is evidence that at pH values higher and lower (2.2 and 7.4) than the PI of BSA adsorption is dramatically decreased due to the lateral electrostatic repulsion between BSA molecules themselves, having the same charge (Li et al., 2005). Accordingly, encapsulation efficiencies for this loading process were also poor, ranging from 0.297±0.017%, for 1 h, to 0.563±0.066%, for 14 h loading. Even though electrostatic attraction seemed to not play a role in adsorption of BSA onto PLA at pH 7.4, some limited adsorption did occur. This

adsorption might be due to hydrophobicity attractions, which are known to exist between proteins and hydrophobic surfaces (Butler et al., 1999).

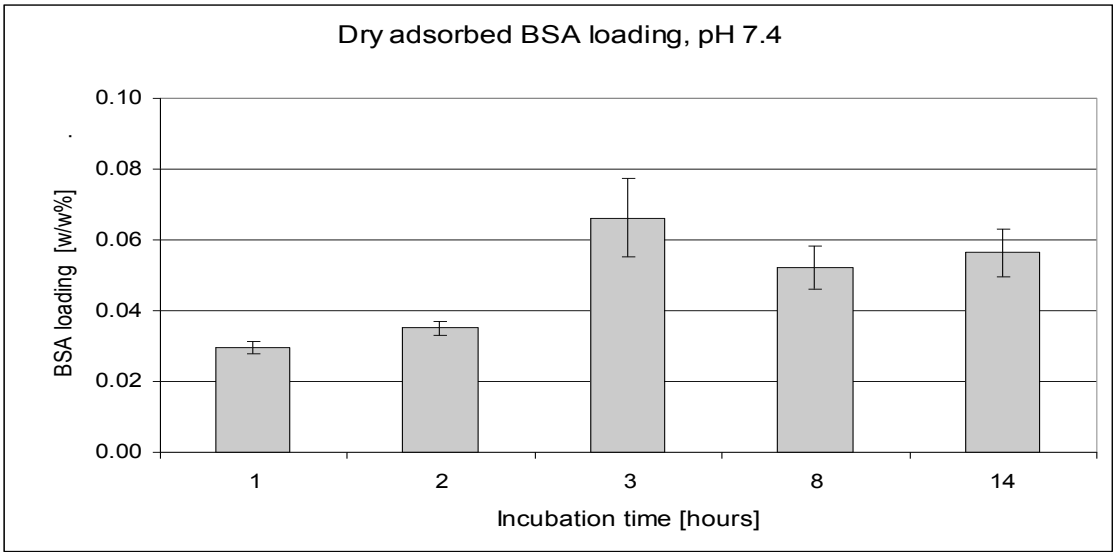

Figure 4-9 Incubation time study. FITC-BSA is loaded onto PLA microbubbles in a pH 7.4 environment (4°C, 10% initial concentration). Means are significantly different, for $P<0.01$, by one way ANOVA test (n=5, ± standard error from the mean)

4.2.1.2.2 *Temperature Effect*

This study was conducted in order to explore whether the aqueous solution temperature affect drug-CA association. The temperatures that were chosen for this study are 4°C, the coldest possible for liquids, done in a cold room, 22°C, room temperature, and 37°C, body temperature carried out in an incubator. The study was carried out for both pH 4.2 and pH 7.4, for 10% initial loading concentration of FITC-BSA. Based on previous results for pH and incubation time, incubation time was set to 3 hours. As seen in Figure 4-10 BSA adsorption decreased with temperature increase. This suggests that the adsorption process of BSA onto

PLA is exothermic, like most of adsorption processes; hence adsorption decreases with increasing temperature.

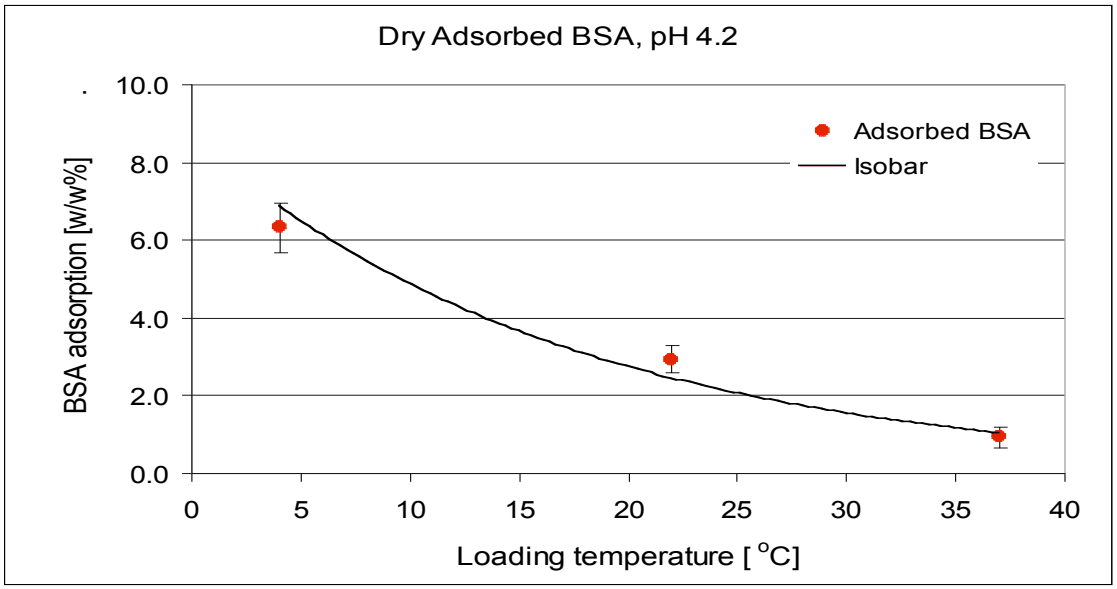

Figure 4-10 Temperature study of dry adsorbed FITC-BSA, incubated in sodium acetate (NaAc) buffer, at pH 4.2, for 3 hours. Initial FITC-BSA loading 10%. Means are significantly different, for $P<0.05$, by one way ANOVA test (n=5, ± standard error from the mean)

This behavior can be described when plotting the adsorption isobar, derived from Langmuir model of adsorption:

$$C = \frac{k\alpha C_m}{1 + kC_m} \qquad \text{eq. 4-2}$$

C_m and C are the maximal and actual concentrations of protein adsorbed, k is the rate constant of protein adsorption and α is a constant. When there is equilibrium between empty surface sites, particles and filled particle sites, k equals:

$$k = \frac{C}{(1-C)C_m\alpha} \qquad \text{eq. 4-3}$$

Langmuir isotherm is an ideal model assuming dynamic adsorption process with adsorbed and un-adsorbed BSA molecules exchange, and no interactions among adsorbed molecules (Li et al., 2005).

In the case of loading at pH 4.2 there is a strong correlation between temperature and adsorption (isobar R^2=0.987).

Encapsulation efficiencies for different loading temperatures, as shown in Figure 4-10, ranged from 59.4±5.6% (for loading at 4°C) to 9.2±2.7% (for loading at 37°C). Those results correlate with the encapsulation percents results, concluding that incubation at 4°C is more suitable for protein dry adsorption than higher temperatures that were tested.

Figure 4-11 shows the protein encapsulation percents results for incubation at pH 7.4, as expected encapsulation percent was less than 1% for all tested temperature conditions. Moreover, there was no significant difference among the loading percents for the different temperatures. Encapsulation percents ranged from 0.578±0.150% (for loading at 4°C) to 0.564±0.062% (for loading at 37°C). There was also no correlation between temperature to extent of adsorption using the Langmuir isobar model (isobar R^2=0.007). This suggests that pH 7.4 solution is not suitable for adsorption of BSA onto PLA; CA and the protein have similar charge, limiting their surface interactions and, therefore, the drug adsorption.

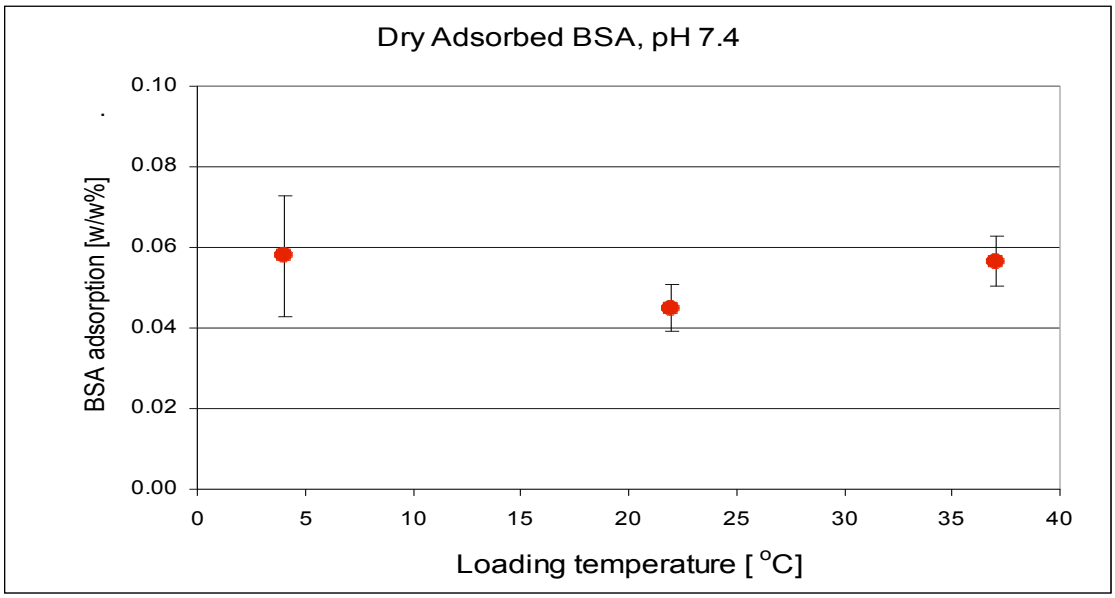

Figure 4-11 Temperature study of dry adsorbed FITC-BSA, incubated in phosphate buffer saline (PBS), at pH 7.4, for 3 hours. Initial FITC-BSA loading 10%. Means were not significantly different, for $P<0.05$, by one way ANOVA test (n=5, ± standard error from the mean)

4.2.1.2.3 *Drug Concentration Effect*

Having determined the effects of time and temperature on drug loading, a study to examine the effect of Initial drug concentration effect study was carried out in order to test if providing more free drug during incubation can improve loading and EE for FITC-BSA onto PLA microbubbles. For this study a wider range, 5%-30%, of initial protein concentrations was used. Dry adsorption conditions were 3 hours incubation at 4°C, based on results presented previously in this chapter. Figure 4-12 shows that the loading percent at pH 4.2 is increased as the initial concentration of protein increases.

It is possible to fit the adsorption results from Figure 4-12 to Langmuir model, described in the previous section, 4.2.1.2.2.

Being able to fit Langmuir model to results means that initially the rate of adsorption is high and then decreases as less surface is available for adsorption. Once the rate of adsorption equals the rate of desorption a dynamic equilibrium is attained.

Figure 4-13 shows Langmuir model plot for our results, it can be seen that our results have a good fit with this model. Meaning, BSA is initially adsorbed fast then slows down and reaches a dynamic equilibrium.

Encapsulation efficiencies for these results ranged from 63.4±2.6% for 5% initial protein concentration to 30.0±3.3% for 30% initial protein concentration. Again, there were no significant differences among encapsulation efficiencies for initial protein concentration ≤20%. This also supports the phenomenon described by Langmuir of dynamic adsorption, where after equilibrium is achieved, microbubbles surface is all taken and addition of BSA will not results in further adsorption.

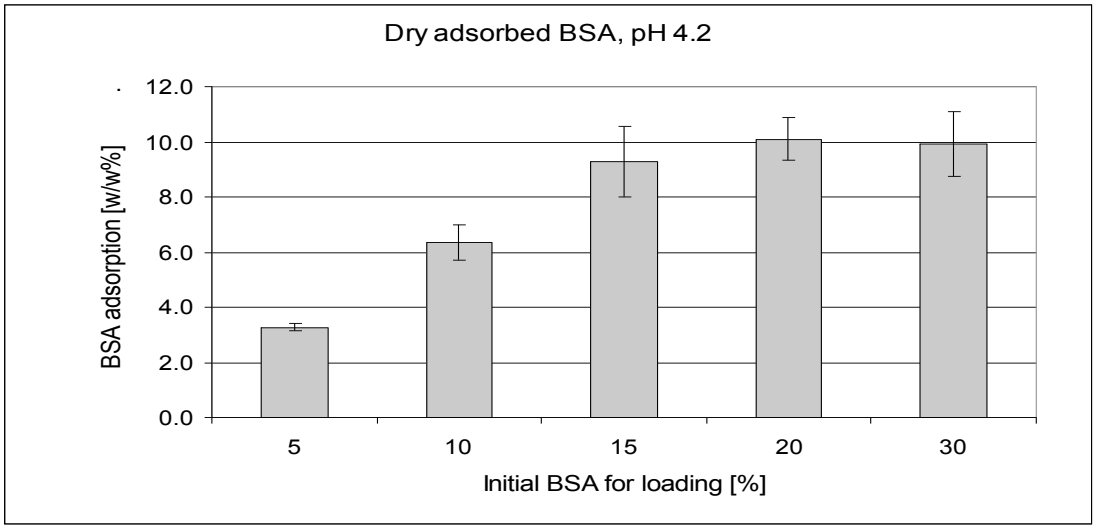

Figure 4-12 Loading percent for PLA loaded with FITC-BSA using Dry adsorption method. Loading in NaAc buffer, pH 4.2, for 3 hours, samples were gently agitated at 4°C. Means are significantly different, for $P<0.01$, by one way ANOVA test (n=5, ± standard error from the mean)

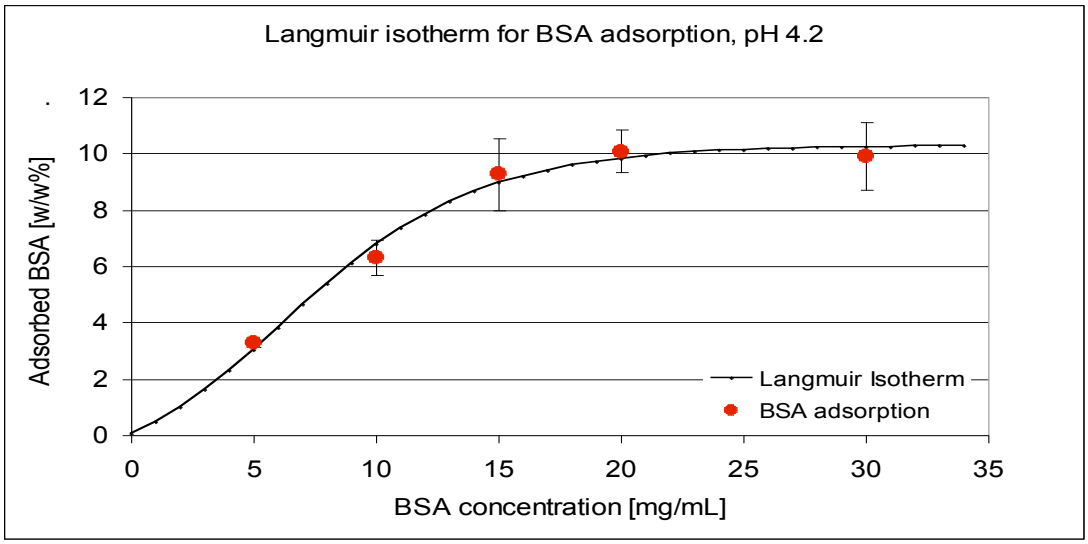

Figure 4-13 Langmuir isotherm plot for BSA adsorption onto PLA CA (R^2=0.9853). Loading conditions: NaAc buffer, pH 4.2, for 3 hours, samples were gently agitated at 4°C.

Figure 4-14 summarizes the initial protein concentration effect for FITC-BSA-loaded PLA at pH 7.4. It can be seen that for increasing concentrations of drug the adsorption of drug is increased. This trend is supported by the encapsulation efficiencies, shown in Table 4-1. This adsorption trend, however, does not fit adsorption model such as Langmuir's model nor first order kinetics. As concluded for previous tested adsorption parameters, temperature and time, pH 7.4 solution is not suitable for adsorption of BSA onto PLA. Since PLA and BSA are negatively charged at this pH adsorption is not controlled here by opposite charging since they repel each other. Hydrophobic interactions are more possible in this situation. Many proteins readily adsorb to hydrophobic polymer surfaces due to an entropic driving force arisen from hydrophobic dehydration and/or conformational changes in protein structure. As a soft protein,

BSA was shown to adsorb to a variety of polymeric and hydrophobic surfaces, among them PLGA (Butler et al., 1999).

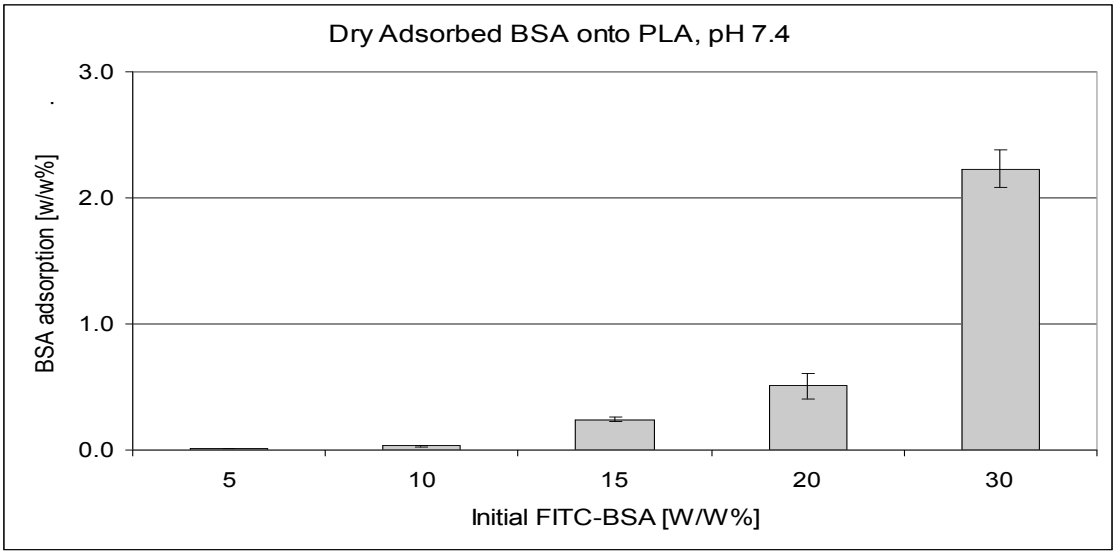

Figure 4-14 EE for PLA loaded with FITC-BSA using Dry adsorption method. Loading in PBS buffer, pH 7.4, loading time is 3 hours, samples were gently agitated at 4°C. Means are significantly different, for $P<0.001$, by one way ANOVA test (n=5, ± standard error from the mean)

Table 4-1 Encapsulation efficiencies percents for dry adsorbed BSA at pH 4.2 and pH 7.4

BSA loading	Dry adsorbed BSA, pH 4.2	Dry adsorbed BSA, pH 7.4
5% BSA	63.45±2.57	0.23±0.01
10% BSA	59.41±5.64	0.31±0.02
15% BSA	56.41±7.12	1.60±0.13
20% BSA	45.80±3.23	2.52±0.51
30% BSA	30.02±3.27	7.27±0.48

4.2.1.2.4 *Incorporation*

Incorporation method is a loading method that can be used for both hydrophilic and hydrophobic drugs. In this method the drug encapsulation step is an integral part of the polymeric microbubbles fabrication process. In the case where the drug is hydrophilic, like FITC-BSA, it is added to the first aqueous phase (see methods section 3.2.6.1). The result is a drug that is encapsulated inside the microbubbles. In case where the drug is hydrophobic it can be added to the first organic phase of methylene chloride. This process will be discussed in details in section 4.2.2.1 for hydrophobic drug model SB.

Unlike the dry adsorption method, which is a post-fabrication drug loading process, enabling many combinations of process variables, incorporation is a more limited/rigid method, allowing change of initial drug concentration only, for a given CA.

Figure 4-15 shows the effect of initial drug concentration on drug loading. For increasing initial concentrations of FITC-BSA there is an increase in the amount of incorporated FITC-BSA, and saturation in loading is achieved for initial concentrations higher than 10%. This trend is confirmed by encapsulation efficiency (EE) calculations shown in Figure 4-16, where EE decreasing for increasing initial FITC-BSA concentration.

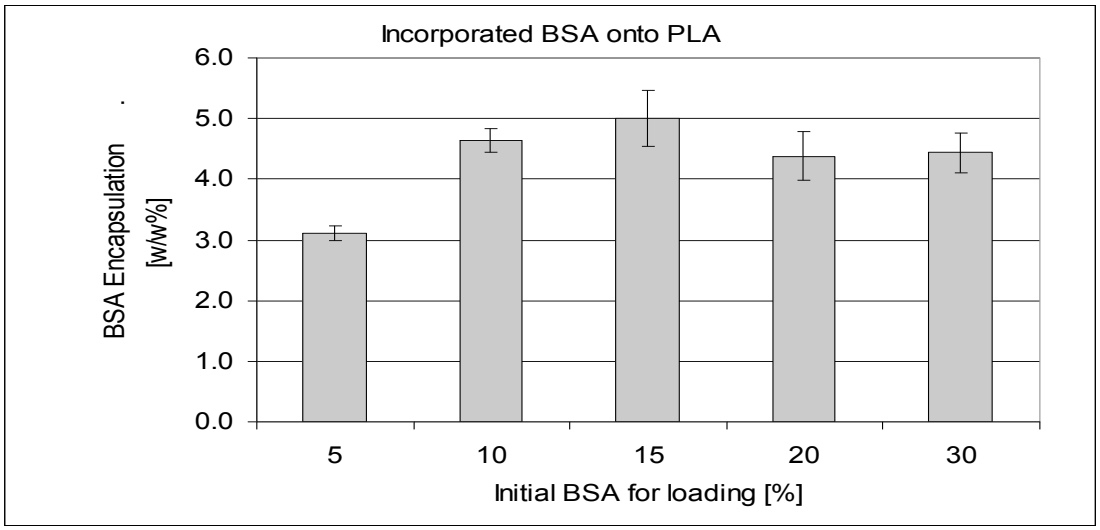

Figure 4-15 Encapsulation percent for PLA loaded with FITC-BSA, using incorporation method. Means are significantly different, for $P<0.05$, by one way ANOVA test (n=3, ± standard error from the mean)

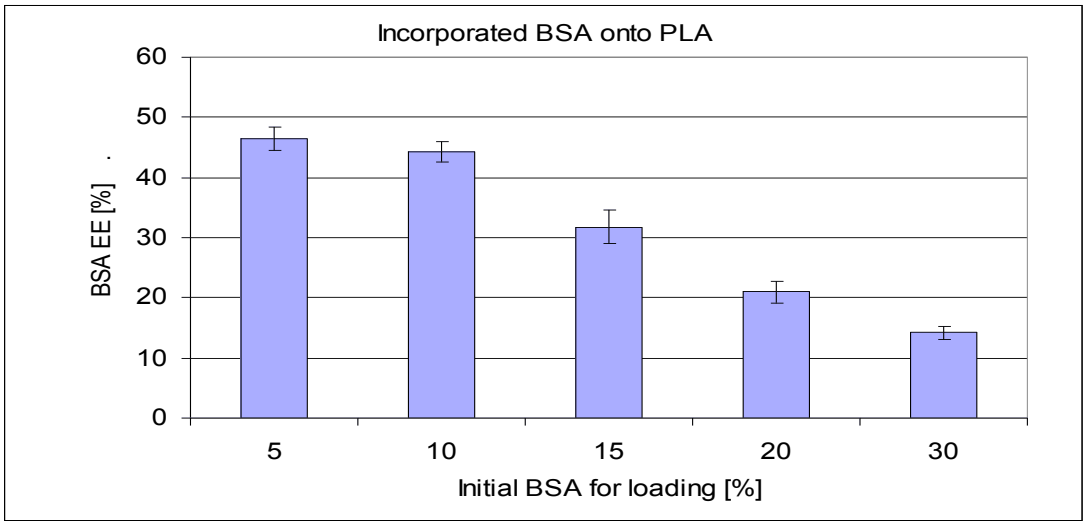

Figure 4-16 EE for PLA loaded with FITC-BSA using incorporation method. Means are significantly different, for $P<0.05$, by one way ANOVA test (n=3, ± standard error from the mean).

4.2.1.3 *Acoustic Studies*

The main acoustic properties that were used as standard tools for evaluating ultrasound signal enhancement and ultrasound signal decay were dose response and time response, respectively. Both tests were performed using the in vitro acoustic set up as shown in Figure 3-2. The system set up assembly and functions are detailed in section 3.2.3, and the protocols for both tests are described in sections 3.2.3.2 and 3.2.3.3.

Dose response was designed to measure echogenicity of increasing doses of CA ranging from 0.0015mg/mL to 0.0150mg/mL. This range of concentration was established in previous work done in our lab and was found to be the smallest range yielding acceptable signal enhancement of more than 20dB. Time response was designed to measure the ultrasound enhancement decay over time, for 15 minutes, for a single dose. A baseline measurement, of stirred PBS, was recorded prior to addition of the CA and was used for all enhancement calculation, as explained in section 3.2.3.

4.2.1.3.1 *Dry Adsorption*

4.2.1.3.1.1 *Incubation pH Effect*

In the dry adsorption method the drug is added post-fabrication, introducing additional step of CA exposure to aqueous solution and additional step of freeze drying. As seen in Figure 4-17 post-fabrication incubation significantly lowered the echogenicity of FITC-BSA loaded CA, in both pH's in comparison to control. Furthermore, acidic pH of 4.2 enhances the hydrolysis of CA in comparison to pH 7.4, which is close to neutral, resulting in a less stable microbubbles population. As biodegradable polymers, PLA and PLGA, contain hydrolysable bonds, hence their most important degradation mechanism is chemical degradation by hydrolysis. Many factors affect PLA and PLGA degradation, such as, polymer molecular weight, polymer water uptake, copolymer composition (for PLGA), polydispersity, structure and pH (Gopferich, 1996, Jain, 2000). Ester bonds can be catalyzed by pH change either acidic or basic. PLA and PLGA

are known to go through faster degradation at low and high pH conditions. The generated monomers, are carboxylic acids, further lowering the pH and accelerate degradation. If the microbubble structure is porous, like in our case, the monomers accumulate within the pores making the immediate vicinity pH more acid, then accelerating the polymer degradation even more. The porous morphology of drug-loaded microbubbles is presented in Figure 4-19 and Figure 4-20, showing FITC-BSA-loaded PLA at pH 7.4 and 4.2, respectively. It can be seen that microbubbles loaded at pH 7.4 barely have any visible pores, whereas microbubbles loaded at pH 4.2 show enlarged surface pores. This morphology strongly supports the acidic pH catalysis of PLA. It has been reported that the extracellular fluid of solid tumors is slightly acidic (pH around 6.8) (Liu et al., 2006 #21). This can be seen as beneficial for drug delivery given the fact that acidic pH accelerates the hydrolysis of our CA.

Going back to echogenicity results, Figure 4-17, CA that were loaded at pH 4.2 were 5.4dB less echogenic than CA loaded at pH 7.4 and 11.9dB lower than control echogenicity.

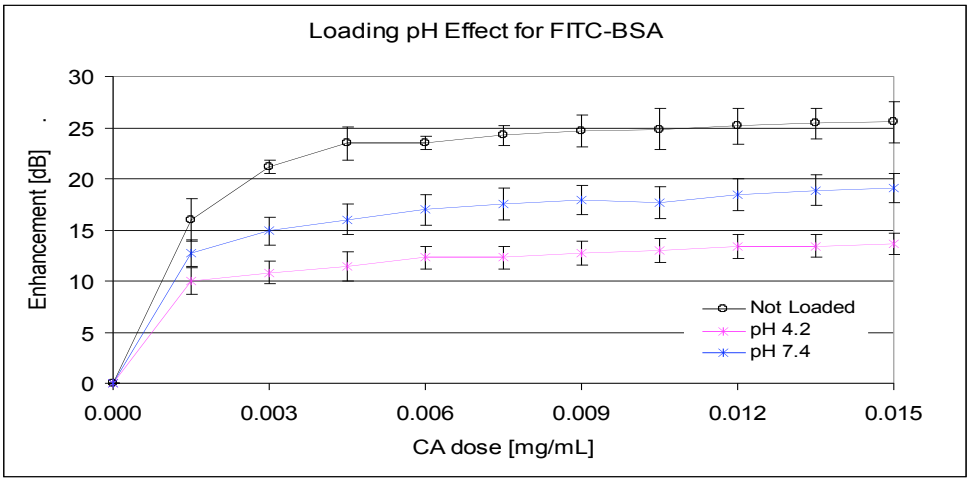

Figure 4-17 Dose response curves of 10% FITC-BSA loaded PLA using dry adsorption method, incubated for 3h at 4°C. Means are significantly different, for $P<0.0001$, by one way ANOVA test (n=5, ± standard error from the mean)

The effect of incubation pH on signal stability, over insonation time period of 15 minutes, is shown in Figure 4-18. Here too, there is a significant (n=5, $p<0.0001$) difference between control group and the loaded groups, and also between the group loaded at pH 7.4 and the group loaded at pH 4.2. At the end of 15 minutes the group that was loaded at pH 4.2 lost 56% of its echogenicity whereas the group that was loaded at pH 7.4 and the control group lost 25% and 21%, respectively. Those results correlate with the dose response curves and morphology and can be explained by enhanced hydrolysis at acidic pH.

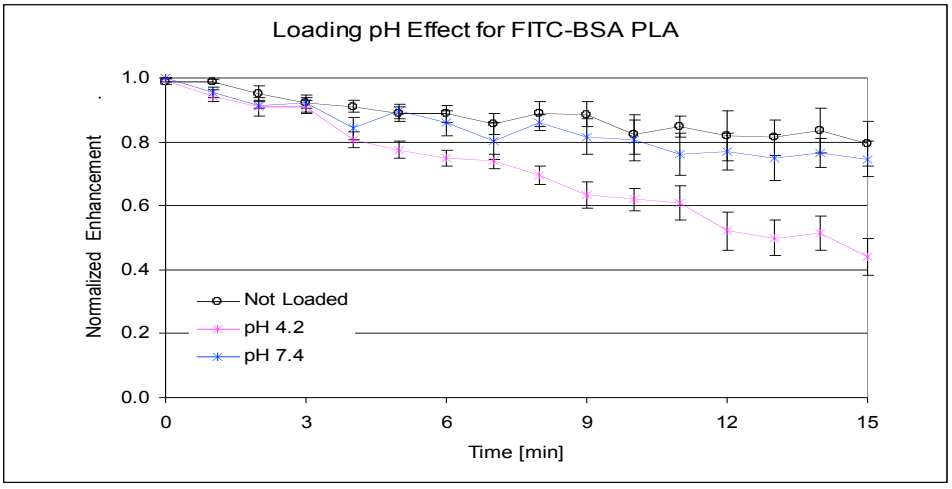

Figure 4-18 Time response curves of 10% FITC-BSA loaded PLA using dry adsorption method, incubated for 3h at 4°C. Means are significantly different, for $P<0.0001$, by one way ANOVA test (n=5, ± standard error from the mean)

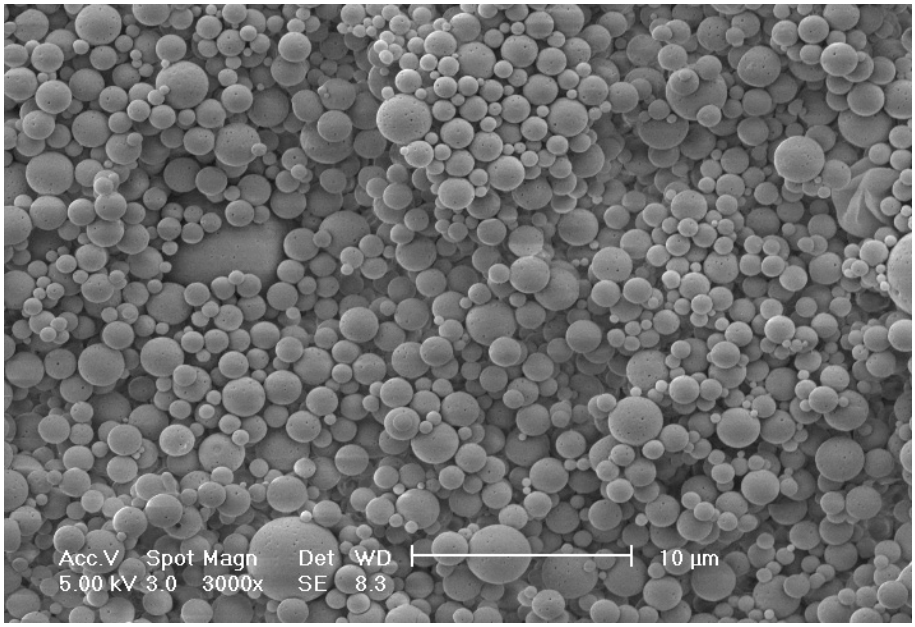

Figure 4-19 Scanning electron micrograph showing the surface morphology of PLA microbubbles loaded with 20% FITC-BSA, using dry adsorption method, pH 7.4, at 3,000X magnification (size bar 10 µm)

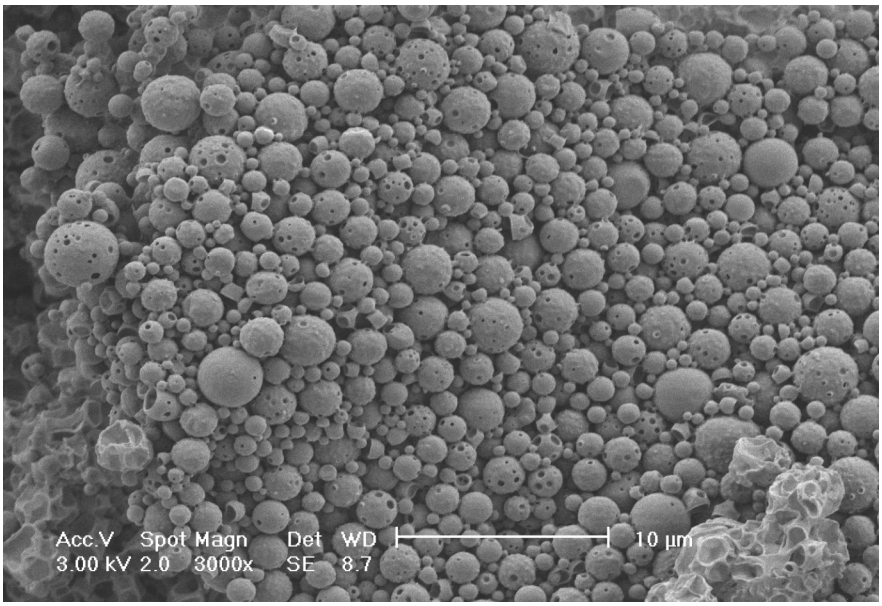

Figure 4-20 Scanning electron micrograph showing the surface morphology of PLA microbubbles loaded with 20% FITC-BSA, using dry adsorption method, pH 4.2, at 4°C for 3 h at 3,000X magnification (size bar 10 µm)

4.2.1.3.1.2 *Loading Incubation Time Effect for pH 4.2*

This study was set to investigate the echogenicity of CA loaded with FITC-BSA for increasing time periods ranging between 3-27 hours. Figure 4-21 shows the dose response results obtained for samples loaded at pH 4.2, temperature of 4°C, and 10% loading. All groups were significantly different than control (n=3, $p<0.0001$), and from one another. As expected, echogenicity decreased dramatically with the increasing time of incubation. Samples that were incubated for more than 14 hours showed no echogenicity. This can also be explained by the acceleration of PLA hydrolysis that occurs at acidic pH, which is further accelerated by the porous structure of the CA (as detailed in the previous section, 4.2.1.3.1.1).

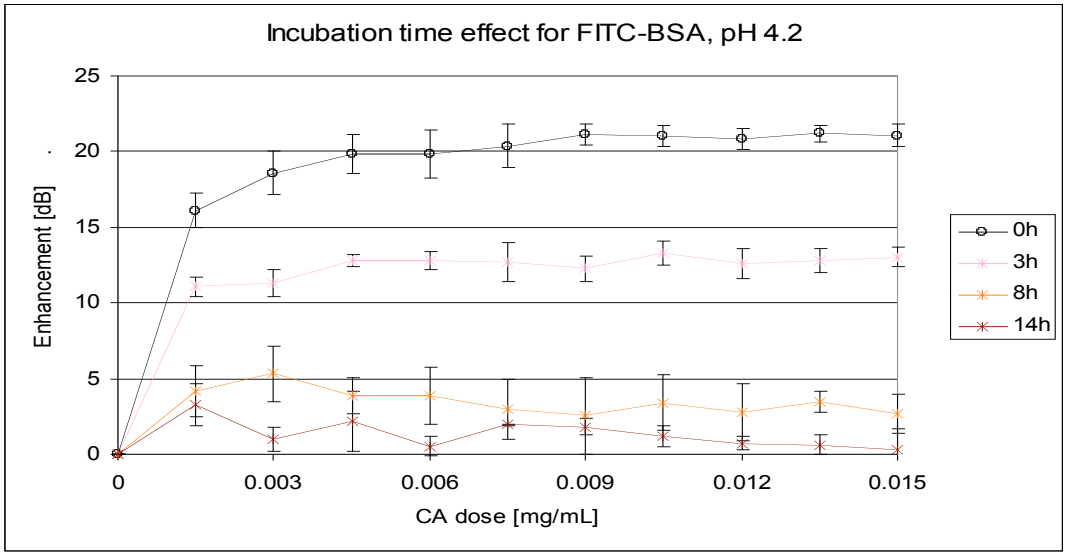

Figure 4-21 Dose response curves of 10% FITC-BSA loaded PLA using dry adsorption method, incubated at 4°C, pH 4.2. Samples incubated for more than 14 hours were non echogenic. Means are significantly different, for $P<0.0001$, by one way ANOVA test (n=3, ± standard error from the mean)

Figure 4-22 shows the time response curves corresponding to previous dose response carried out under the same loading conditions. Loaded groups are significantly different (n=3, $p<0.0001$) than control, and 3h incubation group is different than 8h and 14h, but 8h group is not significantly different (n=3, $p>0.05$) than 14h group. As explained for dose response, here too, acidic incubation conditions take their toll by reducing signal stability over time. Samples that were 8 hours and longer exposed to pH 4.2 environment lost 50% of their echogenicity within less than 3 minutes, compared to control group, where signal loss was 2.4%, up to that time point.

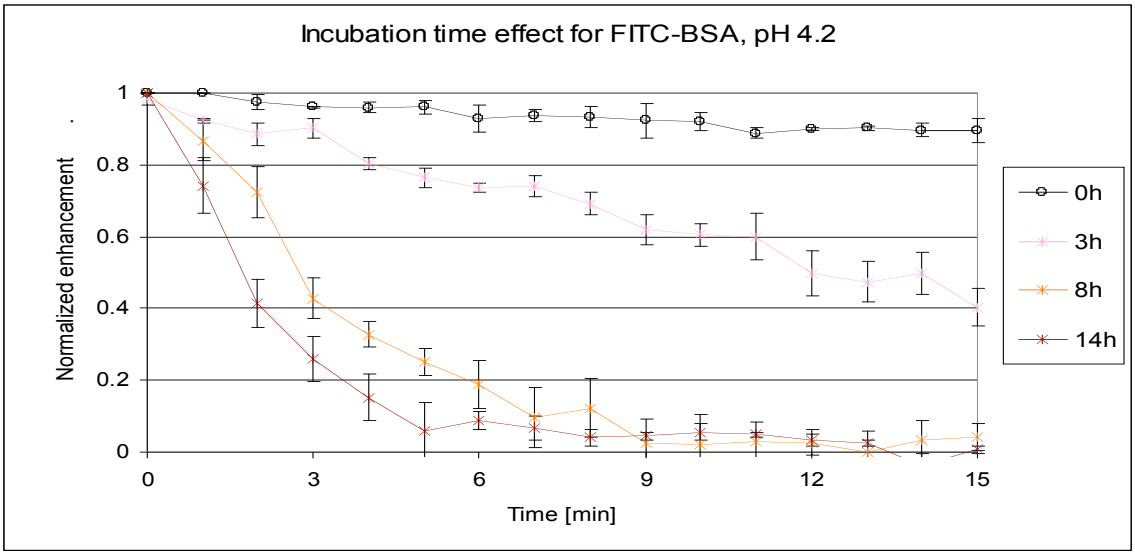

Figure 4-22 Time response curves of 10% FITC-BSA loaded PLA using dry adsorption method, incubated at 4°C, pH 4.2. Samples incubated for more than 14 hours were non echogenic. Means are significantly different, for $P<0.0001$, by one way ANOVA test (n=3, ± standard error from the mean)

4.2.1.3.1.3 *Loading Incubation Time Effect for pH 7.4*

The same incubation time study was carried out at pH 7.4. Here too, CA were loaded with FITC-BSA for increasing time periods ranging between 3-27 hours. Figure 4-23 shows that, for increasing incubation time periods the maximal echogenicity was decreased. All loaded groups were significantly (n=3, $p<0.0001$) less echogenic than the control group. And for 24 hours and above there was no significant difference (n=3, $p>0.05$) in echogenicity for the tested groups. This trend was expected since the less time the CA are exposed for aqueous solution the more it is possible to preserve good echogenic properties.

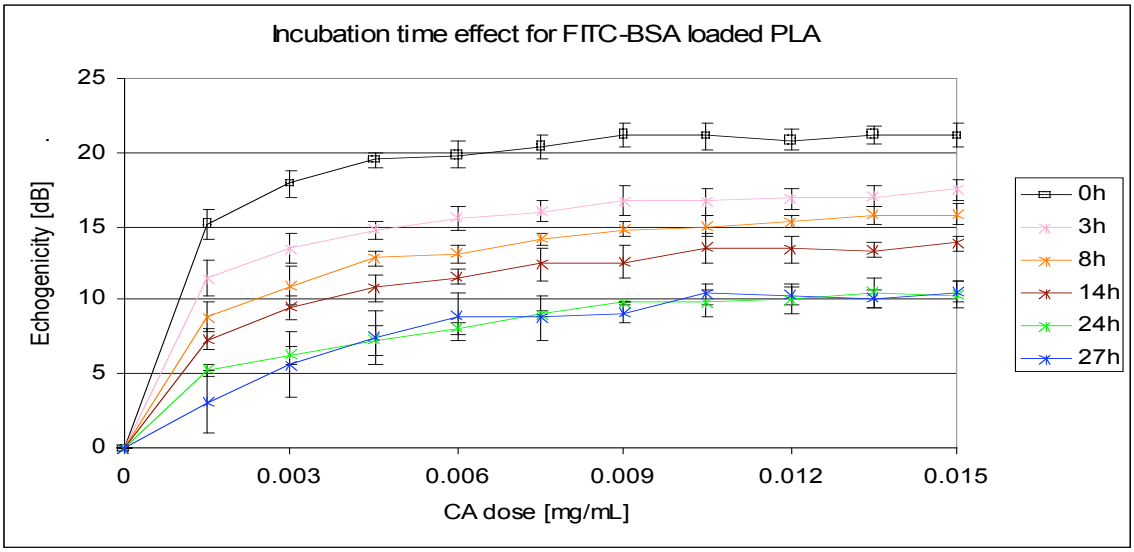

Figure 4-23 Dose response curves of 10% FITC-BSA loaded PLA using dry adsorption method, incubated at 4°C, pH 7.4. Means are significantly different, for $P<0.0001$, by one way ANOVA test (n=5, ± standard error from the mean)

Increasing incubation time periods results in decreasing signal stability as seen in Figure 4-24. All loaded groups were significantly different than control (n=5, $p<0.0001$). For incubation time between 3-14 hours there was no significant difference (n=5, $p>0.05$) in signal

decay. However, signal decay after 24 hours of incubation and after 27 hours were significantly different (n=5, p<0.0001) from one another and from the rest of the groups. Total signal loss (at the end of 15 minutes insonation) for 3-14 hours of incubation was 26.1% (average for all three groups) and 44.8% and 54.9% for 24 hours and 27 hours, respectively. Control signal loss at the end of insonation was 10.4%. Combining echogenicity and stability results, with encapsulation percent results (4.2.1.2.1) all graphs show that beyond 3 hours of incubation there is a significant decrease in both acoustic parameters and no significant increase in drug adsorption. Based on these studies, incubation time for dry adsorbed FITC-BSA should be set to 3 hours. There is a trade off between acoustic properties and drug loading, and both aspects are very important for our drug delivery platform development. In the light of this, 3 hours incubation gave the best trade off for both characteristics.

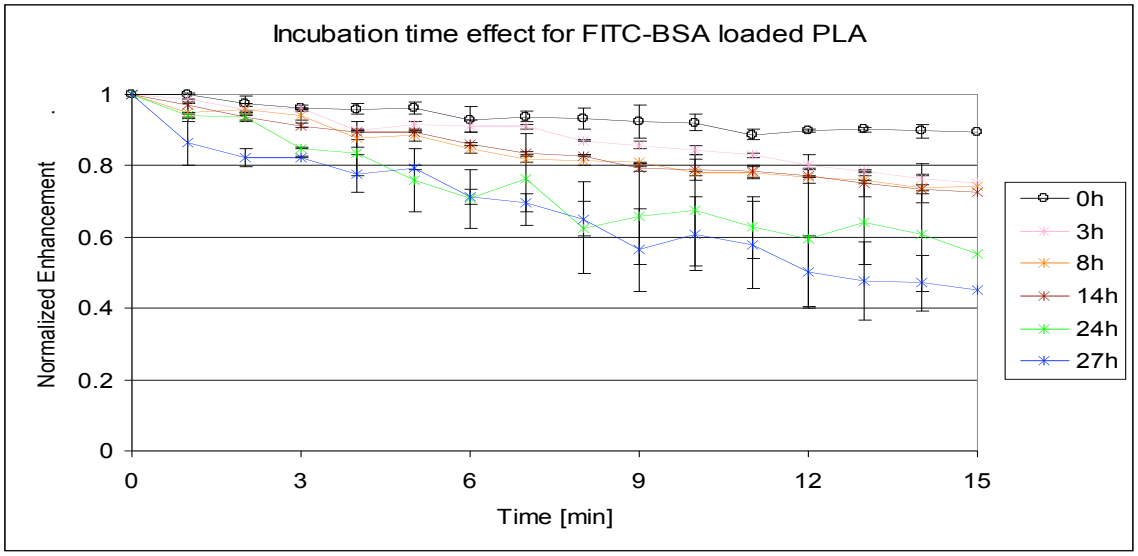

Figure 4-24 Time response curves of 10% FITC-BSA loaded PLA using dry adsorption method, incubated at 4°C, pH 7.4. Means are significantly different, for P<0.0001, by one way ANOVA test (n=5, ± standard error from the mean)

4.2.1.3.1.4 *Drug Concentration effect, pH 4.2*

This study was set to answer whether drug loading concentration has an effect on echogenicity and signal stability, for dry adsorbed FITC-BSA CA. Figure 4-25 shows echogenicity for different loading percents of FITC-BSA, using the dry adsorption method, for 3 hours at pH 4.2 and 4°C. All loaded samples were significantly different ($n=3$, $p<0.0001$) than the control group, but were not significantly different ($n=3$, $p>0.05$) than one another, suggesting that loaded drug percent dose not have an effect on echogenicity of loaded CA, when using dry adsorption. Loaded groups were 10.6±0.6dB (45.2%) less echogenic than control group for the highest CA dose. Suggesting that the acoustically limiting factor is not adsorbed drug amounts on the shell but CA incubation with drug step itself.

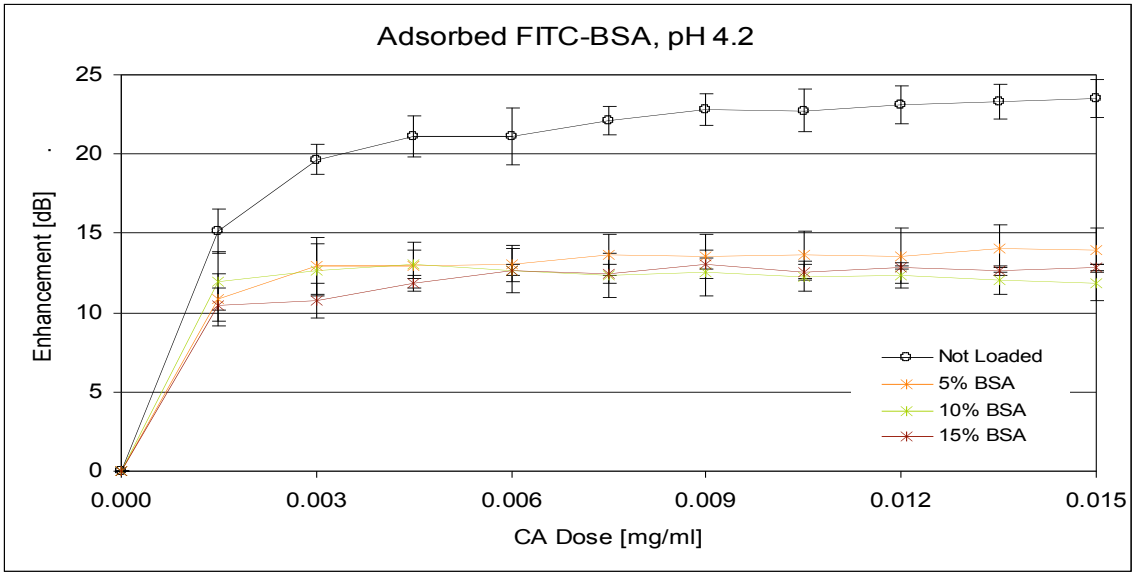

Figure 4-25 Dose response curves of FITC-BSA loaded PLA using dry adsorption method, incubated for 3 hours at 4°C, pH 4.2. Means are significantly different, for $P<0.0001$, by one way ANOVA test ($n=3$, ± standard error from the mean)

Similarly, time response curves, presented in Figure 4-26, show that loaded samples are significantly different than control group but not from one another. Signal decay for loaded groups averaged to 67.1±3.8%, compared to control's signal decay of 8±0.9%. Loaded groups showed similar acoustic properties for both dose and time responses, regardless of drug loading percents, suggesting the acoustically limiting factor is not drug concentration but drug loading incubation process.

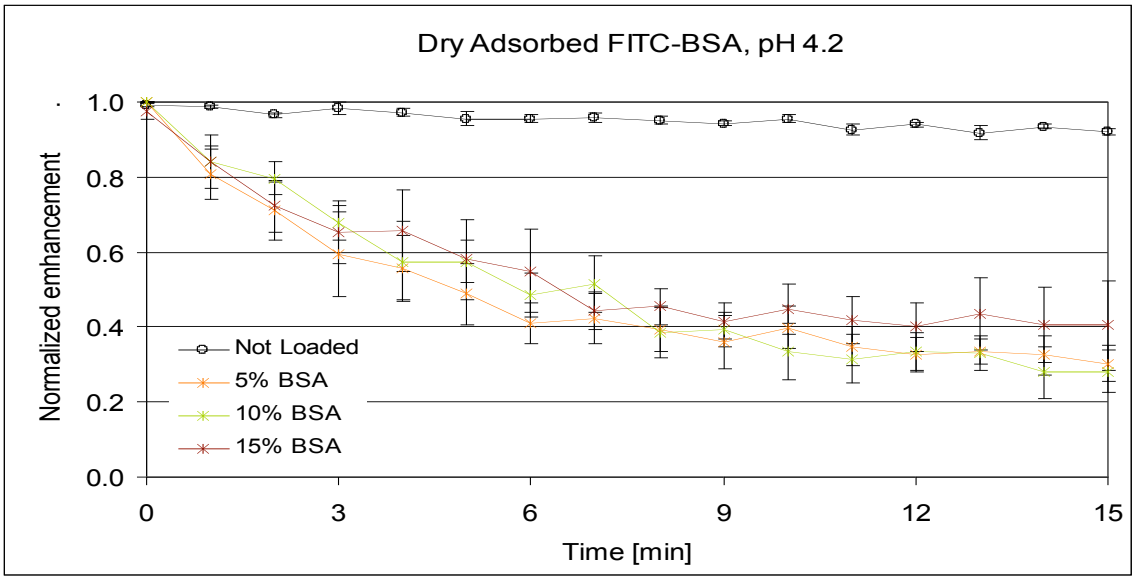

Figure 4-26 Time response curves of FITC-BSA loaded PLA using dry adsorption method, incubated for 3 hours at 4°C, pH 4.2. Means are significantly different, for $P<0.0001$, by one way ANOVA test (n=3, ± standard error from the mean)

4.2.1.3.1.5 *Drug Concentration effect, pH 7.4*

The same drug concentration study was carried out at pH 7.4. Here too, CA were loaded with different concentrations of FITC-BSA. Figure 4-27 shows the echogenicity for different loading percents of FITC-BSA, using the dry adsorption method, for 3 hours at pH 7.4 and 4°C.

As expected due to incubation process itself the echogenicity of loaded CA was significantly ($n=5$, $p<0.0001$) lower than control group. There was no significant difference ($n=5$, $p>0.05$) between the different loading percents, meaning, having different amount of drug adsorbed on the CA surface didn't affect the echogenicity. Loaded groups were 6.6±0.3dB (28.1%) less echogenic than control group for the highest CA dose.

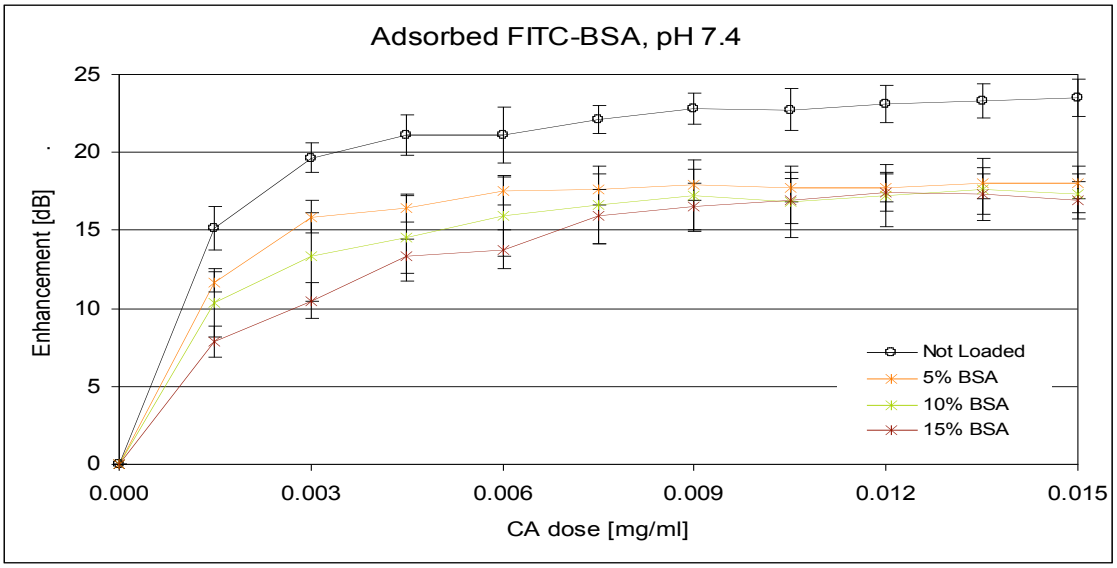

Figure 4-27 Dose response curves of FITC-BSA loaded PLA using dry adsorption method, incubated for 3 hours at 4°C, pH 7.4. Means are significantly different, for $P<0.0001$, by one way ANOVA test ($n=5$, ± standard error from the mean)

Corresponding signal decay curves are shown in Figure 4-28, where loaded groups are significantly different ($n=5$, $p<0.0001$) from the control group, and among the different loading concentrations there are not significant differences ($n=5$, $p>0.05$). Signal loss was 8.0±0.9% for the control group and 20.9±0.3% for the loaded groups, at the end of insonation. These correlate with the dose response results shown in Figure 4-27.

Summarizing this study of different loading percents on echogenicity, at different pH conditions, it can be concluded that at both values of pH the same trend was seen; different drug loading concentrations had no effect on echogenicity nor on signal decay. However, incubation itself was responsible for signal loss at both pH conditions, in comparison to control. Another trend that was observed is the acoustic performance of CA that were incubated in pH 4.2 compared to that of CA loaded at pH 7.4. After incubation at ph 4.2 loaded samples echogenicity was 45.3±2.5% lower than their control, Figure 4-25, whereas after incubation at pH 7.4 the loss was 28.1±1.4% compared to their control, Figure 4-27 (dose response). Comparing signal loss over time for two pH conditions (time response), it is seen that signal loss was 67.1±3.9 and 45.3±2.5% for loading at pH 4.2 and pH 7.4, compared to their control, respectively.

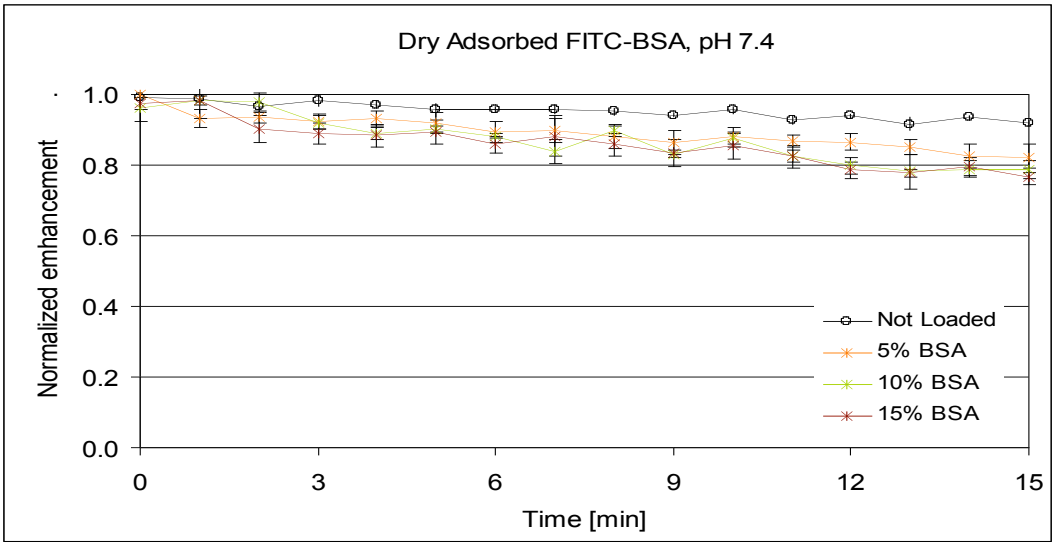

Figure 4-28 Time response curves of FITC-BSA loaded PLA using dry adsorption method, incubated for 3 hours at 4°C, pH 7.4. Means are significantly different, for $P<0.0001$, by one way ANOVA test (n=5, ± standard error from the mean)

As expected, once again, the conclusion is that the amount of drug adsorbed onto the surface of CA is not affecting their acoustic properties; it is the loading process itself, involving incubation time and pH.

4.2.1.3.2 *Incorporation*

This study was done in order to determine whether increasing amounts of loaded drug affect the echogenicity of loaded-CA by incorporation. We hypothesized that in the case of incorporation, unlike adsorption, the drug being an integral part of the shell, would have effect on the CA acoustic properties.

From Figure 4-29 it can be seen that loaded groups are significantly different ($n=5$, $p<0.0001$) than control. Moreover, there are significant differences among the loaded groups themselves, suggesting that different amounts of drug incorporated in the CA shell do have an effect on the echogenicity when using incorporation, as opposed to dry adsorption. As the percent of drug in the shell increases the echogenicity of the loaded CA decreases. The decrease for maximal CA dose is 3.2dB decrease for 5% loading in comparison to control and 4.1dB and 7.2dB decrease for 10% and 15%, respectively. This effect was not seen for other tested loading methods.

As mentioned before, when using the incorporation as loading method drug addition is part of CA fabrication, and the drug results in the shell of the microbubble. This process may alter the shell structure, in such a way that can affect its integrity and stability in aqueous solutions. This fact can be utilized towards ease of drug delivery. Having a more fragile shell that may shatter more easily under the ultrasound, resulting in easier drug dispersion.

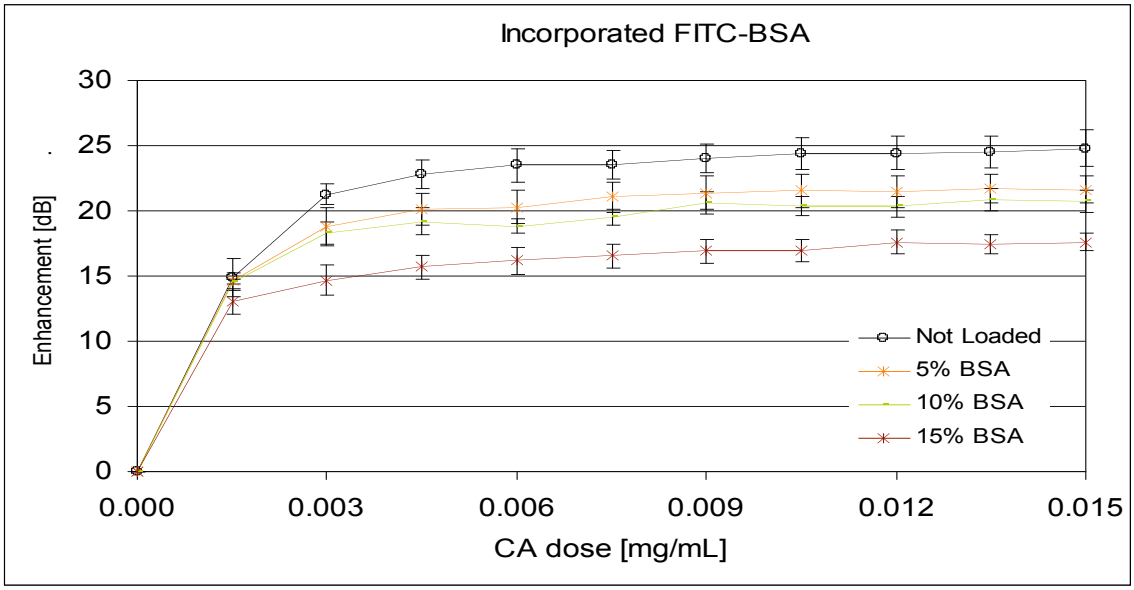

Figure 4-29 Dose response curves of FITC-BSA loaded PLA using incorporation method. Means are significantly different, for $P<0.0001$, by one way ANOVA test (n=5, ± standard error from the mean)

Figure 4-30 shows time response results for incorporated FITC-BSA. Loaded groups, 10% and 15% are significantly different (n=5, $p<0.0001$) than control. Loading of 5% is not different than control, suggesting that 5% drug is not high enough to interfere with shell structure in such a way that would significantly decrease signal stability. There are significant differences among the loaded groups themselves. The signal loss at the end of 15 minutes insonation was 11.0±0.6%, 17.7±2.0% and 21.4±1.8%, for loading percents of 5%, 10% and 15%, respectively. The signal loss for control was 10.2±0.8%. These results agree with the trend showed for dose response (Figure 4-29) and are due to the same effect of shell alterations introduced by incorporation of drug.

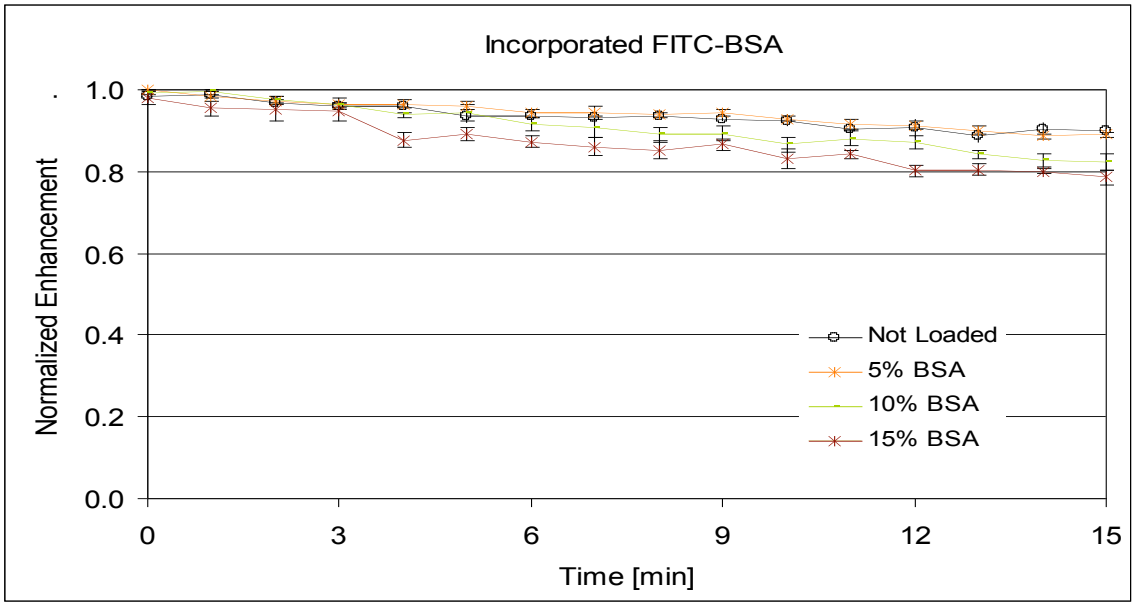

Figure 4-30 Time response curves of FITC-BSA loaded PLA using incorporation method. Means are significantly different, for $P<0.0001$, by one way ANOVA test (n=5, ± standard error from the mean)

4.2.1.4 *FITC-BSA Loading Summary*

In this section, we studied the properties of FITC-BSA loaded PLA microbubbles, i.e., drug loading weight percentage and echogenicity. In the case of loading through incorporation, since this method is an integral part of the microbubbles fabrication process, the only controllable parameter affecting the outcome, is FITC-BSA concentration. On the other hand, dry absorption is a post-fabrication method where several controllable parameters, namely, pH, temperature, and incubation time, affect the loaded microbubbles properties.

Table 4-2 summarizes loading percents (encapsulation) for dry adsorbed and for incorporated FITC-BSA. Dry adsorption is shown for both pH = 4.2 and pH=7.4, for 3h incubation time and a temperature of 4°C, which were shown to yield the highest loading percentage while best preserving echogenicity. For any given initial FITC-BSA concentration,

dry absorption in an environment with a pH = 4.2, yields the highest encapsulation. On the other hand, this setup yields the lowest echogenicity, Table 4-3. Loading a at pH 7.4 maintains good echogenicity, hence, despite the fact they present low encapsulation, those loaded CA can still be good candidates for drug carrying, when using drugs effective at low doses, where 1-2% loading is enough for substantial therapeutic effects.

Table 4-3 also shows that the highest echogenicity is obtained for the incorporation loading method for 10% initial FITC-BSA while still yielding an acceptable level of encapsulation, Table 4-2. Therefore it follows that incorporation is the method of choice for FITC-BSA loading onto PLA microbubbles.

Table 4-2 Loading percent summary for FITC-BSA loaded PLA [%]

Initial FITC-BSA concentration	Dry adsorption (3h, 4°C)		Incorporation
	pH 4.2	pH 7.4	
5%	3.277±0.138	0.011±0.0003	3.113±0.114
10%	6.327±0.638	0.031±0.002	4.288±0.509
15%	9.274±1.269	0.240±0.018	4.173±1.170
20%	10.094±0.778	0.507±0.102	4.380±0.408
30%	9.924±1.196	2.230±0.150	4.438±0.329

Table 4-3 Echogenicity summary for FTIC-BSA loading

	Cold Adsorption (3h, 4°C, 10%)		Incorporation (10%)
	pH 4.2	pH 7.4	
Enhancement [dB]	13.64±1.01	19.04±1.42	20.87±0.87
Enhancement [% of control]	53.43±2.55	74.63±1.40	83.47±4.95
Signal Stability after 15 min [%]	44.11±5.64	76.67±5.46	82.25±2.01

4.2.2 *Sudan Black B (SB)*

4.2.2.1 *Loading Methodology*

Sudan Black B (SB) ($C_{29}H_{24}N_6$, MW 456.55 g/mole) is a lipophilic neutral ink, which is mainly used for staining of fats, and it can also serves as a drug model for hydrophobic drugs, see 2.6.3.2. Due to its hydrophobic nature, SB is most suitable to be encapsulated by incorporation, where it is added to the organic phase. For this reason, we chose SB to model the incorporation of hydrophobic drug onto PLA microbubbles. Below is the chemical structure of SB:

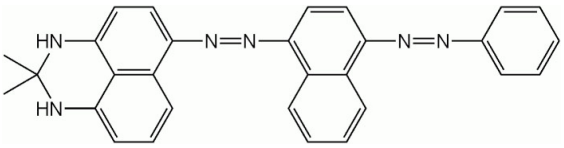

Figure 4-31 Chemical structure of sudan black B.

4.2.2.1.1 *Incorporation*

Different quantities of SB were added to the primary polymer solution to study the concentration effect on loading capacity and acoustic performance. Figure 4-32 shows a scanning electron microscope picture of SB-loaded PLA, which presents smooth surface morphology, i.e., similar to that of plain (non-loaded) CA, Figure 4.1.

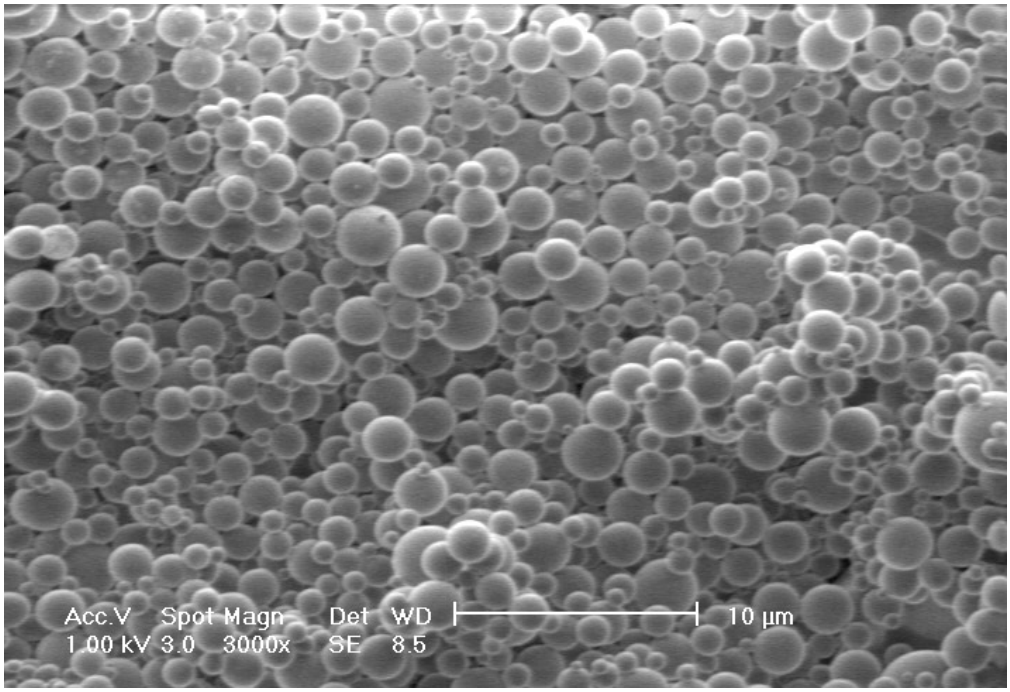

Figure 4-32 Scanning electron micrograph (3000X, size bar 10 µm) showing morphology of PLA microbubbles loaded with 2% SB, through Incorporation. Morphology is similar to non-loaded CA. Size 1.370µm±0.580.

Figure 4-33 shows the effect of SB concentration on actual loading. There is a significant difference ($n=3$, $p<0.05$) between encapsulation percents among all groups. Moreover, encapsulation efficiencies were found to be, 96.3±21.1%, 98.9±6.2%, 96.3±13.9% and 103.5±3.3%, corresponding to 1%, 2%, 4% and 8% initial loading, respectively. It follows, from these results, that SB fits well in the CA shell and any drug concentration that was tested here yields at least 93% encapsulation.

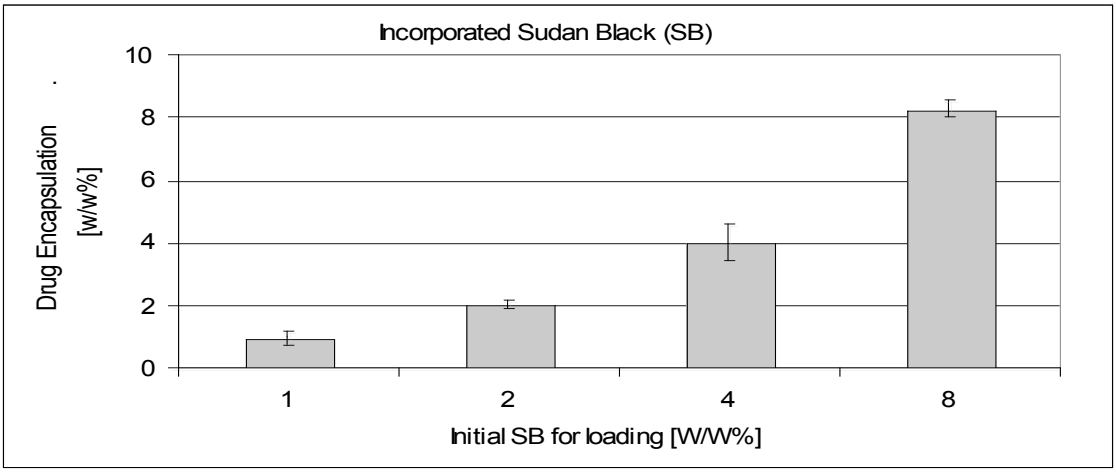

Figure 4-33 Encapsulation percent for SB-loaded PLA, as a function of initial SB concentration, via incorporation method. Means are significantly different, for $P<0.05$, by one way ANOVA test (n=3, ± standard error from the mean)

In order to investigate the hypothesis that SB, as a hydrophobic compound is preferentially encapsulated by incorporation in the organic phase, two encapsulation methods were carried out using two other loading methods, i.e., wet adsorption and dry adsorption. For these tests, we used an initial SB concentration of 4%. Dry adsorption conditions were 4°C in PBS for 1 hour. The encapsulation results are shown in Figure 4-34. The corresponding encapsulation efficiencies are 96.3±13.9%, 40.7±4.9% and 29.3±6.3% for incorporated SB, dry adsorbed SB and wet adsorbed SB, respectively. Based on these results, incorporation was found to be the most suitable method for loading a hydrophobic drug/drug model such as SB.

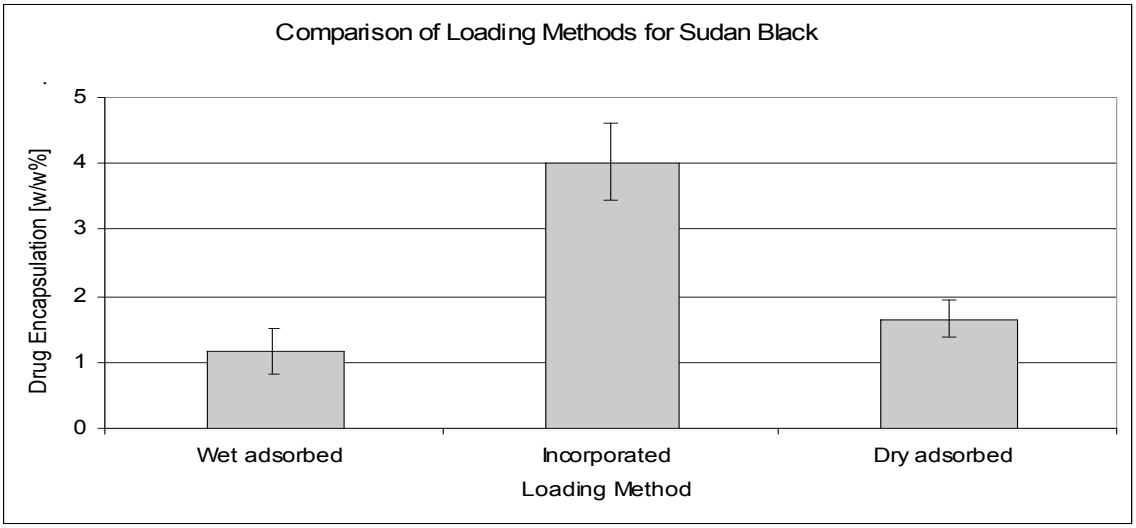

Figure 4-34 Encapsulation percents for SB-loaded PLA, for 4% SB, comparing wet adsorption dry adsorption and incorporation loading methods. loading methods. Loading via incorporation results in the highest SB encapsulation. Means are significantly different, for $P<0.0001$, by one way ANOVA test (n=3, ± standard error from the mean)

4.2.2.2 *Acoustic Studies*

In this section, we study the effects of incorporating increasing amounts of SB on the echogenicity of SB-incorporated PLA. Figure 4-35 shows the dose response obtained for SB-incorporated CA at 0% (control), 2%, 4% and 8%. It can be seen that loaded groups are significantly different than the control (plain CA), all presenting lower echogenicity (n=5, $p<0.0001$). This departure from the control's echogenicity is, once again, attributed to the changes introduced by the drug incorporation step into the CA fabrication process. Furthermore, it can also be learnt that echogenicity is a direct function of SB encapsulation percentage. Notice that this trend is similar to that obtained for incorporated FITC-BSA (which is a hydrophilic model, and for whom dry absorption is the preferred loading method). At the highest CA dose, echogenicity for an SB encapsulation of 2% is 17.4±0.3dB and for 4% and 8% SB-loaded CA, echogenicity increases is 21.9±0.7dB and 22.5±1.1dB, respectively.

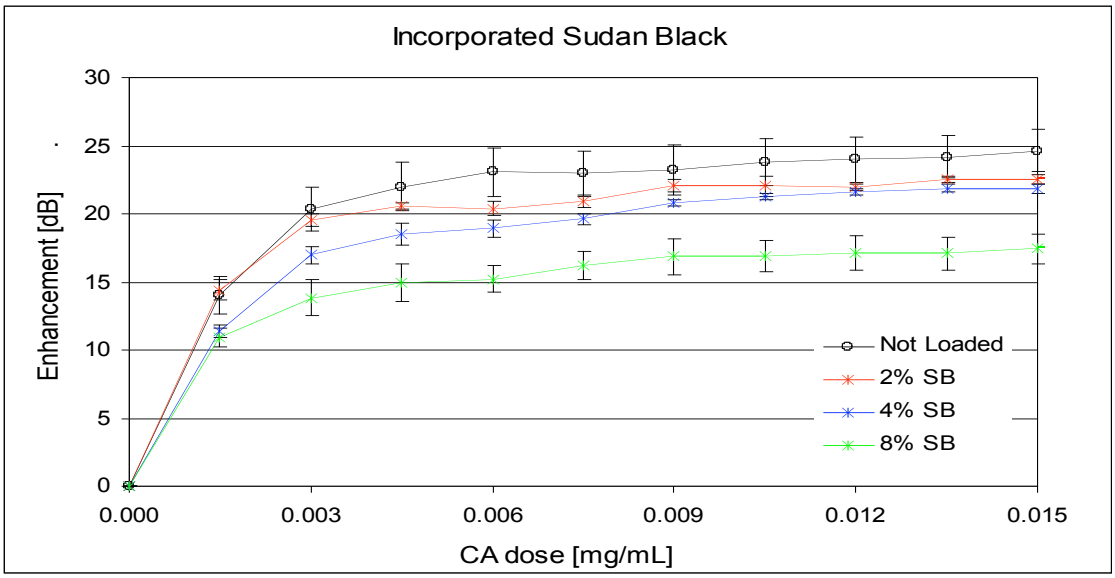

Figure 4-35 Dose response curves of SB loaded PLA using incorporation method. Means are significantly different, for P<0.0001, by one way ANOVA test (n=5, ± standard error from the mean)

Figure 4-36 shows time response results for incorporated SB. Loaded groups, 4% and 8% are significantly different than control. Loading of 2% statistically similar to control, suggesting that 2% loading drug is not high enough to interfere with shell structure in such a way that would significantly decrease signal stability. There are significant differences (n=5, p<0.0001) among the loaded groups themselves. The signal loss at the end of 15 minutes insonation was 5.6±0.7%, 9.0±2.8% and 11.6±3.7%, for loading percents of 2%, 4% and 8%, respectively. The signal loss for control was 7.1±0.7%. These results support the explanation that introduction of a foreign substance (i.e., drug) in the shell structure makes the shell less stable under insonation in aqueous solutions, compared to not loaded shells. However, SB-loaded CA are still

remarkably echogenic, maintaining more than 90% of their enhancement even at the end of 15 minutes of insonation.

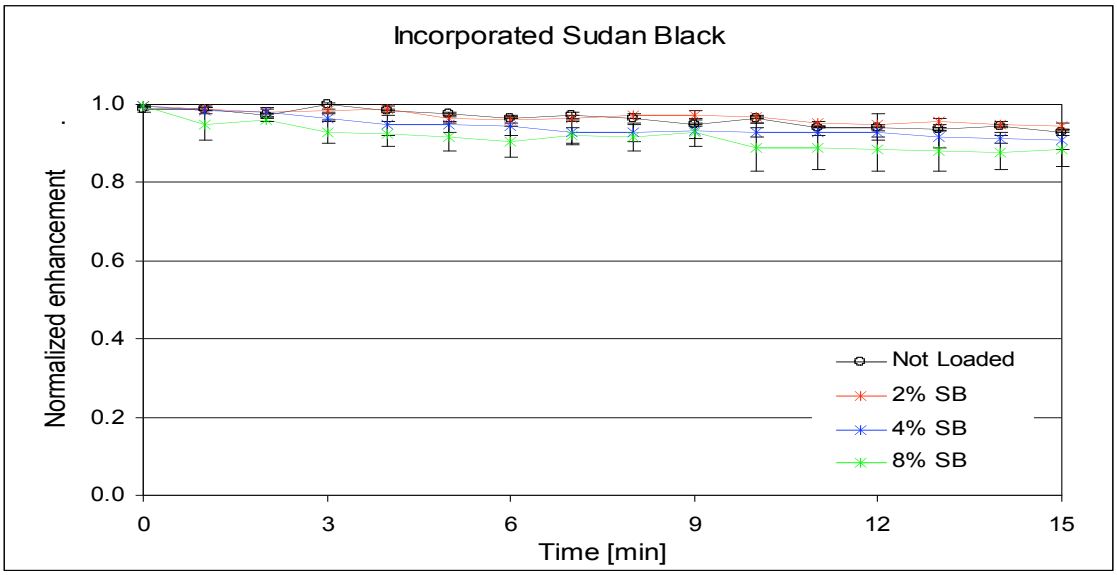

Figure 4-36 Time response curves of SB-loaded PLA using incorporation method. Means are significantly different, for $P<0.0001$, by one way ANOVA test (n=5, ± standard error from the mean)

4.2.2.3 *SB Loaded CA as a Model for Paclitaxel*

SB can serve as a model for a hydrophobic anti cancer drug, such as paclitaxel. In order to evaluate the delivery capability of SB-loaded CA, a comparison with clinical use Paclitaxel is presented below. Paclitaxel is a mitotic-inhibitor anticancer drug, which interferes with normal microtubule breakdown during cell division. It is available in oil or in conjugation with albumin. The FDA approved Abraxane®(protein-bound paclitaxel), developed and manufactured by Abraxis BioScience, for the treatment of breast cancer. Protein conjugated paclitaxel presents less harmful side effects than the oil dissolved version, Taxol, which introduces toxic solvents

into the body (Klaassen et al., 1996; Watanabe et al., 2003; Poole et al., 2006). It is injected intravenously. Its maximal tolerable dose depends on the administration regime, bolus, continues infusion, co-administered drugs and the type of cancer. For comparison with our platform a maximal tolerable dose of 40-80 mg/m^2 that was given to treat breast cancer will be discussed (Kim et al., 2003).

Since no release experiments were done using SB-loaded CA, SB release was calculated for a range of release percent, in order to compare our platform to conventional intravenous SB delivery.

Given the following data it is possible to compare clinical conventional SB drug delivery to SB-loaded CA delivery, as see in Table 4-4:

- Maximal tolerable dose of SB is 40-80mg/m^2 (for calculation 60mg/m^2 was used)
- Body surface area 1.72 m^2 (female, 64 kg, 1.65 m)
- Body fluids 3500mL+ 10,500mL (plasma + interstitial fluid)
- CA injected at: 0.35 mL/kg, 0.04 g/mL, 65 kg body weight (eq. 3-2)

Table 4-4 SB amount [mg] delivered to tumor compared to conventional Paclitaxel administration

Assumed release [%]	SB-loaded CA	Paclitaxel
10	1.78	0.15
30	5.34	
50	8.90	

Table 4-5 Non delivered drug amount [mg] comparing SB remaining on CA to systemic distributed paclitaxel

Assumed release [%]	SB-loaded CA	Paclitaxel
10	16.02	103.05
30	12.46	
50	8.90	

These calculations are based on the following assumptions:

- Tumor fluid volume 20mL (vasculature + interstitial fluid)
- CA loading 2% by incorporation
- CA targeting of 100%

We hypothesized that more and more circulating loaded CA are going to pass through the acoustic window (defined by the placement of US transducer on top of the tumor) with each full blood cycle. This would allow more local release of SB with each cycle. Data presented at Table 4-4 were calculated based on 100% targeting, showing that using our drug-loaded CA delivery system, is capable of carrying enough drug to the target, and even for a hypothetical low release percent (such as 10%) our platform can deliver 11 times more drug than the conventional systemic paclitaxel administration.

The remaining (non-delivered) SB can be calculated as well, Table 4-5 shows that when using the intravenous paclitaxel administration most of the injected drug is circulating and is available for cellular uptake which resents toxic side effects; whereas, using the CA-loaded platform, less drug is carried and hence even for low release percent such as 10%, the remaining SB amount is still, at least, 6 times smaller than in conventional administration. This means that there is less potential for excess of drug toxicity when using drug loaded CA than

conventionally infusing free drug. Minimizing harmful side effects due to drug toxicity is one of the main advantages of developing the current drug delivery platform.

4.2.2.4 *SB Loading Summary*

In this section, we studied the properties of SB loaded PLA microbubbles, i.e., drug loading weight percentage and echogenicity. Incorporation, was pre-selected to be the best method for encapsulating a hydrophobic drug such as SB. A small-scale comparison, Figure 4-34, supported this choice, showing the highest encapsulation percent and highest EE of SB by incorporation compared to dry and wet adsorption. Since incorporation is an integral part of the microbubbles fabrication process, the only controllable parameter, affecting the outcome, is SB concentration. Table 4-6 summarizes the initial loading percent effect on actual encapsulation, where for 4% initial SB concentration, the loading was found to be the most efficient, 61.72±2.90%. Table 4-7 shows that the highest echogenicity is obtained for the 4% and 8% SB concentrations while signal stability is best for 2% SB. Combination of all these parameters, i.e., encapsulation percent, EE, echogenicity and signal stability, points out that 4% SB is the concentration choice for SB loading onto PLA microbubbles using incorporation.

Comparing our drug loaded CA to systemic administration of paclitaxel, a hydrophobic anticancer drug in clinical use, reveals that our drug delivery system has the potential to release more drug in the target site, while presenting smaller drug loss in the body.

Table 4-6 Encapsulation percent and encapsulation efficiency summary for SB loaded PLA [%]

Initial SB concentration for loading	Encapsulation [w/w%]	EE [%]
1%	0.97±0.22	96.32±21.13
2%	2.16±0.10	98.90±6.22
4%	4.02±0.60	96.31±13.91
8%	8.63±0.28	103.48±3.28

Table 4-7 Echogenicity summary for incorporated SB

	Enhancement [dB]	Enhancement [% of control]	Signal Stability after 15 min [%]
2%	17.42±0.31	70.73±1.27	94.42±0.71
4%	21.87±0.71	88.83±1.45	91.00±2.35
8%	22.51±1.14	91.40±4.63	88.40±4.26

4.2.3 *Five-Fluorouracil (5FU)*

Five-fluorouracil is a pyrimidine analogue, ($C_4H_4FN_3O_2$, MW 139.09 g/mole), Figure 4-37, which acts as antimetabolite and immunosuppressive agent, leading cells to apoptosis. It is used as an anti-cancer drug for treating tumors of several organs such as, breast, colon, stomach, pancreas, ovary and lung (Parikh et al., 2003). It is water soluble and has a rapid plasma clearance, leading to a short half life of 10-20 minutes. Encapsulation of this drug into microbubbles can prolong its presence in the circulation and facilitate effective administration in the tumor site.

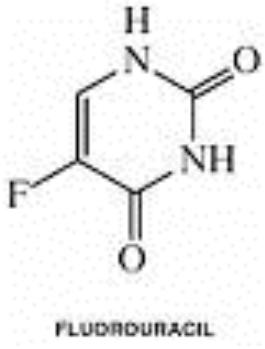

Figure 4-37: Chemical structure of Fluorouracil (5FU), a pyrimidine analogue.

4.2.3.1 *Loading Methodology*

Three different loading methods were tested for 5FU loading onto PLA microbubbles. Dry adsorption and incorporation were previously introduced in this work for FITC-BSA and SB loading. Wet surface adsorption is described in detail in 3.2.6.2.2, in general it is similar to dry adsorption only with respect to the drug final destination, the microbubble surface. Other than that wet adsorption takes place as part of microbubbles fabrication method, at the final stages of hardening, as will be discussed below, 4.2.3.1.2. Figure 4-38 shows the morphology of plain PLA microbubbles (a), and 5FU-loaded PLA, dry adsorbed (b), wet adsorbed (c), and incorporated. It can be concluded that 5FU loading did not affect the microbubbles morphology when using any of the above mentioned loading methods. And loaded microbubbles maintain a smooth surface. The mean size of incorporated CA is similar to the non loaded CA, where the mean size of adsorbed CA is similar for wet and dry adsorption and both show bigger particles mean size. In the case of dry adsorption CA were incubated with the drug, in this process water enter the shell and the microbubbles may swell, and did not shrink back after re-lyophilization (Gopferich, 1996).

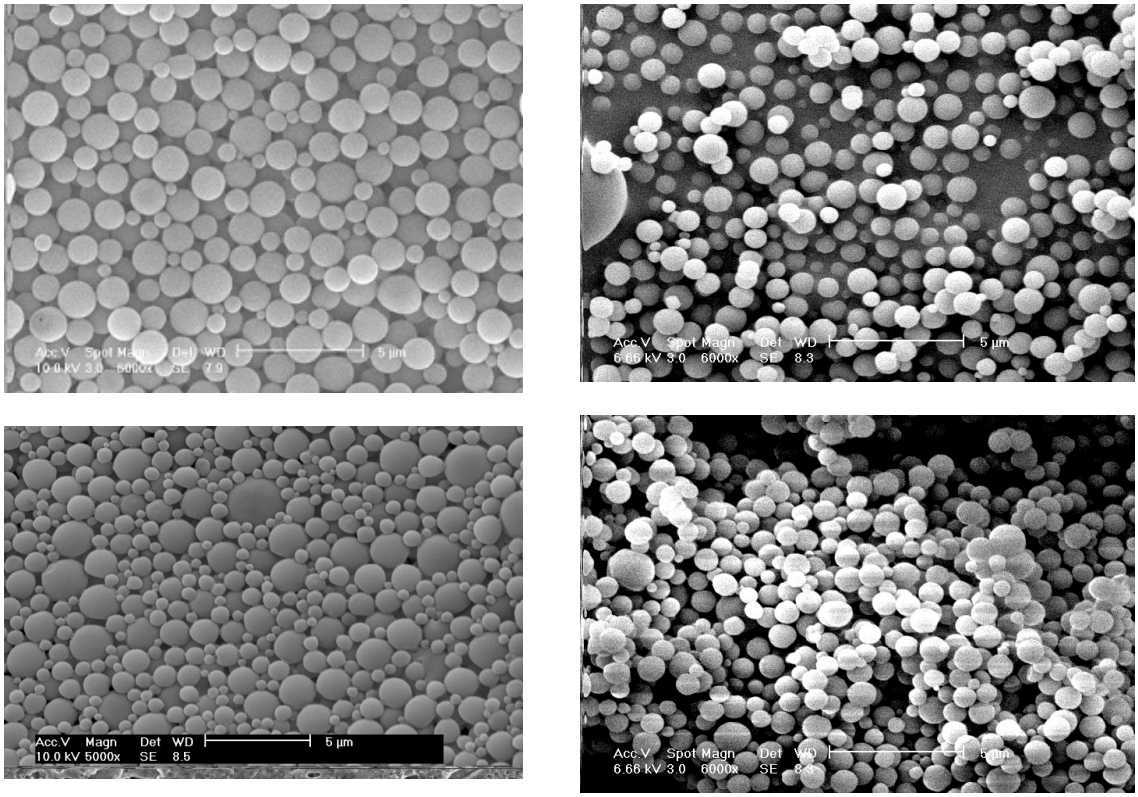

Figure 4-38 Scanning electron micrograph showing the surface morphology of PLA loaded with 5FU using three methods (magnification at 6,000X, size bar 5 µm): A) Plain PLA 1.130±0.190µm, top left, B) Wet adsorbed 5FU 1.479±0.795µm, top right, C) Dry adsorbed 5FU 1.494±0.131µm, bottom left, D) Shell incorporated 5FU 1.119±0.128µm, bottom right.

4.2.3.1.1 *Dry Surface Adsorption*

As a hydrophilic drug, 5FU was dissolved in PBS and incubated with dry microbubbles. Based on previous results with FITC-BSA, dry adsorption conditions were chosen to be at 4C, for 3 hours. Figure 4-39 shows the loading percents for different initial concentrations of 5FU. It can be seen that for an increasing initial concentration of 5FU, there is more drug loading, suggesting the process is not reaching its saturation and there is more surface area available for adsorption. EE supports this trend since values start at 64.85±3.1% for 0.10% initial 5FU and get gradually smaller to 19.94±0.3% for 3% initial 5FU, while the efficiency for 4% 5FU is 25.25±2.7%. Based on these findings it is possible to load more 5FU, providing more drug at the beginning of adsorption process.

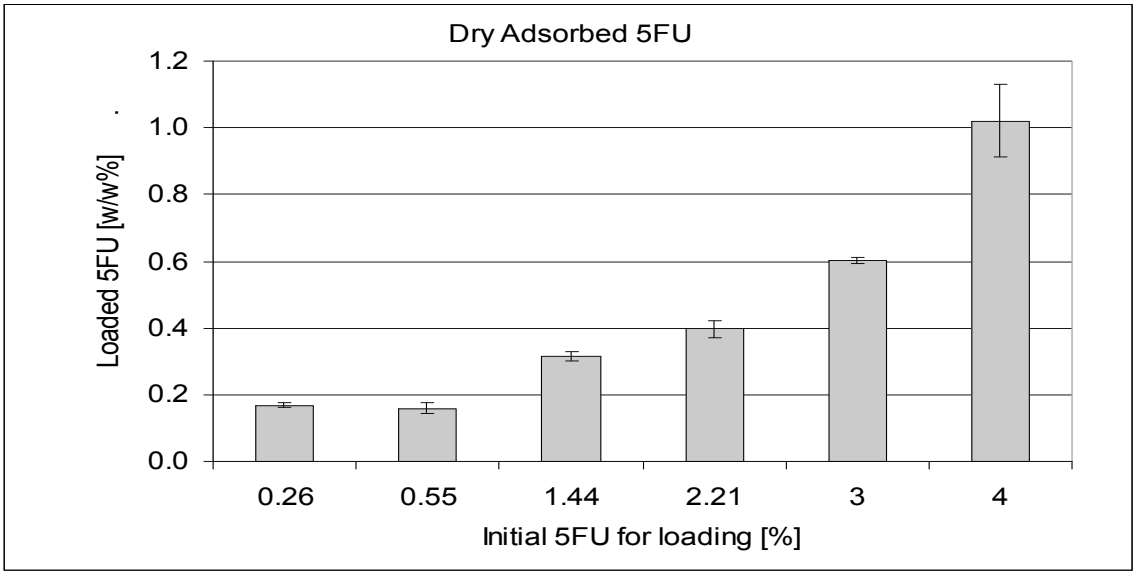

Figure 4-39 Loading percent for 5FU-loaded PLA using dry adsorption method. Loading in PBS buffer, pH 7.4, loading time is 3 hours, samples were gently agitated at 4°C. Means are significantly different, for $P<0.0001$, by one way ANOVA test (n=3, ± standard error from the mean)

4.2.3.1.2 *Wet Surface Adsorption*

Wet adsorption, in contrast to dry adsorption, takes part at the end of microbubbles fabrication. The dry drug is added to the, still wet, microbubbles at the hardening phase. This may have the advantage of allowing greater drug loading, since the drug is expected to adsorb onto the wet thin PVA layer surrounding the microbubbles. Looking at Figure 4-40, it is seen that for increasing initial 5FU concentrations there is an increasing loading.

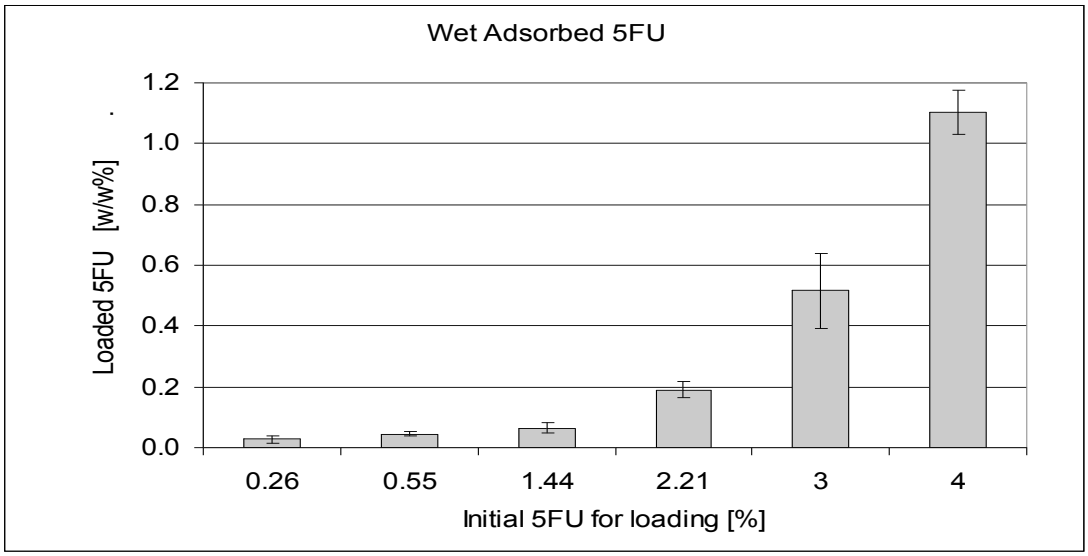

Figure 4-40 Loading percent for 5FU-loaded PLA using wet adsorption method. Means are significantly different, for $P<0.0001$, by one way ANOVA test ($n=3$, ± standard error from the mean)

However, when comparing these results to dry adsorption, Figure 4-41, there were significant differences for loading percents for the smaller concentrations of initial 5FU, i.e., 0.26%-1.44% ($n=3$, $p<0.0001$), but for the higher initial 5FU concentrations both methods yield similar loadings. The encapsulation efficiencies of dry adsorption were 1.8 times higher (in average) than wet adsorption for 0.26%-3% initial 5FU concentrations, in favor of dry adsorption. For 4% 5FU there was no significant difference ($n=3$, $p>0.05$) in encapsulation efficiencies of wet and dry adsorption. This contradicts our hypothesis that 5FU adsorption would be greater when loading at the wet phase than at dry. One of the main differences between wet adsorption and dry adsorption is the incubating solution. In the case of dry adsorption the incubation solution is PBS, pH 7.4, whereas, wet adsorption is done as part of microbubbles hardening process so the solution is a mix of DI water and hexane (non-polar solvent). As a polar material, 5FU, is more soluble in PBS than in hexane, making it more

available for adsorption. Hexane is a non polar solvent in nature, and 5FU may be aggregated in its present compromising its availability to adsorption (Sherertz et al., 1987).

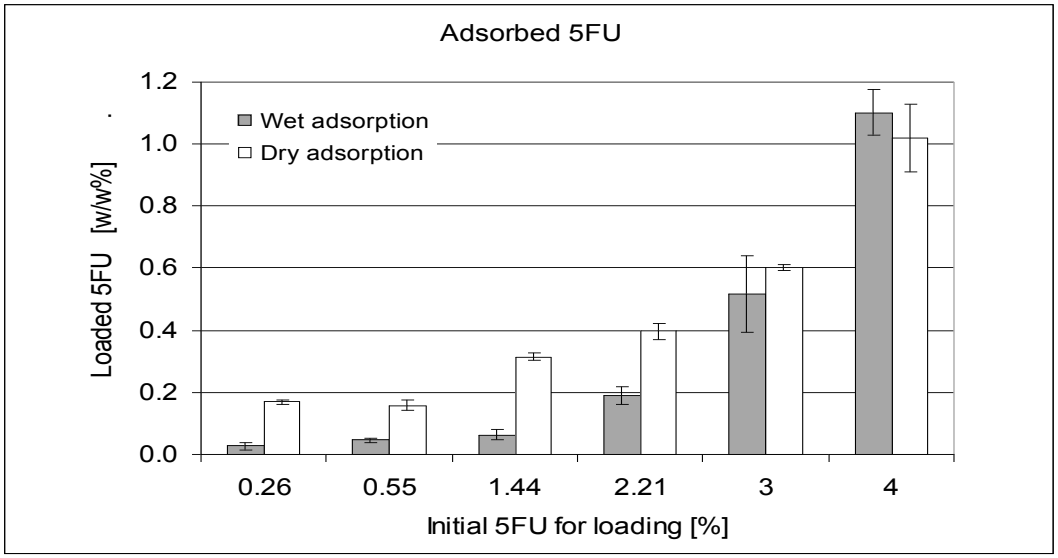

Figure 4-41 Loading percent comparing 5FU-loaded PLA using wet adsorption and dry adsorption. Means are significantly different, for $P<0.0001$, by two way ANOVA test (n=3, ± standard error from the mean)

4.2.3.1.3 *Incorporation*

Five-FU is a hydrophilic drug and was incorporated to PLA microbubbles through addition to the aqueous phase, similar to FITC-BSA. Results are presented in Figure 4-42, showing the initial concentration effect of 5FU on encapsulation. From Figure 4-42 it can be seen that there is no clear trend of initial concentration affecting 5FU encapsulation. Loading percents for all initial 5FU concentration were poor. This is supported by EE values of 10.9±1.1% for 0.26% initial 5FU that are decreased to 1.0±0.2% for 1.44% initial 5FU and it further decreased to less than 1% efficiency for 4% initial 5FU. In summary, these results show that incorporation is not a favorable method for loading 5FU onto PLA microbubbles. When adding a hydrophilic drug

to the inner aqueous phase of a double emulsion, there is a higher drug concentration gradient in that phase; this drives a more rapid diffusion of drug to the outer aqueous phase resulting in loss of drug (Wong et al., 2001).

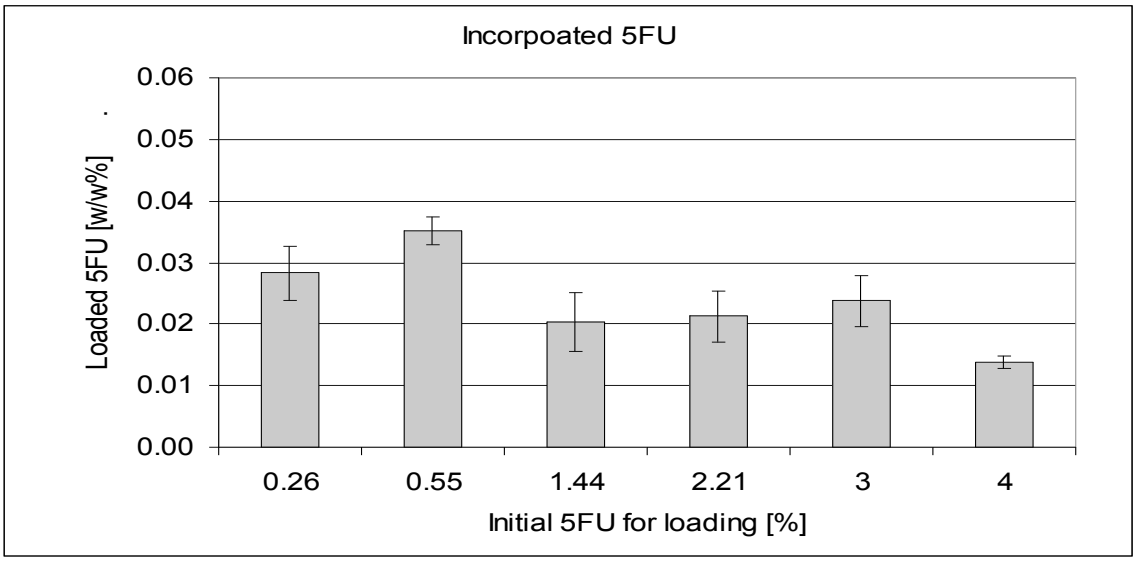

Figure 4-42 Encapsulation percent for 5FU-loaded PLA using incorporation method. Means are significantly different, for $P<0.01$, by one way ANOVA test (n=3, ± standard error from the mean).

4.2.3.2 *Acoustic Studies*

4.2.3.2.1 *Dry Adsorption*

Dry adsorbed 5FU dose response curves are shown in Figure 4-43. It can be seen that loaded groups are significantly different than control (n=3, $p<0.0001$), however, there are statistical similarities (n=3, $p>0.05$) among the loaded groups. This suggests that 5FU concentration dose not have an effect on the echogenicity of loaded PLA microbubbles.

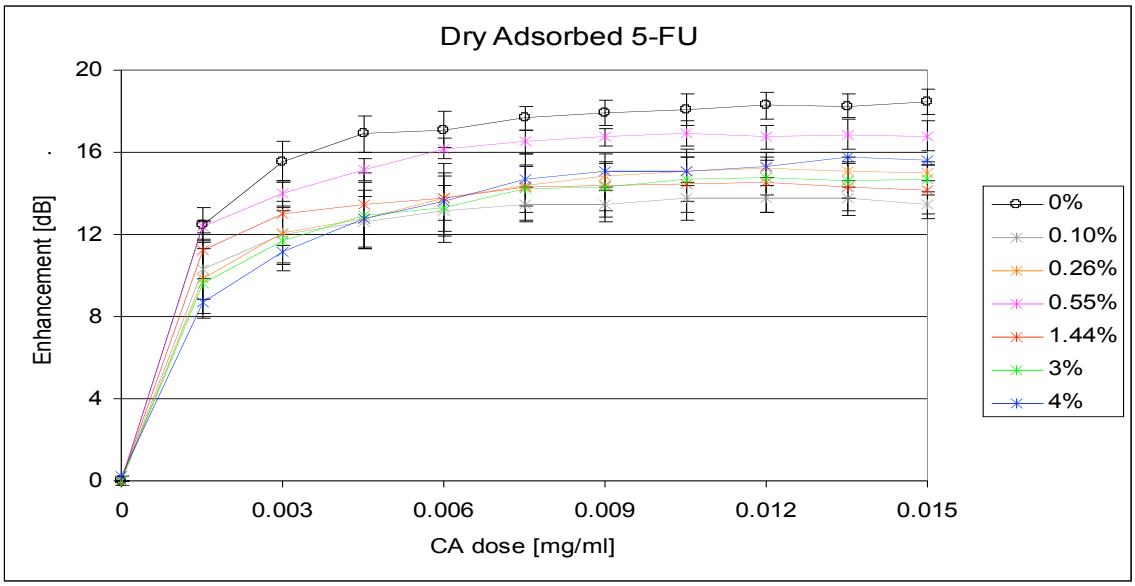

Figure 4-43 Dose response curves of 5FU-loaded PLA using dry adsorption method. Means are significantly different, for $P<0.0001$, by one way ANOVA test (n=3, ± standard error from the mean)

Time response curves, Figure 4-44, follow the same trend. Loaded samples are significantly different than control (n=3, $p<0.0001$), and there are statistical similarities (n=3, $p>0.05$) among the loaded groups. Signal decay for control was 9.5±1.0% and for loaded samples, in average, 34.1±2.5%.

This suggests, again, that in dry adsorption the incubation with drug is the meaningful step in lowering loaded CA echogenicity, but echogenicity is not affected by loading percent for itself. The same conclusion was found for BSA, where incubation conditions were having a significant effect on acoustic properties, whereas drug concentration did not.

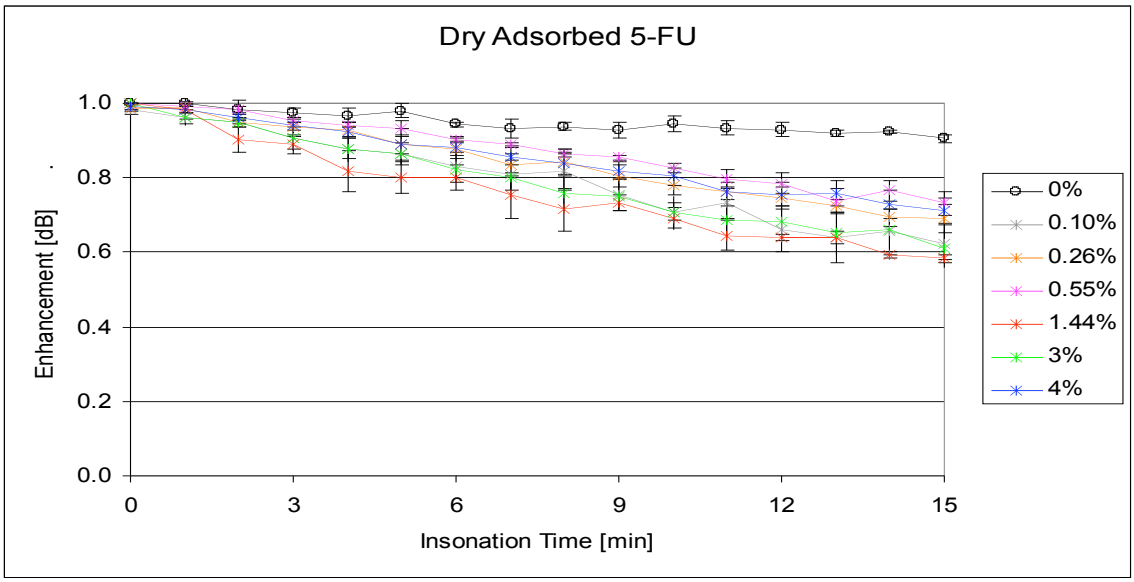

Figure 4-44 Time response curves of 5FU-loaded PLA using dry adsorption method. Means are significantly different, for P<0.0001, by one way ANOVA test (n=3, ± standard error from the mean)

4.2.3.2.2 *Wet Adsorption*

Dose response curves for wet adsorbed 5FU are presented in Figure 4-45, showing loaded samples are not significantly different than control (n=3, p>0.05), suggesting that, since wet adsorption is a process done at the very end of fabrication it dose not interfere with microbubbles integrity nor shell structure. Similarly, different loading percents did not have a significant clear trend, suggesting that different amounts of drug present on CA surface do not affect CA's echogenicity.

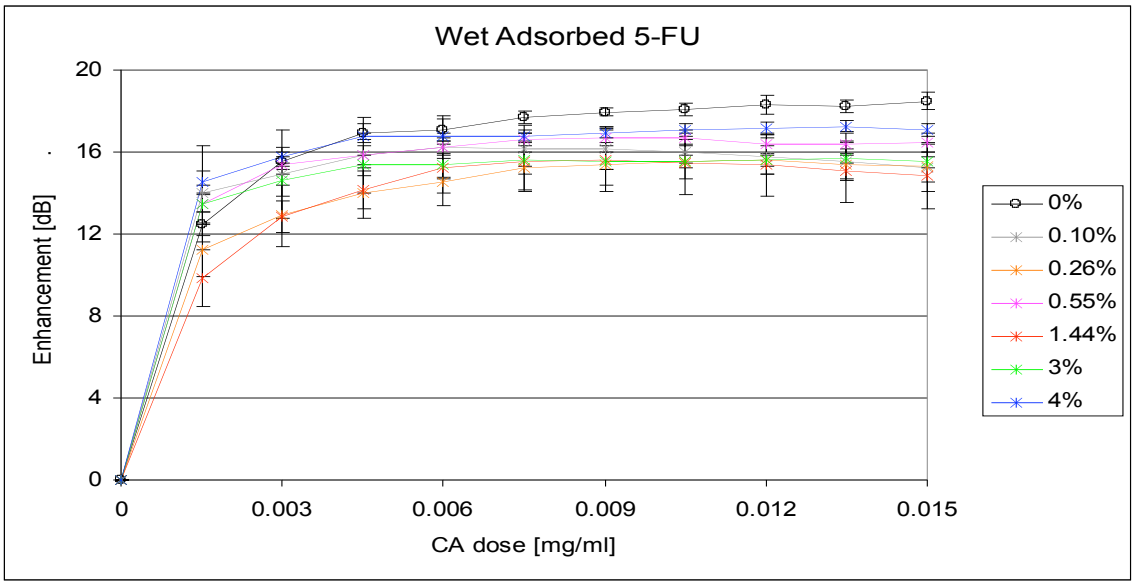

Figure 4-45 Dose response curves of 5FU-loaded PLA using wet adsorption method. Means are significantly different, for $P<0.0001$, by one way ANOVA test (n=3, ± standard error from the mean)

The corresponding time response curves are presented in Figure 4-46 showing the same trends of drug percent and drug loading on signal decay over time. Signal decay for control was 11.0±0.8% and for loaded samples, in average, 9.9±3.4%, having no significant difference (n=3, $p>0.05$). Time response results also suggest that there is no effect of signal decrease for loaded samples in comparison to control and that drug percent on the shell dose not contribute to signal decay.

For both adsorption methods, dry and wet, 5FU loading concentration did not have an effect on echogenicity nor on stability. However, the loading process itself lowered the echogenicity and signal stability of dry adsorbed 5FU CA more than wet adsorbed CA; dry adsorption of 5fU CA lowered echogenicity by 3.9±1.2 dB whereas wet adsorption lowered it by 2.8±0.9 dB. Wet adsorbed 5FU-CA maintained 90.1±1.5% of signal over 15 minutes of insonation whereas dry

adsorbed 5FU-CA maintained only 65.9±2.5% of signal. A full comparison is presented at Table 4-11. These trends can be related to the difference between the two loading procedures, dry adsorption having an extra post-fabrication incubation step that was shown here to allow the initiation of hydrolysis of CA and reduce their acoustic properties.

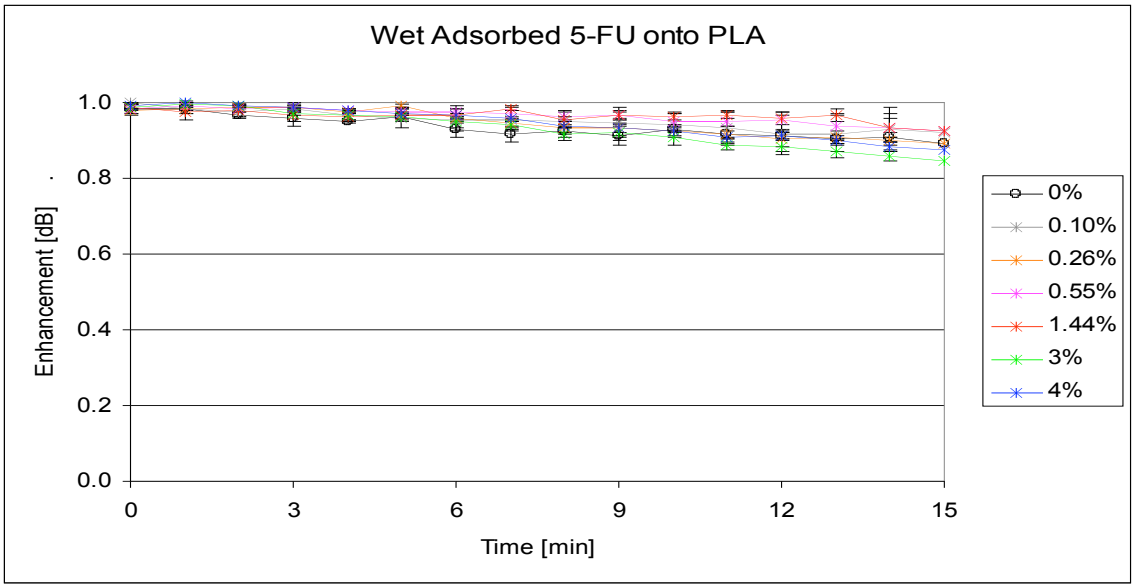

Figure 4-46 Time response curves of 5FU-loaded PLA using wet adsorption method. Means are significantly different, for P<0.0001, by one way ANOVA test (n=5, ± standard error from the mean)

4.2.3.2.3 *Incorporation*

Five-FU was incorporated into the CA shell by mixing into the first aqueous phase. The results of this process on the loaded CA echogenicity are presented in Figure 4-47. It shows that loaded samples are not significantly different than control (n=5, p>0.05), as opposed to incorporation of FITC-BSA and SB, sections, ⁋4.2.1.4.2 and ⁋4.2.2.2. Five-FU is a relatively small molecule (MW=130.08), in comparison to FITC-BSA, which is a considerably large

protein (MW ~66 kDa), and introduces less interference when incorporated in the inner shell of CA. SB on the other hand is a small molecule like 5FU, however, its incorporation in the shell is done via dissolution with the polymer in the organic phase, as opposed to 5FU which is initially dissolved in the first aqueous phase. SB and 5FU have different starting points in incorporation process which might affect their integration inside the shell later on. For this reason concentration of loaded 5FU did not have an effect on echogenicity, Figure 4-47, as opposed to SB where the loaded drug concentration did affect echogenicity, Figure 4-35.

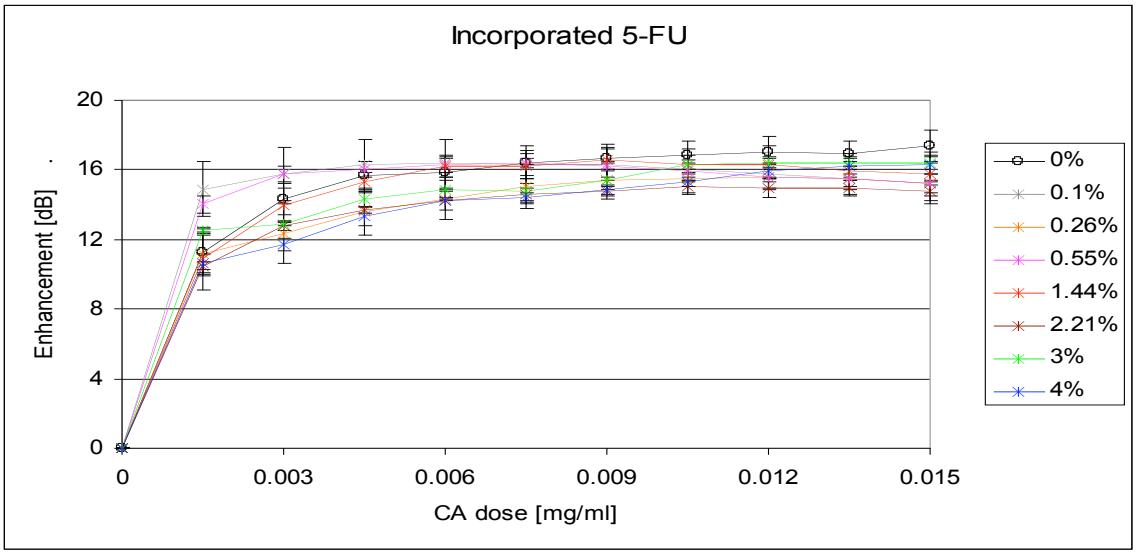

Figure 4-47 Dose response curves of 5FU-loaded PLA using incorporation method. Means are significantly different, for $P<0.0001$, by one way ANOVA test ($n=5$, ± standard error from the mean)

Time response curves, Figure 4-48, show no significant difference between control and loaded samples of concentrations 0.10% to 2.21%. However, 3% and 4% loaded CA are significantly different than control ($n=5$, $p<0.0001$). This suggests that beyond 3%

incorporation of 5FU does interfere with CA integrity, despite its relative small size, and lowers its stability in aqueous solution, such as the one used in time response test.

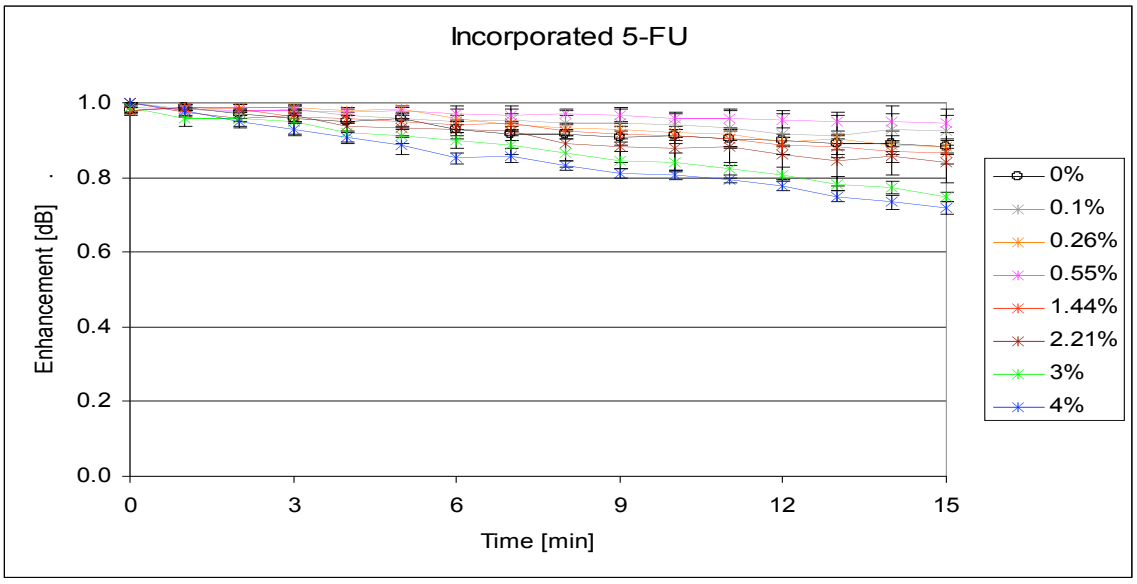

Figure 4-48 Time response curves for 5FU-loaded PLA using incorporation method. Means are significantly different, for $P<0.0001$, by one way ANOVA test (n=5, ± standard error from the mean)

4.2.3.3 *5FU-Loaded CA Compared To Clinically Available 5FU*

5FU is clinically available for at least 30 as an anticancer drug, administered by itself or along with other chemotherapeutic drugs such as irinotecan, doxorubicin and oxaliplatin. It is given by intravenous short or continuous infusions, or as a cream preparation applied on the skin for skin cancers (Bukowski et al., 1992; Yip et al., 2003; Hanauske et al., 2007). Its maximal tolerable dose depends on the administration regime, bolus, bolus followed by continues infusion, or continuous infusion, and on co-administered drugs. For comparison with

our platform a maximal tolerable dose of 400 mg/m^2 that was given to treat solid colorectal tumors will be discussed (Hanauske et al., 2007).

Since no release experiments were done using 5FU-loaded CA, 5FU release was calculated for a range of release percent, in order to compare our platform to conventional intravenous 5FU delivery.

Given the following data it is possible to compare clinical conventional 5FU drug delivery to 5FU-loaded CA delivery, as see in Table 4-8:

- Maximal tolerable dose of 5FU is 400mg/m^2
- Body surface area 1.9 m^2 (male, 75 kg, 1.73 m)
- Body fluids 3500mL+ 10,500mL (plasma + interstitial fluid)
- CA injected at: 0.35 mL/kg, 0.05 g/mL, 75 kg body weight (eq. 3-2)

Table 4-8 5FU amount [mg] delivered to tumor for conventional 5FU administration and 5fU-loaded CA ultrasound induced release

	5FU-loaded CA			Conventional 5FU
Assumed release [%]	Dry adsorbed	Wet adsorbed	Incorporated	
10	1.34	1.44	0.18	1.09
30	4.02	4.33	0.55	
50	6.69	7.22	0.92	

Table 4-9 Non delivered 5FU amount [mg] for conventional 5FU administration and 5fU-loaded CA ultrasound induced release

	5FU-loaded CA			Conventional 5FU
Assumed release [%]	Dry adsorbed	Wet adsorbed	Incorporated	
10	12.05	12.99	1.65	758.9
30	9.37	10.11	1.29	
50	6.69	7.22	0.92	

These calculations are based on the following assumptions:

- Tumor fluid volume 20mL (vasculature + interstitial fluid)
- CA loading 1.01%, 1.10% and 0.14% (dry adsorption, wet adsorption and incorporation, respectively)
- CA targeting of 100%

We hypothesized that more and more circulating loaded CA are going to pass through the acoustic window (defined by the placement of US transducer on top of the tumor) with each full blood cycle. This would allow more local release of 5FU with each cycle. Data presented at Table 4-8 were calculated based on 100% targeting, but even if targeting was less than 100% we could still deliver more drug using our platform than the conventional delivery, just by increasing the injected dose or concentration, up to the maximal tolerable dose of 400 mg/m^2 (which is 760 mg for a 75 kg, 173 cm male). In the current calculations we showed a total of 13.4mg, 14.4mg and 1.84mg of total 5FU carried by CA, for dry adsorption, wet adsorption and incorporation, respectively (compared to the maximal tolerable dose of 760 mg for a 75 kg, 173 cm male).

The remaining (non-delivered) 5FU can be calculated as well, Table 4-9 shows that when using the intravenous 5FU administration most of the injected drug is circulating and is

available for cellular uptake which resents toxic side effects; whereas, using the CA-loaded platform, less drug is carried and hence even for low release percent such as 10%, the remaining 5FU amount is still, at least, 58 times smaller than in conventional administration. This means that there is less potential for body 5FU toxicity when using 5FU loaded CA than conventionally infusing free 5FU. Minimizing harmful side effects due to drug toxicity is an important virtue of developing a drug delivery platform.

4.2.3.4 *5FU Loading Summary*

Based on the loading percents of 5FU, presented on Table 4-10, it is seen that by dry adsorption it is possible to load more 5FU onto PLA than by using wet adsorption, and incorporation. Incorporating of hydrophilic drugs in the primary aqueous phase creates a large drug concentration gradient that drives the drug out to the outer aqueous phase.

From the acoustic performance results there is no effect of drug concentration on signal enhancement (dose response curves) for any of the methods used to load PLA with 5FU. For signal stability (time response curves) it can be concluded that wet adsorption did not reduce the signal for loaded CA for all tested concentrations of 5FU. Using incorporation, it can be seen that for the higher doses of 5FU, 3% & 4%, signal stability decreased in 13.5% and 16.4% respectively, compared to control, over a period of 15 minutes of insonation. For dry adsorbed samples, no trend was seen for signal decrease for the different loading concentrations, however, the maximal signal decrease was 21.8% (for 1.44% 5FU, compared to control) whereas the maximal signal decrease for wet adsorption was 4.5% (for 3% 5FU, compared to control).

In conclusion, based on acoustic performances, that are briefly summarized in Table 4-11, wet adsorption was found to be the best loading method for 5FU onto PLA.

Both 5FU and BSA showed best loading using the same method, dry adsorption. Both loaded drugs showed no effect of different drug loadings on acoustic properties using dry adsorption. When incorporating 5FU and BSA same trend was seen where the highly loaded

CA had lowered signal stability in comparison to low loadings that did not have an effect on signal stability. These similarities are due to the fact that they are both polar molecules.

Table 4-10 Encapsulation percent summary for 5FU loaded PLA

	Dry adsorption	Wet adsorption	Incorporation
0.26%	0.169±0.008	0.028±0.012	0.028±0.002
0.55%	0.158±0.016	0.046±0.007	0.035±0.005
1.44%	0.315±0.014	0.064±0.016	0.020±0.004
2.21%	0.397±0.025	0.191±0.028	0.021±0.004
3.00%	0.602±0.009	0.515±0.123	0.024±0.001
4.00%	1.020±0.110	1.102±0.073	0.014±0.005

Table 4-11 Echogenicity summary for 5FU-loaded PLA CA

	Dry adsorption	Wet adsorption	Incorporation
Enhancement [dB]	15.26±0.47	15.72±0.35	15.57±0.22
Enhancement [% of control]	66.92±11.93	85.08±3.50	84.24±1.20
Signal Stability after 15 min [%]	65.87±2.50	90.10±1.54	84.64±3.44

Comparing calculated drug release of 5FU from our platform to systemically administered 5FU it can be seen that wet and dry adsorbed 5FU both carry high enough 5FU, so that even for a small release such as 10%, our platform may deliver more drug than the conventional systemic delivery. Combining result from all tests and calculations it can be concluded that wet

adsorption gives the best combination of drug content and acoustic enhancement and stability and may be able to deliver more drug than conventional systemic administration.

4.2.4 *Doxorubicin (DOX)*

Doxorubicin ($C_{27}H_{29}NO_{11}$, MW 543.52 g/mole), is an anthracycline antibiotic, anti cancer drug having a strong activity against various solid tumors by binding to DNA strands and inhibiting cellular functions (Lin et al., 2005; Sinha & Lewis, 1981). The motivation to encapsulated DOX and administer it as a local treatment originates from its high cardio toxicity even when administered in low doses. Figure 4-49 shows the chemical structure of DOX.

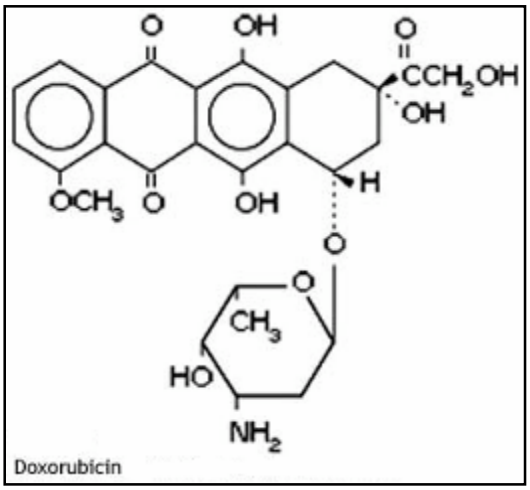

Figure 4-49 DOX chemical structure.

DOX was found to have high cardio toxicity even when administered in low doses, it acts as a vasodilatant and might also cause necrosis in its injection site. Minding this, and the hydrophilic nature of DOX, traditional drug administration is limited, and there is a need to encapsulate the potent drug. DOX is a fluorescent material that can be easily detected and quantified.

4.2.4.1 *Choice of Polymer*

DOX encapsulation percent was tested for three different loading methods, i.e., dry adsorption, wet adsorption and incorporation. Each method was tested for two shell materials, PLA and PLGA. Based on the different chemical properties of PLA and PLGA we hypothesized each polymer would demonstrate different drug loading capacity. Due to the presence of methyl groups on every lactic acid molecule, PLA has a more hydrophobic nature than PLGA. The loading process steps and quantities are detailed in section 3.2.6.

4.2.4.2 *Loading Methodology*

4.2.4.2.1 *Dry Surface Adsorption*

The following study was set to determine the effects of initial DOX concentration on drug loading for PLA and PLGA using the dry adsorption method. Based on previous results with FITC-BSA, section 4.2.1.2.1, the best pH set up that was found was when the polymer and the drug had opposite charging. The pKa of DOX is 9.17, and the pI of each polymer is 3.85 and 6.4 for PLA and PLGA, respectively. Hence the adsorption was done at pH 6.8, where the polymers are negatively charged and the drug is positively charged. Based on FTIC-BSA results, section 4.2.1.2.2, incubation temperature was set to 4°C. Figure 4-50 shows incubation time study for DOX-PLGA, for 1.44% initial DOX concentration at 4°C. Loading percent for more than 24 hours was similar. Based on results with BSA, section 4.2.1.3.1.2, excess of incubation might contribute to a decrease in echogenicity, hence, incubation time for DOX was set to be 24 hours, since this was the minimal time to reach a drug loading peak.

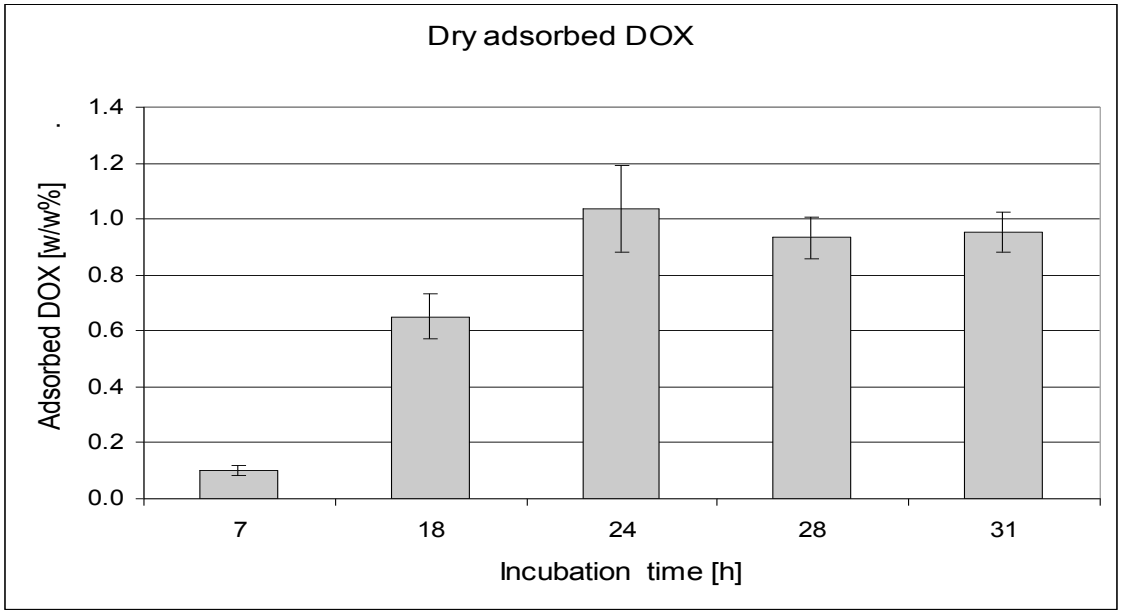

Figure 4-50 Incubation time study for dry adsorbed DOX onto PLGA, for 1.44% loading, done at 4C. Means are significantly different, for $P<0.0001$, by one way ANOVA test (n=3, ± standard error from the mean)

Once DOX dry adsorption conditions were established it was possible to study the shell polymer effect on encapsulation. Figure 4-51 shows the encapsulation of DOX for different initial DOX concentrations, comparing PLA and PLGA shell polymers. DOX-loaded PLA experiments were carried out by John Eisenbrey (Figure 4-51 to Figure 4-56) and are presented here for the sake of comparison. It can be seen that PLGA loading percentage was higher than PLA for all tested initial DOX concentrations, by a factor of 10, at least. This trend was tested by a two way ANOVA analysis. PLA hydrophobicity affects its ability to adsorb hydrophilic substances such as DOX onto its surface (Tamber et al., 2005).

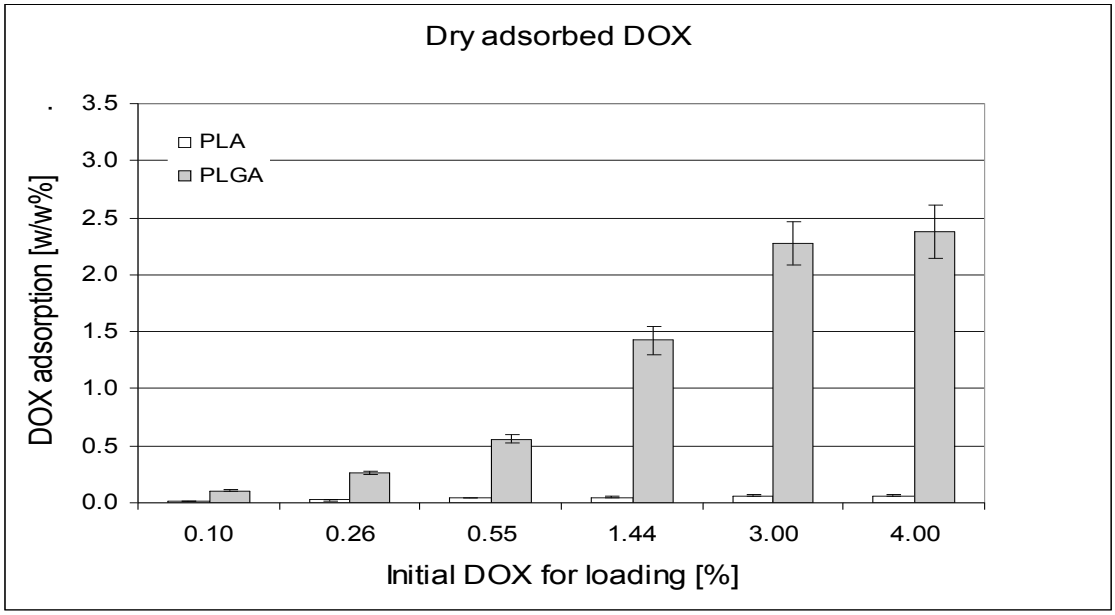

Figure 4-51 Encapsulation percent for CA loaded with DOX, dry adsorption method, comparing loading percent onto PLA and PLGA. DOX loading onto PLGA is higher than PLA loading by a factor of 10, at least. Means are significantly different, for $P<0.0001$, by two way ANOVA test (n=3, ± standard error from the mean)

Figure 4-52 shows Langmuir model plot for results for PLGA ($\alpha=5.6483$, $k=0.2023$), it can be seen that our results have a good fit with this model. Being able to fit Langmuir model to results means that initially the rate of DOX adsorption is high and then decreases as less surface is available for adsorption. Once the rate of adsorption equals the rate of desorption a dynamic equilibrium is attained. Dry adsorption of DOX onto PLGA reaches its equilibrium at 28% at that point the maximal possible loading percent of DOX that can be loaded is 2.45%. Dry adsorption of DOX onto PLA achieves equilibrium at 0.5% and the maximal possible loading percent of DOX is 0.043%.

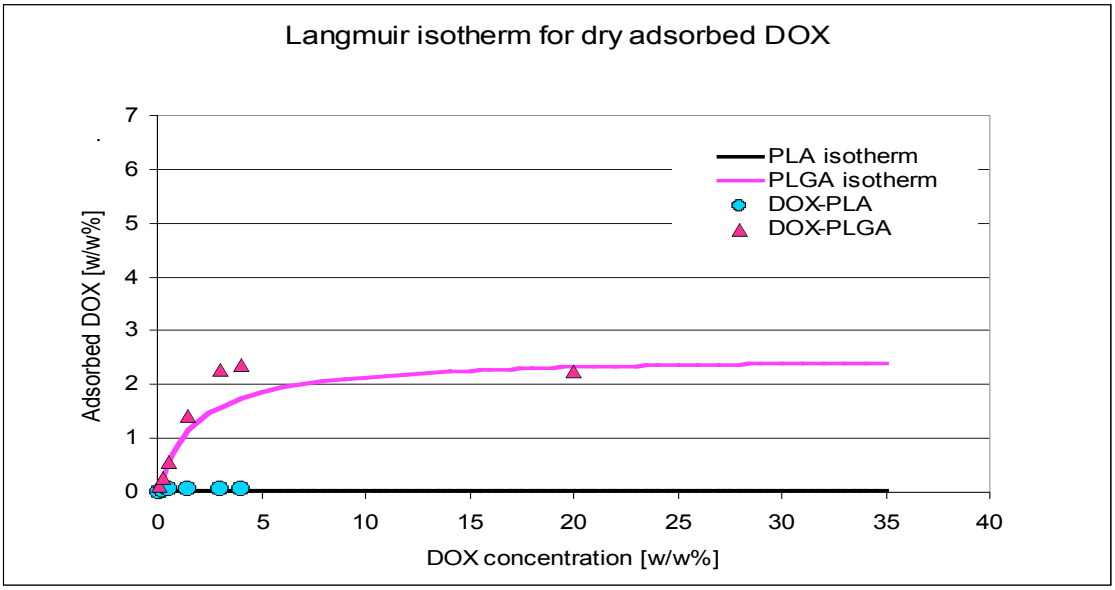

Figure 4-52 Langmuir isotherm plot for DOX dry adsorption onto CA, comparing PLA (R^2=0.5669) and PLGA (R^2=0.9645) shell materials. Loading conditions: DI water, pH 6.8, for 24 hours, samples were gently agitated at 4°C

A potential concern that could arise from using this loading method is the burst of lightly attached drug, before the loaded CA arrive to their target. As seen in some preliminary experiments, Chapter 5, this effect is present, and about 42% of dry adsorbed DOX falls off the CA as they are inserted into the aqueous solution. Since DOX is cardio-toxic this effect should be taken into account when considering which loading method is most suitable for attachment of DOX. A full comparison of DOX loaded CA to current clinically used DOX is brought at the end of this chapter, 4.2.4.4.

4.2.4.2.2 *Wet Surface Adsorption*

The same study was carried out for wet adsorption loading. Figure 4-53 shows the results for wet adsorbed DOX onto PLA and PLGA. It can be seen that for the first 4 initial DOX

concentrations, the loading percent for PLA and PLGA was similar. This is supported by EE calculations that show 100% efficiency for those groups (initial DOX of 0.10% to 1.44%). A significant difference between the two polymers' loading is seen at 4% initial DOX concentration.

In summary, for DOX concentrations equal to and smaller than 3% there was no difference seen between PLA loading to PLGA loading, when using wet adsorption (n=3, p>0.05).

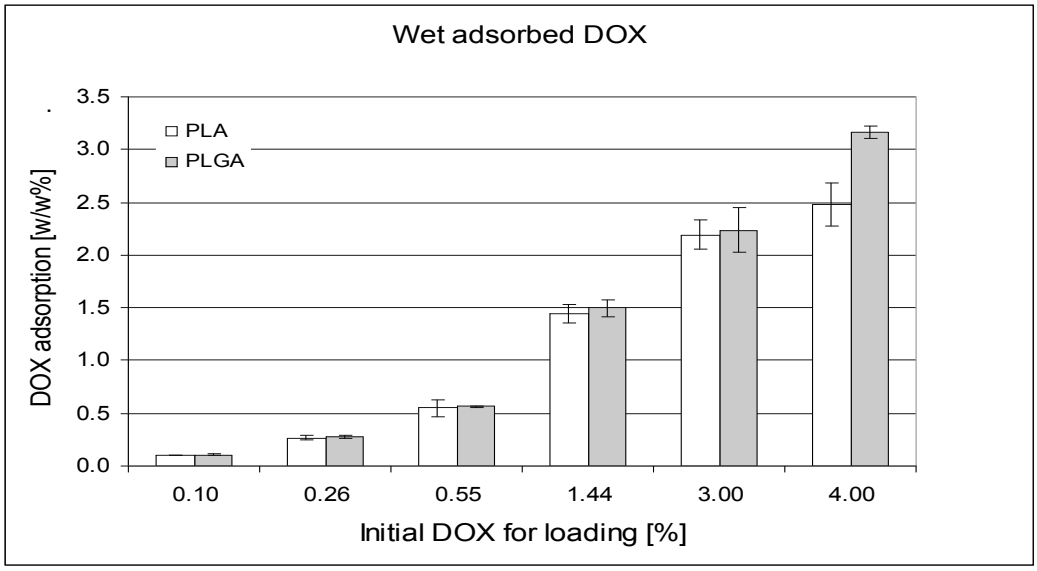

Figure 4-53 Encapsulation percent for PLGA loaded with DOX, wet adsorption method. Means are significantly different, by two way ANOVA: $p<0.0001$ for concentration factor, and $P>0.05$ for polymer factor analysis (n=3, ± standard error from the mean)

Langmuir isotherm fit is shown in Figure 4-54 for the adsorption of DOX onto each of the polymers (for PLA: $\alpha=6.2848$, $k=0.1740$; PLGA $\alpha=9.5902$, $k=0.1149$). It can be seen that wet adsorption of DOX onto CA made of either polymer follows the Langmuir model; where a rapid adsorption is followed by a slower adsorption until a dynamic equilibrium is reached between adsorption and desorption. When extending the model to the point where equilibrium is

achieved DOX adsorption to PLA would be ~3.7 w/w% and DOX adsorption onto PLGA would be ~5.8 w/w%. These findings are expected based on the differences in chemical properties of PLA and PLGA.

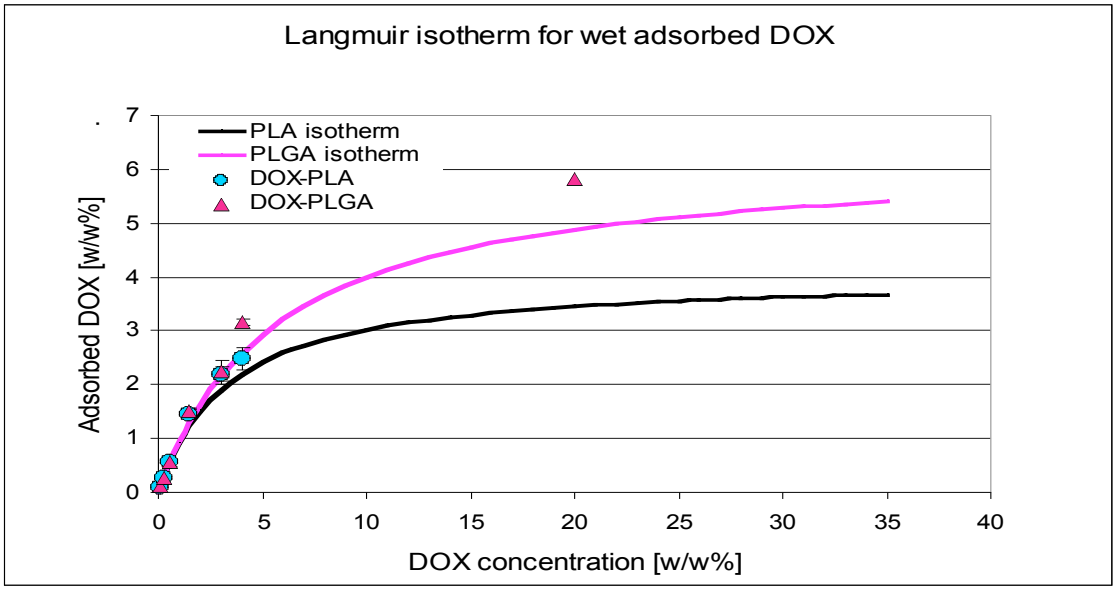

Figure 4-54 Langmuir isotherm fit for wet adsorbed DOX onto PLA (R^2=0.9429) and PLGA (R^2=0.9369). Solid lines indicate isotherm fit for each polymer, extended to adsorption equilibrium.

Figure 4-55 shows a comparison of dry adsorbed DOX onto PLGA and wet adsorbed DOX onto PLGA using the Langmuir model plot. It is seen that wet adsorption has more loading potential than dry adsorption and that the maximal drug loading percent are 6.2% and 2.45% for wet and dry adsorptions, respectively.

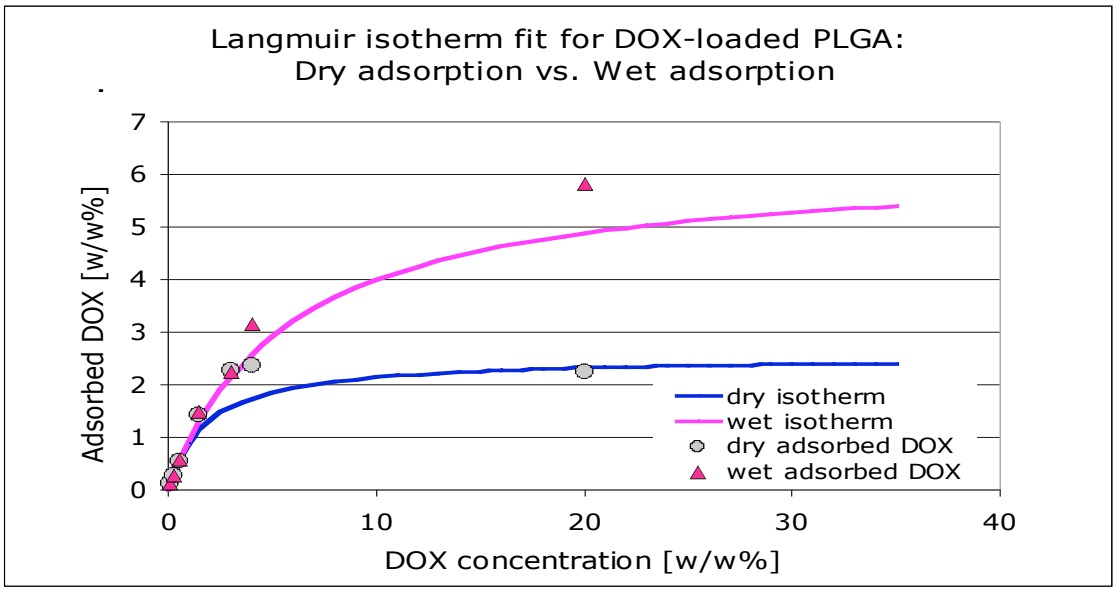

Figure 4-55 Langmuir isotherm fit for DOX-loaded PLGA comparing wet and dry adsorptions, R^2=0.9369 and R^2=0.9645, respectively). Solid lines indicate isotherm fit for each method, extended to adsorption equilibrium

Another important aspect in comparing the two adsorption methods is the burst of lightly attached drug, before the loaded CA arrive to their target. As seen in some preliminary experiments, Chapter 5, about 35% of wet adsorbed DOX and 42% of dry adsorbed DOX is detached when added to aqueous solution. Since DOX is cardio-toxic this effect should be taken into account when considering which loading method is most suitable for attachment of DOX. A full comparison of DOX loaded CA to current clinically used DOX is brought at the end of this chapter, 4.2.4.4.

4.2.4.2.3 *Incorporation*

Due to the hydrophilic nature of DOX it was incorporated by addition to the aqueous phase of the first step of microbubble fabrication. Results for DOX loading onto PLA and PLGA

using incorporation as loading method are presented in Figure 4-56. It can be seen that for all tested initial concentration (but 0.55%) there is significant difference between DOX loading percent onto PLA and onto PLGA. PLA EE peaks at 0.55% DOX (EE=68.97±9.0%) and then decreases. Whereas, PLGA EE starts at 100% for DOX concentration 0.26% and 0.10%, and decreases for 0.55% DOX and above, down to 48.51±3.0% for 4% initial DOX. This can be attributed to the formation of larger pores in the PLA microspheres, due to their chemical structure, which results in easier loss of the inner phase drug to the outer phase (Wong et al., 2001).

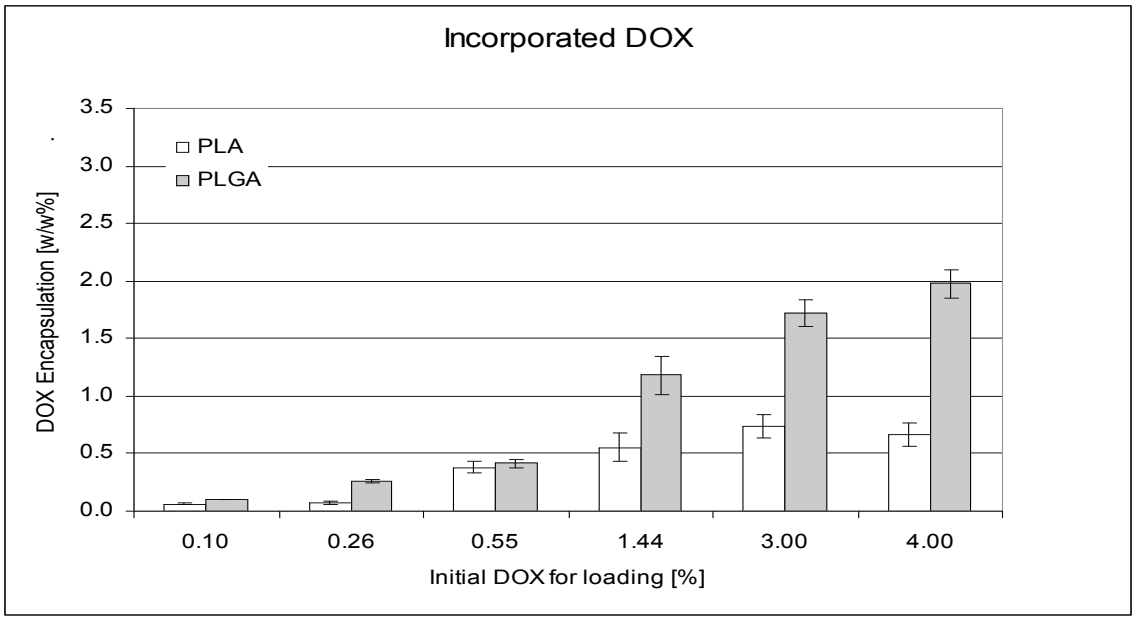

Figure 4-56 Encapsulation percent for PLGA loaded with DOX, using incorporation method. Means are significantly different, for $P<0.0001$, by two way ANOVA test (n=3, ± standard error from the mean)

Summarizing DOX loading, it can be concluded that PLGA was a better match for DOX loading when using dry adsorption or incorporation. For wet adsorption loading PLGA demonstrated better DOX loading for the highest tested concentration of 4%. Based on these findings, PLGA was chosen for further exploration of loading effects on echogenicity.

4.2.4.3 *Acoustic Studies*

4.2.4.3.1 *Dry Adsorption*

Conditions for dry adsorption of DOX were chosen based on previous work with FITC-BSA and are reasoned in ¶4.2.1.2. Briefly, temperature was 4°C, incubation time was 24 hours and pH 6.8. The present study was set in order to test weather initial concentration of drug can affect the loaded CA echogenicity and signal stability. Figure 4-57 shows the dose response curves for different initial DOX concentrations. All loaded samples were significantly different than control. Loaded groups had some statistical similarities ($n=3$, $p>0.05$) and there is no clear trend of concentration affecting echogenicity. This suggests, what was seen before for FITC-BSA, ¶4.2.1.3.1.4 and ¶4.2.1.3.1.5, and 5FU, ¶4.2.3.2.1, that when using dry adsorption the incubation process, or the freeze drying/rehydration is responsible for echogenicity loss and not the quantity of drug that is loaded. Similarly, when looking at the corresponding time response curves, Figure 4-58, all loaded samples were significantly different than control, but were not statistically different than one another ($n=3$, $p<0.0001$). This follows the same trend seen for dose response, where different drug loading do not have an effect on drug-loaded CA signal enhancement. Here too, the main loss of signal enhancement origins from the loading procedure itself, exposing the CA to an aqueous solution for 24 hours.

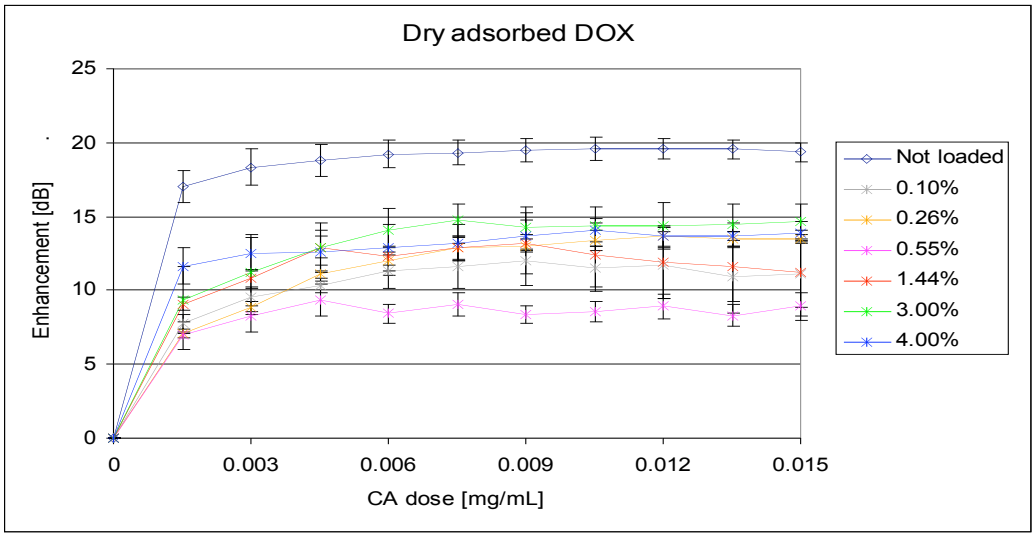

Figure 4-57 Dose response curves of DOX-loaded PLGA using dry adsorption method, incubated for 24 hours at 4°C, pH 6.8. Means are significantly different, for P<0.0001, by one way ANOVA test (n=3, ± standard error from the mean)

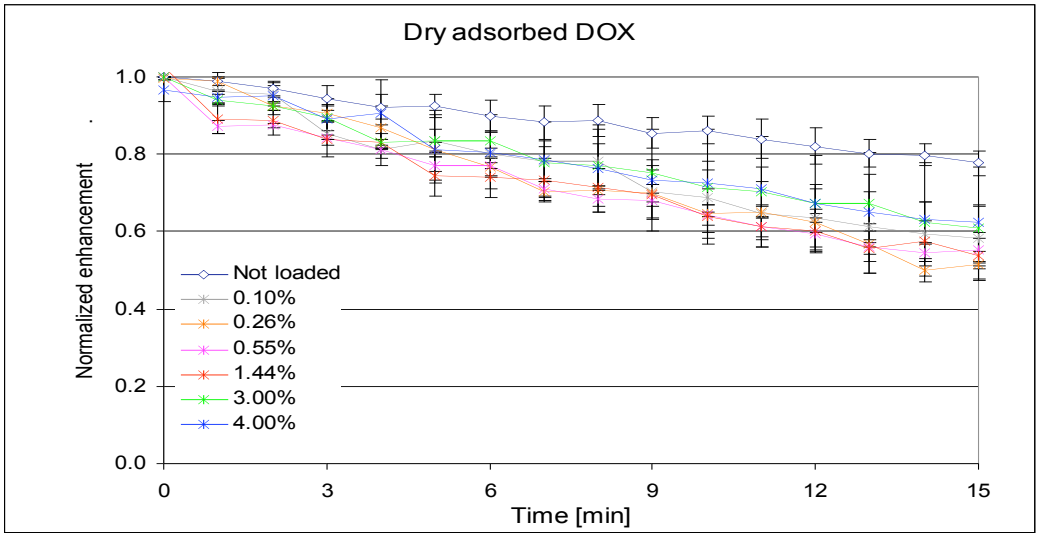

Figure 4-58 Time response curves of DOX-loaded PLGA using dry adsorption method, incubated for 24 hours at 4°C, pH 6.8. Means are significantly different, for P<0.0001, by one way ANOVA test (n=3, ± standard error from the mean)

4.2.4.3.2 *Wet Adsorption*

The present study was set in order to test whether initial concentration of drug can affect the loaded CA echogenicity and signal stability when using wet adsorption method. As mentioned before, wet adsorption is very different than dry adsorption since loading takes place as part of last steps of CA fabrication. In wet adsorption the drug is added to the CA while they are still wet and not completely formed, and without exposing the CA to an additional step of aqueous incubation. This is an advantage in using wet adsorption in comparison to dry adsorption. Figure 4-59 shows the results for wet adsorbing DOX onto PLGA microbubbles, using different DOX concentrations. It can be seen that 0.10% and 0.26% DOX groups are not significantly different than control ($n=3$, $p>0.05$), while other initial DOX concentrations are. However, for the 3% and 4% initial DOX there was a significant decrease in echogenicity ($n=3$, $p<0.0001$), 35.60±4.66% and 49.14±7.25%, respectively. This suggests that echogenicity is compromised for highly loaded CA.

These findings may be correlated to the way that DOX is loaded by wet adsorption. In this process the drug is added to the microbubbles before they have hardened. It is possible that they are more susceptible to adsorb drug at this stage. Minding this and the fact that our microbubbles are porous, it is possible that drug is adsorbed deep into the pores and not only onto the outer surface, in such a way that may make the shell more rigid. A change in shell elasticity may affect the CA resonance and, consequently, its echogenicity. Altering the shell structure may also reduce its integrity and increase its exposure to hydrolysis, which would result in greater signal loss, as seen in Figure 4-60.

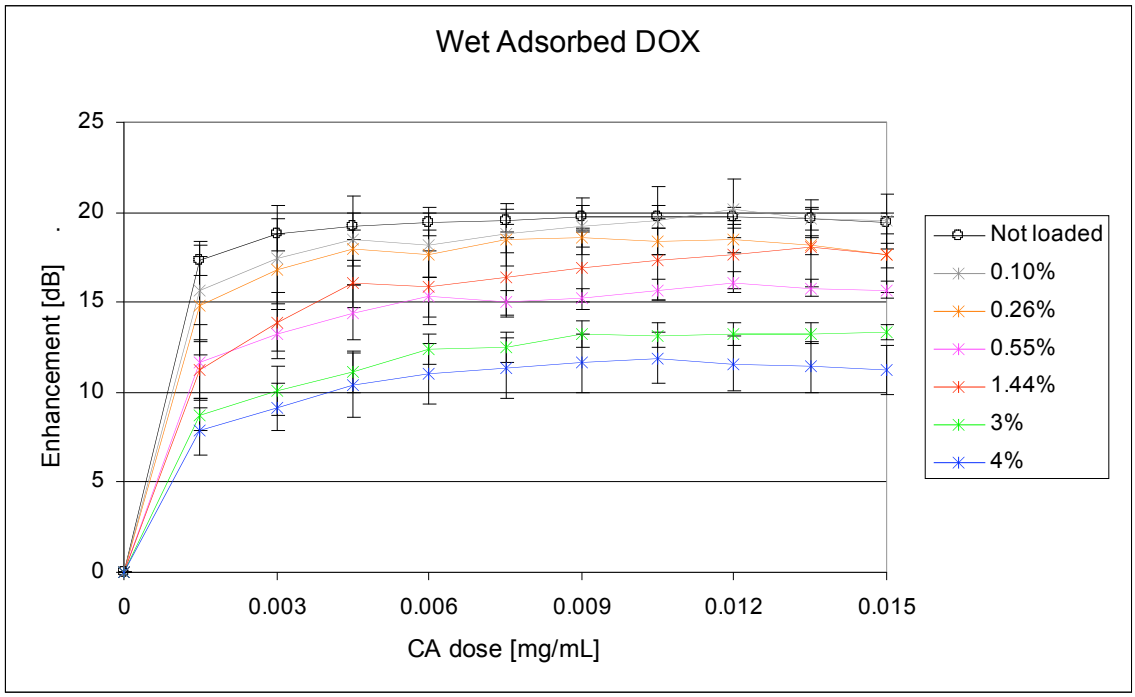

Figure 4-59 Dose response curves of DOX-loaded PLGA using wet adsorption method. Means are significantly different, for P<0.0001, by one way ANOVA test (n=3, ± standard error from the mean)

Figure 4-60 shows the corresponding time response curves. All loaded groups were significantly different than control. There were no statistical differences (n=3, p>0.05) among the lower concentrations (0.10%-0.55%), however, the top 3 concentrations were significantly different than one another (n=3, p<0.0001). This follows the trend seen in dose response, Figure 4-59, where highly loaded CA has compromised signal stability. Signal loss at the end of 15 minutes of insonation was found to be 37.4±2.3 for three smaller DOX loadings, in average, and 40.9±12.4 and 49.7±7.7, for 3% and 4%, respectively.

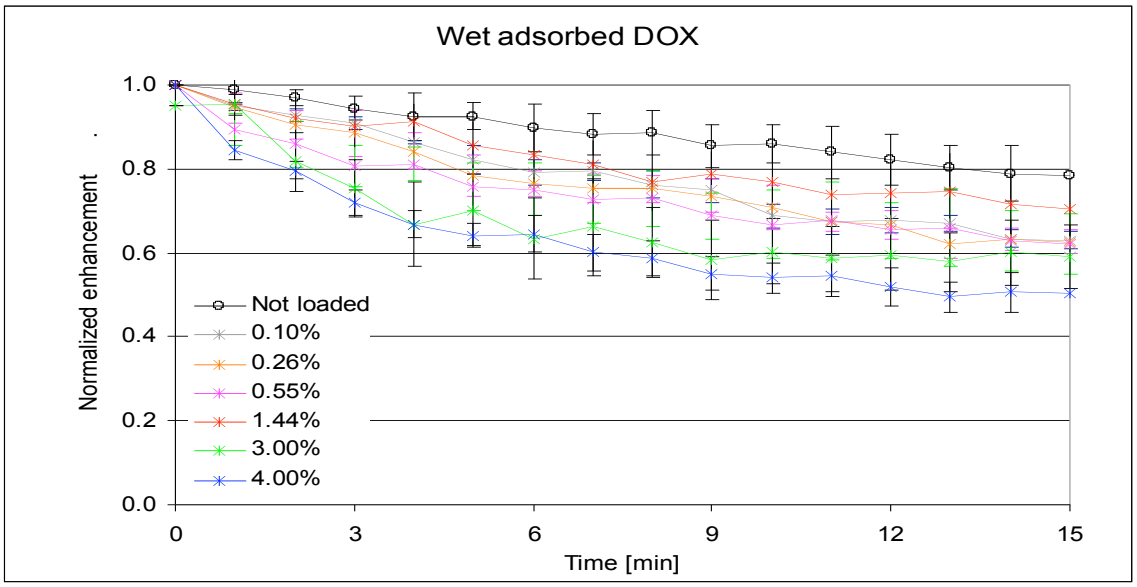

Figure 4-60 Time response curves of DOX-loaded PLGA using wet adsorption method. Means are significantly different, for P<0.0001, by one way ANOVA test (n=3, ± standard error from the mean)

4.2.4.3.3 *Incorporation*

This study was set to learn about the effect of different drug loadings on echogenicity for incorporated DOX. Figure 4-61 shows the dose response curves for different DOX concentrations using drug incorporation. All loaded samples were significantly different than control (n=3, p<0.0001). No statistical differences were found among different loading concentrations (n=3, p>0.05). Suggesting that different DOX loadings do not affect echogenicity, as opposed to FTIC-BSA and SB, sections 4.2.1.3.2 and 4.2.2.2, where increase in drug loading increased echogenicity compromise.

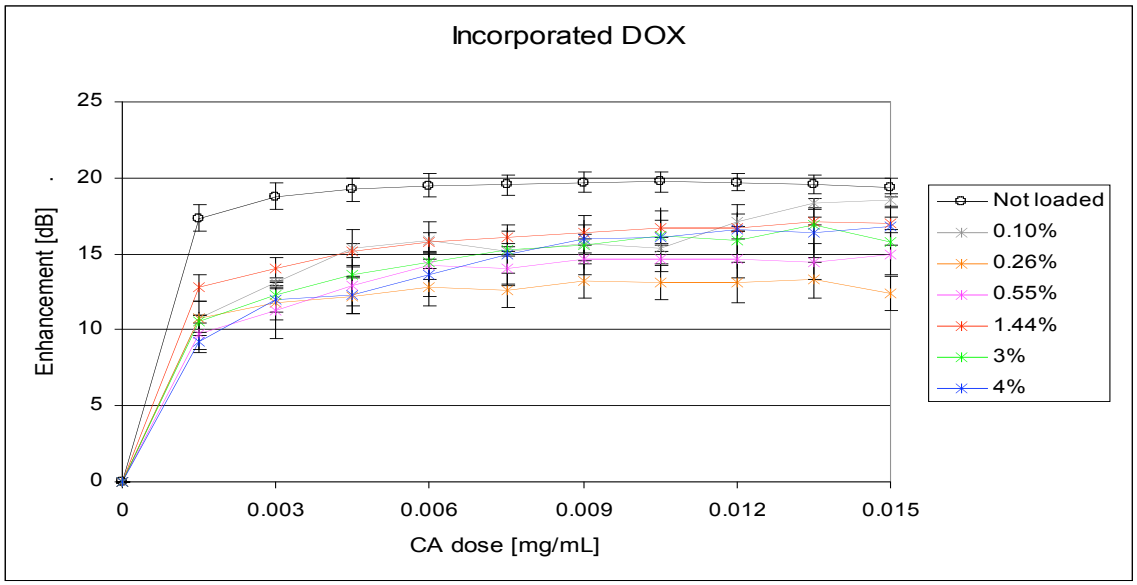

Figure 4-61 Dose response curves of DOX-loaded PLGA using incorporation method. Means are significantly different, for P<0.0001, by one way ANOVA test (n=3, ± standard error from the mean)

Figure 4-62 shows the corresponding time response curves, demonstrating the same trend as dose response curves, Figure 4-54. All loaded samples were significantly different than control (n=3, p<0.0001), but not statistically different then one another (n=3, p>0.05). Signal stability was decreased in 52.4±2.0% for loaded samples, in average, where control signal loss was 21.6±4.8%. This suggests that by incorporating DOX, the CA integrity is compromised and loaded CA have loose half of their signal enhancement after 15 minutes of insonation. This however is not a good enough reason to rule out this method since having CA with half life of 15 minutes is qualified for imaging.

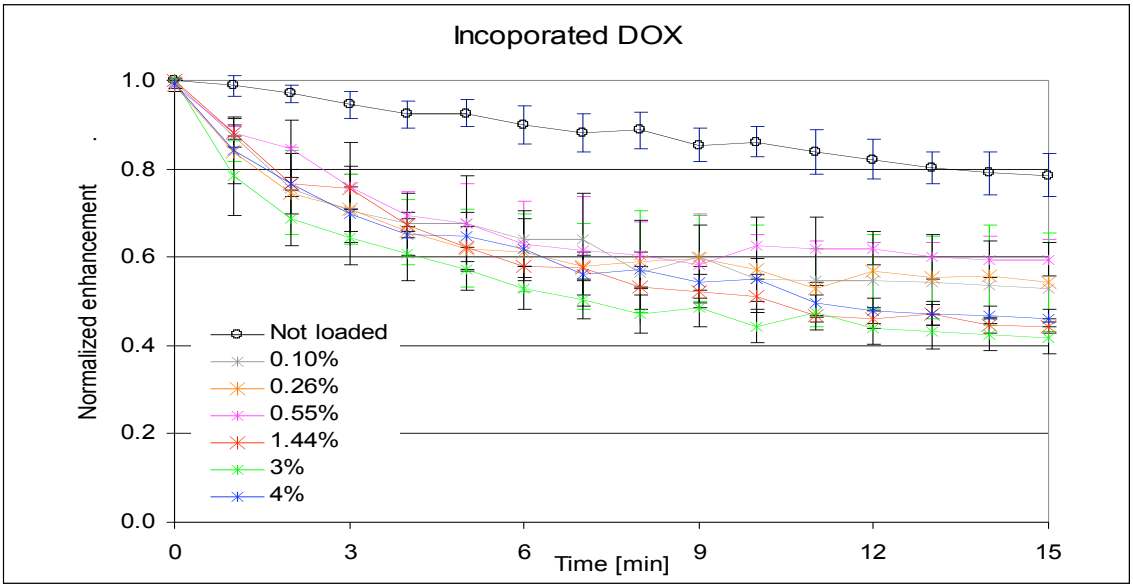

Figure 4-62 Time response curves of DOX-loaded PLGA using incorporation method. Means are significantly different, for P<0.0001, by one way ANOVA test (n=3, ± standard error from the mean)

4.2.4.4 *DOX-Loaded CA Compared To Clinically Available DOX*

- Doxorubicin is clinically available as a free drug, in the form of doxorubicin hydrochloride or encapsulated in liposomes, called liposomal doxorubicin, both of which are approved by the FDA for treating several cancers. Free DOX administration results in short half life of 10-20 minutes, due to rapid cellular uptake, and hence high cytotoxcitiy. Having DOX carried by liposomes increases its half life to 60-80 hours for solid tumors (Gabizon et al., 2008) which reduces its cytotoxicity. However, these liposomes are rapidly taken by macrophages and deposited in the liver, reducing their intrinsic activity by 40-50% (Amantea et al., 1997; McLoon and Wirtschafter, 1999). Given the following data it is possible to compare liposomal DOX drug delivery to DOX-loaded CA delivery, as see in

Table 4-12:

- Maximal tolerable dose of DOX is 40-60mg/m^2 (50mg/m^2 used to calculate)
- Body surface area 1.9 m^2 (male, 75 kg, 1.73 m)
- Body fluids 3500mL+ 10,500mL (plasma + interstitial fluid)
- DOX release enhanced by insonation, using 5MHz transducer, 0.68MPa, 30min.
- CA injected at: 0.35 mL/kg, 0.25 g/mL, 75 kg body weight (eq. 3-2)
- DOX burst from CA 45.0%, 25.5% and 13.5% (dry adsorption, wet adsorption and incorporation, respectively)

Table 4-12 DOX amount [mg] delivered to tumor comparing liposomal DOX administration and DOX-loaded CA ultrasound induced release

	DOX-loaded CA			Liposomal DOX
	Dry adsorbed	Wet adsorbed	Incorporated	
No ultrasound	0.093	0.074	0.021	0.068
With ultrasound	0.100	0.079	0.025	

Table 4-13 Non delivered DOX amount [mg] for liposomal DOX administration and DOX-loaded CA ultrasound induced release

	DOX-loaded CA			Liposomal DOX
	Dry adsorbed	Wet adsorbed	Incorporated	
No ultrasound	0.007	0.011	0.008	0.068
With ultrasound	0.008	0.011	0.008	

These calculations are based on the following assumptions:

- Tumor fluid volume 20mL (vasculature + interstitial fluid)
- Liposomal delivery is 50%
- CA loading 2.37%, 3.16% and 1.98% (dry adsorption, wet adsorption and incorporation, respectively)
- CA targeting of 100%

We hypothesized that more and more circulating loaded CA are going to pass through the acoustic window (defined by the placement of US transducer on top of the tumor) with each full blood cycle. This would allow more local release of DOX with each cycle. Based on data presented at Table 4-12, DOX burst from loaded CA contributes most of DOX release in the tumor, 45.5%, 26.3% and 13.7% for dry adsorbed, wet adsorbed and incorporated DOX, respectively. Future work should be dedicated towards minimizing DOX burst effect. One way to eliminate burst effect was suggested by Yang et al., where DOX was conjugated to PLGA and then encapsulated in PLGA microspheres (Yang et al., 2001). Using this method drug release profile was of zero order and spanned over one month. Ideally drug delivery system should have minimal initial burst effect, so that more drug would be available for release at the target site.

The amount of drug left on the carrier, Table 4-13, is 0.068 mg DOX in liposomes whereas 0.008-0.011 mg is left on CA. This means that there is less potential for body DOX toxicity when using DOX loaded CA than liposomal CA. Minimizing harmful side effects due to drug toxicity is one of the main advantages of developing the current drug delivery platform.

Drug delivery using our platform can be increased by changing the following parameters: injecting higher CA concentration within the safety limits, injecting more CA solution (without changing its CA concentration), improving loading of CA (it is possible to use a combination of two loading methods to get higher loading), improving US release by achieving a better understanding of the release mechanisms involved in our platform.

4.2.4.5 *DOX Loading Summary*

Table 4-14 summarizes the encapsulation percents for the three loading methods used to load DOX onto PLGA, it is seen that for smaller initial DOX concentration (0.10%-0.55%) the encapsulation is 100% efficient (excluding 1.44% initial DOX, that yield 75% efficiency using incorporation). Based on drug loading for the full range of initial DOX concentrations, the highest yielding encapsulation method is wet adsorption. Using either adsorption method, one of the limiting factors of loading is number of adsorption sites on the CA. From results presented at Table 4-14 it is impossible to identify that limit since saturation has not been reached and as we add more initial DOX we still get more drug loaded on the microbubbles. An additional test was done to verify this assumption and indeed for 20% initial DOX the loading percents were 2.34±0.60 and 5.82±0.52 for dry adsorption and wet adsorption, respectively. Those loading percents are showing the potential of our microbubbles to carry more DOX using either adsorption method. All of these results were fit to Langmuir model the adsorption limits were confirmed; the adsorption loading percent limits were 0.04%, 2.69% for dry adsorbed DOX onto PLA and PLGA, respectively, and 2.45% and 6.23% for wet adsorbed DOX onto PLA and PLGA, respectively.

Loading by wet adsorption was explored for 30 minutes incubation time period, in order not to interfere with microbubbles fabrication method. It is possible to set another study of time optimization for wet adsorption of DOX in order to explore if more DOX can be adsorbed.

Table 4-14 Loading percent summary for DOX-loaded PLGA

	Dry adsorption	Wet adsorption	Incorporation

0.10%	0.108±0.004	0.108±0.007	0.098±0.006
0.26%	0.264±0.025	0.275±0.017	0.260±0.013
0.55%	0.559±0.068	0.564±0.017	0.415±0.056
1.44%	1.423±0.207	1.499±0.135	1.183±0.286
3.00%	2.276±0.338	2.236±0.478	1.719±0.199
4.00%	2.373±0.405	3.164±0.061	1.979±0.215

Table 4-15 summarizes the acoustic properties of DOX-loaded PLGA. It can be concluded that wet adsorption and incorporation have similar echogenicity values, however, by incorporation less signal is lost over insonation time of 15 minutes.

Table 4-15 Echogenicity summary for DOX-loaded PLGA CA

	Dry adsorption	Wet adsorption	Incorporation
Enhancement [dB]	12.22±0.90	15.84±0.61	16.04±0.86
Enhancement [% of control]	63.18±4.62	81.70±3.46	82.15±4.42
Signal Stability after 15 min [%]	42.98±1.73	38.73±2.67	52.39±2.03

When comparing delivery of DOX from DOX-loaded CA to liposomal DOX, it can be seen that loading by wet and dry adsorption methods result in 47.3% and 15.7% more drug delivery, respectively. Using any of the three loading method the amount of DOX left on the carrier is at least 6 times smaller than when using liposomal DOX administration. Based on this and on the acoustic performance and the loading percents, wet adsorption is the best method among the three for loading DOX onto PLGA microbubbles.

4.2.5 *Drug Loading Comparison*

In this chapter we presented the loading effects on the acoustic capabilities of drug loaded CA and compared drug delivery using our platform to available clinical data.

When loading a protein drug such as BSA, by dry adsorption it was seen that loading incubation conditions, i.e., temperature, time, pH, had a dramatic effect on loading percent and drug loaded CA acoustic capabilities. Even though the best drug loading was achieved at incubation at acidic pH, at these conditions shell hydrolysis was accelerate and echogenicity and signal stability were compromised. When using a pH of 7.4 BSA loading was poor but the echogenicity and signal stability were good (maintaining 76% of acoustic capabilities). This strongly demonstrates the trade off trend between loading capacity and acoustic performance. Dry adsorption was not a suitable method for loading a non polar drug such as SB, as expected, due to its minimal solubility in aqueous incubation solution. When using dry adsorption to load 5FU and DOX drug concentration did not have an effect on acoustic properties but incubation step itself lowered loaded CA echogenicity and signal stability. The exposure to aqueous solution was found to initiate shell hydrolysis and compromise acoustic capabilities.

Using wet adsorption it was seen that more DOX could be loaded by this method compared to the other two loading method. In wet adsorption drug is dissolved in the residues of non polar solvent (hexane). DOX was preferably attracted to the CA surface when using a non polar solvent than when dry adsorbing it from an aqueous solution. Five fluorouracil, on the other hand, was found have more loading when using dry adsorption than wet adsorption. These results are affected by the chemical nature of each of the drugs, 5FU being water soluble and DOX being bound to HCl to become water soluble, and demonstrates the versatility of using different loading methods to suit different drugs.

Drug amount incorporated into the CA shell was found to affect their acoustic properties for BSA, SB and 5FU. This means that incorporating a foreign substance in the shell introduces a disruption in the shell structure, such that can affect the elasticity of the shell (leading to a

change in resonance capability) or expose the shell to hydrolysis. Both effects may lead to compromised echogenicity and signal stability of loaded CA. When incorporating a hydrophilic drug using CA that was fabricated in a double emulsion process (W/O/W) drug might leak out from the inner aqueous phase to the outer aqueous phase due to concentration gradient, resulting in smaller loading percent compared to other loading methods. This was the case of DOX, BSA and 5FU, all water soluble agents.

SB, 5FU and DOX delivery was compared to conventional drug delivery data. In the case of 5FU and SB calculations based of experimental data and assumptions suggested the potential of delivering more drug using our delivery platform than the available systemic delivery. In the case of DOX actual experimental release data were compared to systemic delivery of DOX from liposomes. And again our platform was found to deliver more drug than the systemic administration of liposomal DOX. However, there is still need to improve DOX release percents from our PLGA microbubbles, and minimize DOX burst effect.

SB, 5FU and DOX non-delivered drug amount were 6, 58 and 6 times smaller than the systemic exposure of the conventionally administered drugs, respectively. This is an important feature of our local drug delivery platform that may result in minimizing harmful side effects associated with cellular toxicity of chemotherapeutic drugs.

4.3 *In Vivo Tests*

4.3.1 *Ultrasound Enhancement in Rabbit Kidney*

This test was set as part of a bigger study testing the echogenicity of CA fabricated in our lab. One rabbit was dedicated to test SB-PLA (4% loaded by incorporation) against PLA control. Injections of CA summary are presented in below Table 4-16.

Table 4-16 Injections summary for rabbit kidney, using Sudan-PLA (4% incorporated) and BSA-PLA (15% dry adsorbed, pH 7.4, 4°C)

Rabbit #2 R47350	PLA (control)	BSA-PLA	SB-PLA
Injection #	6,7	4,5	1,2,3,8,9
Enhancement duration [min]	5	4	4
Enhancement quality	Powerful Intense	Fair Less intense	Very good Intense

It can be seen from Table 4-16 that plain PLA CA had better echogenicity, powerful and intense, in comparison to both loaded PLA. SB-PLA CA had better echogenicity than BSA-PLA as expected. This correlates with in vitro experiments, where SB-PLA demonstrated 22.3dB echogenicity, Figure 4-35, and signal stability of 91.0% after 15 minutes of insonation, Figure 4-36, and BSA-PLA 17.1dB, Figure 4-27, maintaining 79.1% of signal after 15 minutes of insonation, Figure 4-28. Figure 4-63 shows color Doppler image of rabbit kidney before and after injection of SB-loaded PLA CA. This figure qualitatively demonstrates the enhancement effect of our SB-loaded CA. The intense signal was seen for at least 4 minutes.

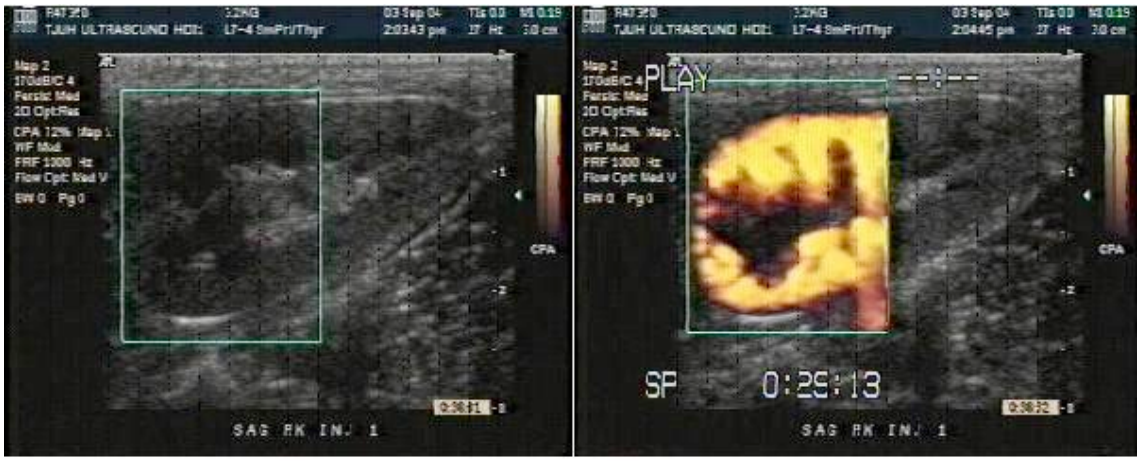

Figure 4-63 Color Doppler image of a rabbit kidney before (left) and after injection of SB-loaded PLA. Four percent of SB were loaded using incorporation. CA was injected through the ear vein. Power Doppler imaging was done with a broad bandwidth L12-5 transducer (5-12 MHz), a PRF of 700 kHz and a mechanical index of 0.33.

4.3.2 *Lymph Node and Lymph Channels Dyeing*

Sentinel lymph node is the hypothetical first lymph node or group of nodes reached by metastasizing cancer cells from a tumor. Sentinel lymph nodes identification plays a role is the staging and treatment of several kinds of cancer. The need to locate lymph channels that drain primary tumors, and serve as spreading channels for migrating cancer cells, led to the development of techniques for this purpose (Mathelin et al., 2007). Some of those techniques rely on injection of radio-labeled substance and a blue dye near the tumor and require an invasive step to visualize it, which bares its own risks. The lymph nodes that are shown to pick up the dye are considered sentinel lymph nodes and are removed for pathological examination for cancer cells identification. Development of a CA that carry a dye and use of ultrasound (lymphosonography) may be offered as an alternative (Goldberg, Merton, Liu, Murphy, & Forsberg, 2005).

The purpose of the present study was to see if these CA can enhance sentinel lymph nodes (SLNs) on ultrasound imaging by subcutaneous injection, and test the ability of drug loaded CA

to travel along lymph channel reaching to their lymph nodes. For this purpose sudan black loaded CA are most suitable since their color is visibly detectable and can be matched with ultrasound signal enhancement. In this study 4 rabbits were used and imaged using Sudan-PLA (2%, incorporated). The contrast agent was identified upon autopsy because of its intense blue color. Table 4-17 summarizes the injections.

Table 4-17 Injection summary of SB-PLA for rabbit lymph nodes and lymph channels lymphosonography and staining in four rabbits

	Injections to the left body side	Injections to the right body side
Rabbit #919: Leg	SB-PLA 0.25mL of 50mg/mL CA Figure 4-62	Control (Sonozoid) Figure 4-62
Lymph node		SB-PLA: 0.25mL of 50 mg/mL CA Strong enhancement from lymph node Sudan quantification: 0.27mg
Rabbit #918: Foot	Control (PLA) No staining	SB-PLA: 0.25mL of 50 mg/mL CA Staining at injection site
Rabbit #917: Isolated node	Control (PLA) Echogenic	SB in saline (control) 0.001g/mL SB quantification: 0.36mg
Kidney		Control (PLA)
Rabbit #916: Leg	SB-PLA 0.25mL of 50 mg/mL CA Very echogenic SB quantification: 0.28mg Figure 4-65	Control (PLA) Very echogenic No staining Figure 4-65

Figure 4-64 shows the sentinel lymph nodes of rabbit #919 legs after injections. On the left is SLN from the leg that received SB-PLA and on the right is the right leg SLN that was injected with plain CA, control. It can be seen that the SB was staining the SLN. Figure 4-65 shows the same injections for rabbit #916, it is clear that SB-PLA CA reached the SLN, as confirmed by echogenicity.

Figure 4-64: Sentinel lymph nodes of rabbit legs after injections: Left - Sudan-PLA in of 0.25mL of 50mg/mL Sudan-PLA (2%, incorporated), right – control

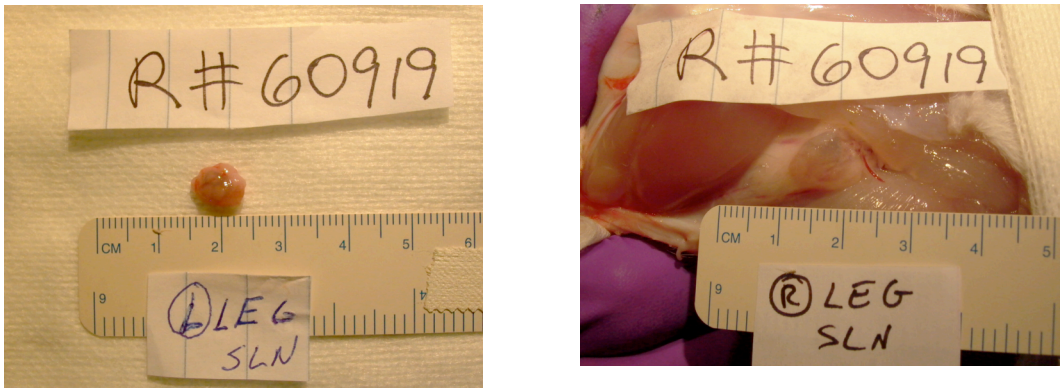

Figure 4-65: Sentinel lymph nodes of rabbit legs after injections: Left - SB-PLA in of 0.25mL of 50mg/mL SB-PLA (2%, incorporated), right – control

These results demonstrate the potential of PLA contrast agent to serve as a CA and for identification and discrimination of SLN to act as a benign imaging method which will allow

the surgeon to make critical decisions about the extent of spread of the cancer and the need for lymph node removal.

5. Drug Release - Preliminary Results and Future Work

5.1 *Drug Release*

As explained in the introduction to this work, chapter 1, the long term goal of this project is to use these CA as drug carriers and use ultrasound to release their payload. In light of this aim, some preliminary experiments were done to assess drug release using ultrasound in vitro. Those preliminary results are presented below.

Drug release in general is affected by many parameters mainly preparation conditions and release conditions. In the case of drug release in vivo the release conditions are pre-set limiting the release to physiological environment properties, hence the best way to affect drug release is by optimizing its loading. This chapter presents several effects of drug loading on drug release.

5.1.1 *Effect of Loading Method*

Loading method was found to have a significant effect on drug loading, as seen in chapter 4. We hypothesized that loading method will also have an effect on drug release. The detailed protocol for drug release experiments in given in Appendix J. Briefly, 10mg of dry drug-loaded CA were suspended in 1mL PBS, the suspension was added to the sample vessel including 50mL of PBS, and stirred. Ultrasound was turned on after time zero sample was taken out. Samples of 700µL were taken out every 2 minutes, centrifuged to separate free drug from CA, and plated for fluoresces or absorbance detection. Figure 5-1 shows the comparison of loading methods, using 1.44% DOX, applying ultrasound frequency of 5MHz for 30 minutes. It can be seen that release percents were poor over time, and no increase in release was seen over time for incorporated DOX and wet adsorbed DOX. DOX release from dry adsorbed samples was 15% over a period of 30 minutes of insonation. These trends were unexpected. The only difference among the loading methods is their drug burst effect. Drug burst effect is due to the detachment of poorly attached drug immediately when dry drug-loaded CA are added to solution. This effect is unwanted, and should be minimized if possible. One way to minimize it, would be to

add another step of preparation prior to insertion of drug loaded CA into solution. In this step dry-loaded CA are dipped in solution, and then collected by centrifugation separating free burst drug form bound drug. It can be seen that when the drug was surface adsorbed onto the CA surface, in the cases of dry and wet adsorption, the burst effect was 32% and 13% higher than for incorporated drug burst, respectively.

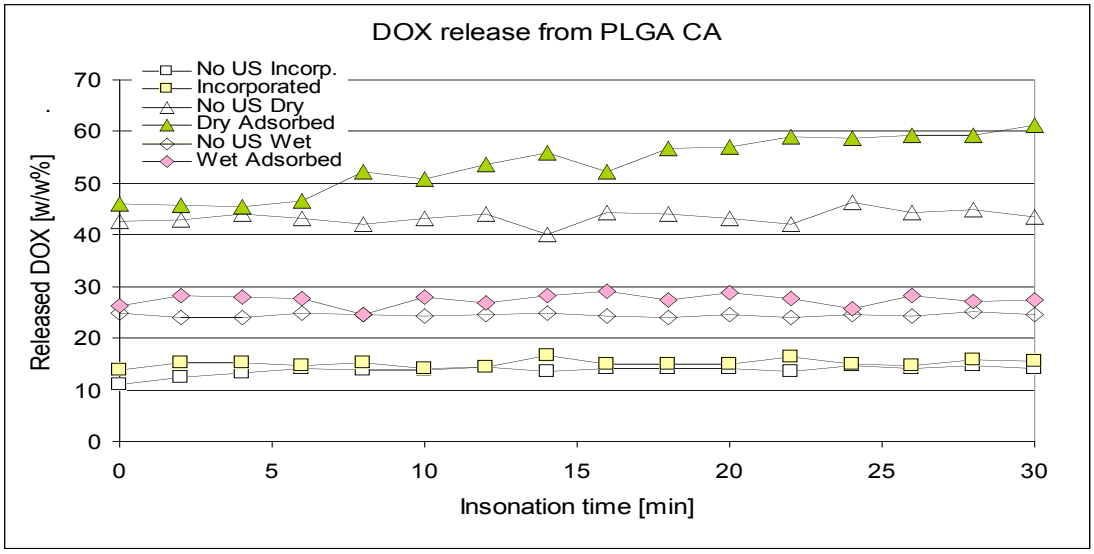

Figure 5-1 Ultrasound triggered DOX release comparison for three loading methods: incorporation, dry adsorption and wet adsorption. Control, stirred sample for 30 minutes without ultrasound, for each group is shown (in matching open shape). Experimental conditions: 5MHz, energy level 4, 1.44 % DOX.

Burst effect depends on microbubble surface morphology, shell porosity and drug loading method among other parameters (Wong et al., 2001). One step that is done in order to minimize burst is washing of loaded microbubbles before freeze drying them to make sure the frozen ones would not include free drug.

Incorporation, on one hand, is a method where drug is part of the shell composition and hence it is less affected by these effects, on the other hand, however, incorporated DOX was not released using the current ultrasound regime. Adsorption, as mentioned in the introduction, is attachment of drug onto the surface of microbubbles by non-covalent forces, such as, polarity, hydrogen bonds and electrostatic attractions. It is expected that adsorbed drug would be released more easily than incorporated drug. Wet adsorbed drug showed a 19% smaller burst effect than dry adsorbed drug.

The one fact that is common for all three methods is that freeze drying is taken place after drug is loaded. Some preliminary tests that were done in our lab suggested that freeze drying itself plays a part in interfering with drug-microbubble integrity, and exposing the loaded CA to burst effect. One possible way to overcome the harm of freeze drying is to protect the loaded CA with a lyoprotector agent, i.e. sugar, before freeze drying. Some preliminary experiments with mannitol were done in our lab testing mannitol as a lyoprotector. In that experiment different ratios of mannitol:PLA were used 0.15:1, 0.25:1, 0.5:1, 1:1. Mannitol was added to the wet microbubbles suspension just before they were frozen and lyophilized. A ratio of 0.25:1, mannitol:PLA was found to yield the most echogenic CA.

5.1.2 *Effect of PVA Concentration*

In order to improve drug release by ultrasound several approaches were taken. One of them was to explore the surfactant, PVA, and to investigate if its concentration had any effect on drug release. The surfactant is used to stabilize microbubbles integrity and prevent them from aggregating. There are several factors regarding surfactant that can be explored in respect to drug release i.e., type, concentration and molecular weight. In this preliminary experiment surfactant concentration effect on drug release was assessed, Figure 5-2. It can be seen that increasing PVA concentrations results in increase in drug release. This is supported by the fact that surfactant protects microbubbles from aggregating. When using less surfactant it is possible

that microbubbles tend to aggregate, having less surface area available for drug to be exposed to the medium, and be released.

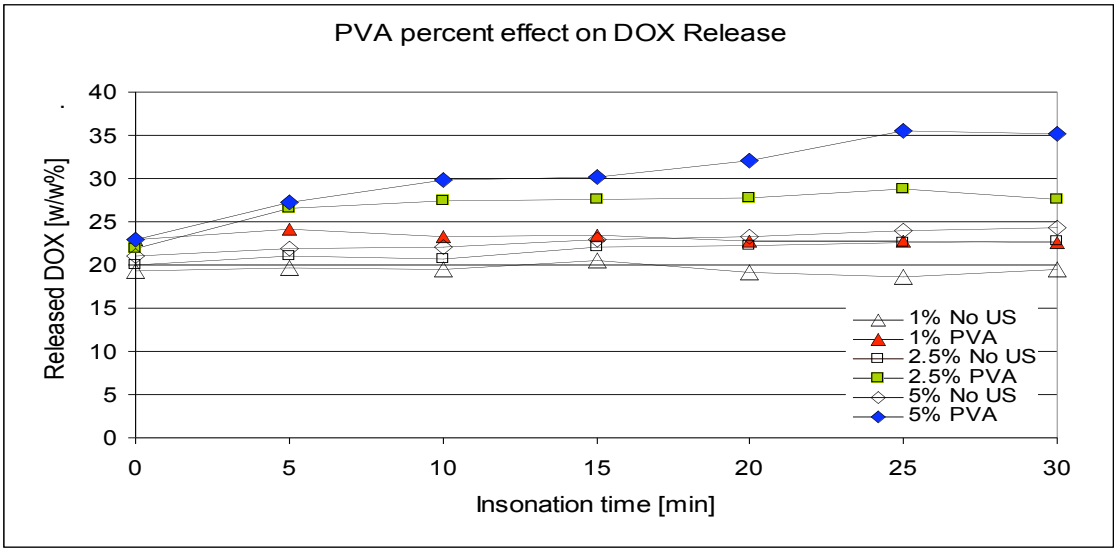

Figure 5-2 PVA concentration effect on DOX release. DOX was loaded using dry adsorption method, 3% drug. PVA concentrations vary from 1% to 5%. Control, stirred sample for 30 minutes without ultrasound, for each group is shown (in matching open shape). Experimental conditions: 5MHz, energy level 4.

This experiment shows the potential of changing PVA concentration and affecting drug release, it would be interesting to expand it for higher concentrations of PVA, and to other PVA with different molecular weights and see if drug release can be optimized or burst effect could be minimized. Other surfactants may also be considered for future research.

5.1.3 *Effect of Ultrasound Frequency*

The effect of ultrasound frequency on drug release was widely tested, for different systems of drug delivery. In order to optimize drug release we wanted to find the best set up conditions.

This optimization was done for FITC-BSA loaded PLA using 15% drug and dry adsorption method. Results are shown in Figure 5-3. It can be seen that using 7.5 MHz yield the most released FITC-BSA. It would be interesting to expand this experiment for PLGA and other drugs, and also to correlate the results with size distribution and attenuation.

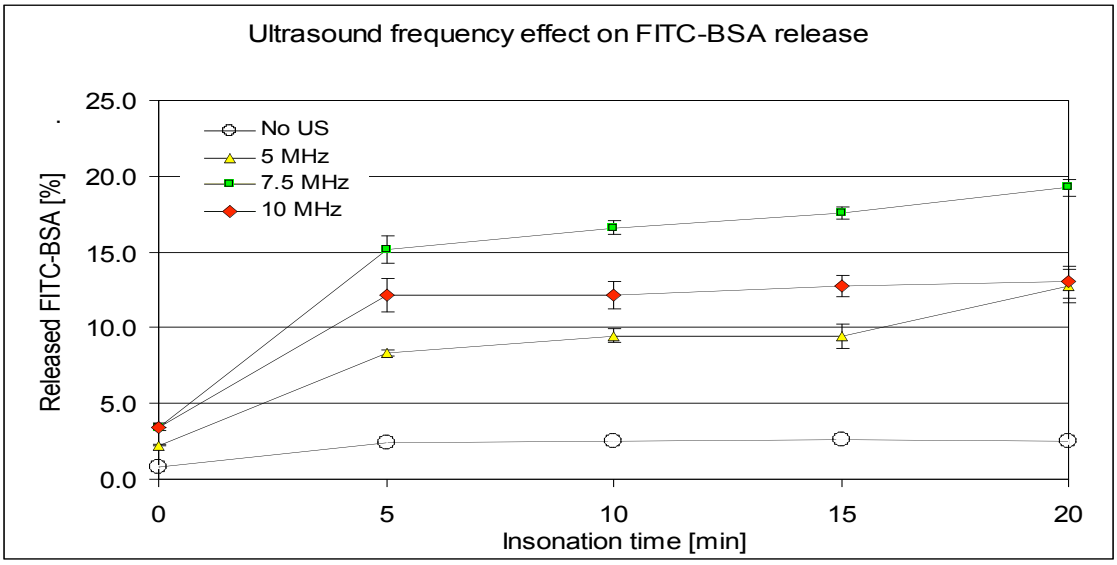

Figure 5-3 Ultrasound frequency effect on FITC-BSA release from PLA. FITC-BSA was loaded using dry adsorption method, 15% protein, 3 h, at 4°C. ultrasound was operated at energy level 4 (n=3, $p<0.0001$).

5.2 *Mixing Nanobubbles and Microbubbles*

Nanoparticles for drug delivery are widely investigated now especially because they can offer several advantages based on their size alone, over micron sized vehicles. Similarly to microbubbles/microspheres, nanoparticles can carry drugs and bear targeting agents to facilitate their accumulation in the target site. However, nano bubbles have more surface area per volume

to offer for surface attachment and conjugation than microbubbles. Being in the size range of tenths to hundredths of microns they can penetrate deep into tissues through fine capillaries and are generally take up efficiently by cells, having the potential to mimic macromolecules in vivo (J. Liu, Li, Rosol, Pan, & Voorhees, 2007; Panyam & Labhasetwar, 2003). Translating this to cancer drug delivery, nanoparticles can carry chemotherapeutic agents and easily leak from the neo-vascularization endothelial layer directly into the tumor tissue.

Cheng et al. investigated the ability to control polymeric nanoparticles size by changing parameters within their preparation method. Solvent type, polymer concentration and solvent:water ratio were reported to affect nanoparticles size. When conjugating those nanoparticles with targeting agents, nanoparticles demonstrated enhanced accumulation in prostate cancer tissue (Cheng et al., 2007). Rapoport et al. reported on injecting nano-micelles to the circulation of tumor inoculated mice, which were passively targeted to the tumor. After extravasating into the tumor tissue by leakage from the neo-vascularization, nano-micelles coalesced to form micro-micelles. Ultrasound energy that was applied (20 kHz) caused cavitation of micro-micelles and drug release (Rapoport et al., 2007).

Echogenic nanobubbles are still under investigation and development (Oeffinger & Wheatley 2004; Gao et al., 2008), however, nanobubbles can still be used to enhance drug delivery to solid tumors in mixtures with microbubbles. In this fashion, nanobubbles provide the drug payload delivery and the microbubbles provide ultrasound imaging enhancement and drug release mechanism. Based on this hypothesis, we used a mixture of drug loaded PLGA microbubbles with PLA nanobubbles that were fabricated in our lab, to test echogenicity and DOX release in vitro.

Nanobubbles were prepared by Seunglee Kwon. Briefly, PLA nanobubbles were prepared using a solvent diffusion method with acetone. When tested they did not show echogenicity. PLGA microbubbles were loaded with 3% DOX using wet adsorbed method. Two mg of nanobubbles and 1mg of microbubbles were mixed and suspended in 800µL of PBS. An initial

dose of 120µL of this suspension was added to a 50mL PBS in a stirred sample vessel. Ultrasound was turned on using a 5MHz frequency, energy level 4 for 30 minutes. Samples of 700µL were taken out each 10 minutes starting a time zero just before ultrasound was turned on.

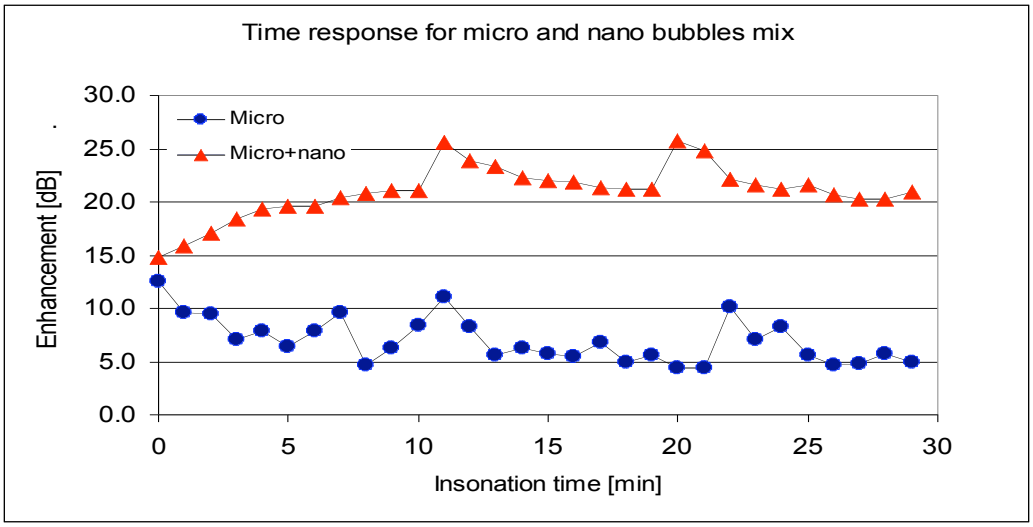

Figure 5-4 Time response curves for DOX-loaded microbubbles in comparison to a mixture of DOX-loaded microbubbles and nanobubbles. Conditions: 3% DOX was loaded onto PLGA using wet adsorbed method. Ultrasound frequency was 5MHz, energy level 4.

The results for time response curves are shown in Figure 5-4. The high peaks at 10 minutes and 20 minutes intervals are artifacts of pipettor tip insertion for sampling purpose. It can be seen that microbubbles alone showed a normal signal decay over time of insonation, as seen for all previously tested polymeric CA. The mixture of nano and micro bubbles yield an increase in signal stability over time of insonation. These findings suggest that addition of nanobubbles increases the stability of presenting microbubbles, the mechanism for this phenomenon should be further explored.

Drug release study was done with the same set up as time response where, 10mg of PLGA loaded microbubbles were suspended in 1mL PBS. One mL of this suspension was added to 50mL PBS in a sample vessel. The sample was insonated for 30 minutes, and 700µL samples were taken out every 10 minutes. For the nano/microbubbles mixture test 20mg of nanobubbles was suspended with 10mg of DOX loaded microbubbles in 1mL of PBS. One mL of mix suspension was added to a 50mL PBS in a sample vessel. Ultrasound was turned on and samples were taken out 700µL were taken out each 10 minutes starting a time zero just before ultrasound was turned on. The same procedure was done for 20mg nanobubbles alone.

Figure 5-5 shows DOX release results for mixture of nano and microbubbles in comparison to microbubbles alone, with and without ultrasound. It can be seen that ultrasound enhanced DOX release for both microbubbles and nano/microbubbles mixture in comparison to samples that were not insonated, in 2.5% and in 4.5%, respectively.

Deng et al., investigated cavitation and cavitation threshold in vitro using polystyrene nanoparticles as cavitation nuclei (Deng et al., 1996). They explored the cavitation dependence on particle size and concentration as well as medium viscosity. Polystyrene particles of diameter 0.1-1µm, used in concentration of $6*10^{10}$ particles/mL had a threshold of 4.43±0.66 MPa when using a 4.3 MHz spherical transducer. Larina et al., used nanoparticles to lower cavitation threshold in tumor vicinity and used it to enhance free drug delivery that was co-injected with the nanoparticles (Larina et al., 2005b). In light of these findings our experiment should be repeated and expanded for a wider range of nano:micro bubbles ratios, and include a thorough investigation of cavitation phenomenon for our in vitro set up.

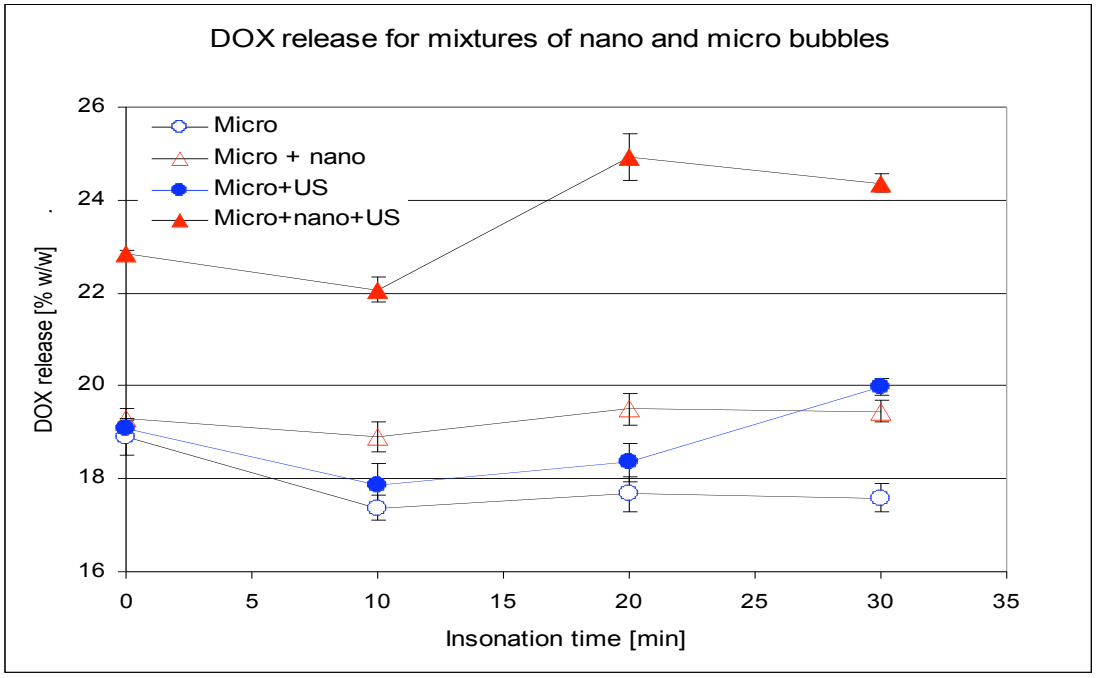

Figure 5-5 DOX release from mixtures of micro and nanobubbles with and without ultrasound. Conditions: 3% DOX was loaded using wet adsorption method, ultrasound frequency 5MHz, energy level 4. Solid with ultrasound, non-solid no ultrasound. Means are significantly different, for $P<0.05$, by one way ANOVA test (n=3, ± standard error from the mean)

5.3 *In Vivo Feasibility Test in Tumor Model*

This feasibility test was done to test BSA-loaded PLA and SB-loaded PLA CA acoustic performance on animal model, as additional part of a larger animal study. The details of animal model, tumor induction and imaging tools are detailed below.

Animal model: Mice that were induced with tumors originating from inoculated breast cancer (melanoma) cells 7 weeks prior to imaging, detailed protocol is presented in Appendix B. Contrast enhanced ultrasound evaluations of the melanoma xenografts were performed 7 weeks after tumor implantation.

Ultrasound imaging: Mice were imaged using a Sonoline Elegra scanner (Siemens Medical Solutions, Issaquah, WA) and a 7.5 MHz linear array transducer. All imaging parameters were kept constant before and after contrast administration (Mechanical Index below 0.5 was used to limit the amount of bubble destruction). The time between injections was at least 10 minutes to allow the contrast agent to clear the blood pool. Upon completion of the study, the mice were euthanized with an intracardiac injection.

Contrast agents in test: Forty mg of CA were weighted and placed in vials ready for use. Just before injection 1mL of saline was added to one CA vial, and the vial was gently shaken to properly suspend the CA. Mice were injected with Sudan-PLA (4%, loaded by incorporation) and PLA-BSA (5%, loaded by adsorption). Injected dose was 10μl/kg of loaded-CA (0.04 g/ml/kg) into the tail vein.

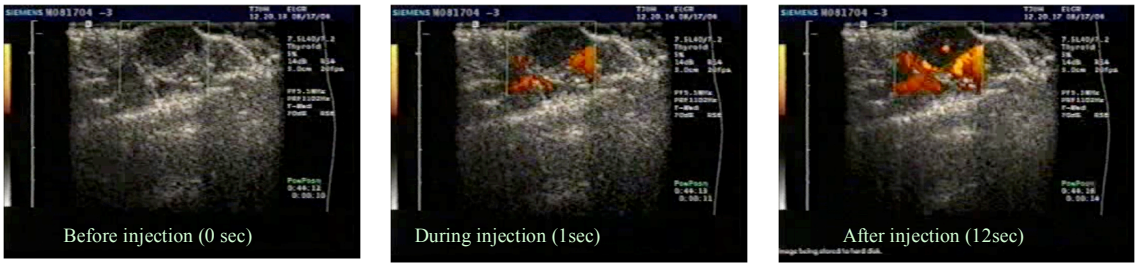

Figure 5-6 A time sequence of pictures showing the progress of perfusion of FITC-BSA-loaded PLA before injection (time zero, left) and after injection (1 sec later, middle, and 12 sec after injection, right) injection to the tail vain of a mouse. The CA seen to perfuse to the blood vessels feeding the tumor and some of it starts to show inside the tumor itself. Conditions: Elegra scanner (Siemens) with 7.5MHz probe.

When injecting BSA-loaded PLA CA there was a good echogenicity coming back from the periphery of the tumor, the enhancement increased in a pulsatile fashion as more CA was coming into the insonation field. The enhancement effect lasted 6 minutes. The sequence of

images in Figure 5-6 show the progress of contrast starting just before injection time (zero) to 12 seconds later.

When injecting SB-loaded PLA there was a good enhancement that lasted more than 11 minute. The CA progressed inside the tumor but didn't penetrate deep since this tumor was too large (1.5cm*2 cm) and the center was probably necrotic. These results show the potential to use our drug-loaded CA in vivo and demonstrate their stability. Further study is necessary to quantify dose response and drug delivery in vivo.

6. Conclusions and Recommendations

Polymeric CA that were developed in our lab are capable of carrying drugs of different characteristics as well as enhancing ultrasound signals. Those CA were demonstrated to serve as dynamic platform for three loading methods, shell incorporation, wet adsorption and dry adsorption. The advantages and disadvantages of each method regarding the nature of the loaded model drugs and drugs were discussed. The loading process parameters, i.e., temperature, pH, drug concentration, incubation time, affecting drug loading were analyzed. Based on this work a complex relationship was found to exist among the drug itself, its loading method and CA shell polymer. And each loaded substance was found to have its own set of loading parameters and loading method.

The final recommendations regarding the model drugs are to use incorporation for protein drugs, although it did not yield the highest loading it maintained the best echogenicity, when using a hydrophobic drug the best loading was obtained by incorporation of the drug and this was confirmed by echogenicity as well.

The final recommendations regarding loading of anticancer drugs are to use wet adsorption for loading 5-FU onto PLA CA and for loading DOX onto PLGA CA.

Moreover, our CA can carry anticancer drugs that are in clinical use and known to have important therapeutic effects, which are compromised by their reactivity and toxicity.

The potential of ultrasound to enhance the release of drug loaded PLA and PLGA CA was preliminarily studied and more experiments are currently being carried out to further understand the factors affecting drug release in the present system.

Additional further experimentation may be done on cell cultures and in vivo:

- Assessment of effects of insonation in different regimes (frequency, pressure, duty cycle) on drug release, and drug release effects on cancer cell death in cell cultures.
- Understanding the mechanism by which ultrasound acts on our CA and enhances drug release.

- In vivo tests to prove drug delivery and drug efficacy on tumor induced animal models.
- In vivo tests to quantify the ultrasound effect on drug delivery and drug efficacy.

Since our long term goal is to produce drug loaded CA systems serving as actual products in the cancer therapeutic field, further thought should be dedicated to finding a suitable technique to sterilize them. This aspect is already being explored.

An integral part of the drug delivery system that we are developing is its targeting capabilities to cancer tumor cells. The CA surface activation and attachment of targeting agents is currently under advanced research.

Our micro-sized drug -loaded CA can also be used in mix with nano-size polymeric CA. This is another vast field of interest that is pursued in our lab in parallel to this work, and several preliminary experiments were already done in this direction.

To conclude, this research was carried out in order to further develop a biodegradable chemotherapeutic drug delivery system and understand its capabilities to carry drugs, where ultrasound is used for imaging and therapeutic effects enhancement. Cancer is a worldwide concern and even though the road for its elimination is still long, major research is dedicated towards minimizing it.

7. List of References

Alexandrov, A. V. (2006). Ultrasound enhanced thrombolysis for stroke. [Journal Article]. *International Journal of Stroke, 1*, 26-29.

Amantea, M. A., Forrest, A., Northfelt, D. W., & Mamelok, R. (1997). Population pharmacokinetics and pharmacodynamics of pegylated-liposomal doxorubicin in patients with AIDS-related Kaposi's sarcoma. *CLINICAL PHARMACOLOGY & THERAPEUTICS, 61*(3), 301-311.

Arap, W., Pasqualini, R., & Ruoslahti, E. (1998). Cancer treatment by targeted drug delivery to tumor vasculature in a mouse model.[see comment]. *Science, 279*(5349), 377-380.

Basude, R., & Wheatley, M. A. (2001). Generation of ultraharmonics in surfactant based ultrasound contrast agents: use and advantages. *Ultrasonics, 39*(6), 437-444.

Baxter, L. T., & Jain, R. K. (1991). Transport of fluid and macromolecules in tumors : III. Role of binding and metabolism. *Microvascular Research, 41*(1), 5-23.

Bekeredjian, R., Grayburn, P. A., & Shohet, R. V. (2005). use of ultrasound contrast agents for gene or drug delivery in cardiovascular medicine. [Journal Article]. *Journal of the American College of Cardiology, 45*(3), 329-335.

Bukowski, R. M., Inoshita, G., Yalavarthi, P., Murthy, S., Gibson, V., Budd, G. T., et al. (1992). A Phase I Trial of 5-Fluorouracil, Folinic Acid, and Alpha-Pa-Interferon in Patients With Metastatic Colorectal Carcinoma. [Journal Article]. *Cancer, 69*(4), 889-892.

Butler, S. M., Tracy, M. A., & Tilton, R. D. (1999). Adsorption of serum albumin to thin films of poly(lactide-co-glycolide). [Journal Article]. *Journal of Controlled Release, 58*(3), 335-347.

Charrois, G. J. R., & Allen, T. M. (2004). Drug release rate influences the pharmacokinetics, biodistribution, therapeutic activity, and toxicity of pegylated liposomal doxorubicin formulations in murine breast cancer. *Biochimica et Biophysica Acta (BBA) - Biomembranes, 1663*(1-2), 167-177.

Cheng, J., Teply, B. A., Sherifi, I., Sung, J., Luther, G., Gu, F. X., et al. (2007). Formulation of functionalized PLGA-PEG nanoparticles for in vivo targeted drug delivery. [Journal Article]. *Biomaterials, 28*, 869-876.

Correas, J.-M., Bridal, L., Lesavre, A., Mejean, A., Claudon, M., & Helenon, O. (2001). Ultrasound contrast agents: properties, principles of action, tolerance, and artifacts. [Journal Article]. *European Journal of Radiology, 11*, 1316-1328.

Chumakova, O. V., Liopo, A. V., Evers, M. B., & O., E. R. (2006). Effect of 5-Fluorouracil, Optison and ultrasound on MCF-7 cell viability. [Journal Article]. *Ultrasound in Medicine and Biology, 32*(5), 751-758.

Cui, W., Bei, J., Wang, S., Zhi, G., Zhao, Y., Zhou, X., et al. (2005). Preparation and evaluation of Poly(L-lactide-co-glycolide) (PLGA) microbubbles as a contrast agent for myocardial contrast echocardiography. [Journal Article]. *Journal of Biomedical materials research Part B: Applied Biomaterials, 73B*, 171-178.

Dalecki, D. (2004). Mechanical bioeffects of ultrasound. [Journal Article]. *Annual reviews in Biomedical Engineering, 6*, 229-248.

Dayton, P., Klibanov, A. L., Brandenburger, G. H., & Ferrara, K. W. (1999). Acoustic radiation force in vivo: a mechanism to assist targeting of microbubbles. [Journal Article]. *Ultrasound in Medicine & Biology, 25*(8), 1195-1201.

de Jong, N., Hoff, L., Skotland, T., & Bom, N. (1992). Absorption and scatter of encapsulated gas filled microspheres: Theoretical considerations and some measurements. *Ultrasonics, 30*(2), 95-103.

Deng, C. X., Xu, O., Apfel, R. E., & Holland, C. K. (1996). Inertial cavitation produced by pulsed ultrasound in controlled host media. [Journal Article]. *The Journal of the Acoustical Society of America, 100*(2), 1199-1208.

De Rosa, G., Quaglia, F., La Rotonda, M. I., Apple, M., Alphandary, H., & Fattal, E. (2002). Poly(lactic-co-glycolide) microspheres for the controlled release of oligonucleotide/polyethylenimine complexes. [Journal Article]. *Journal of Pharmaceutical science, 91*(3), 790-799.

Delius, M., Ueberle, F., & Gambihler, S. (1994). Destruction of gallstones and model stones by extracorporeal shock waves. *Ultrasound in Medicine & Biology, 20*(3), 251-258.

Eassa, W. A., Sheir, K. Z., Gad, H. M., Dawaba, M. E., El-Kenawy, M. R., & Elkappany, H. A. (2008). Prospective Study of the Long-Term Effects of Shock Wave Lithotripsy on Renal Function and Blood Pressure. *The Journal of Urology, 179*(3), 964-969.

El-Sherif, D. M., Lathia, J. D., Le, N. T., & Wheatley, M. A. (2003). Ultrasound degradation of novel polymer contrast agents. [Journal Article]. *Journal of Biomedical materials research, 68A*(1), 71-78.

El-Sherif, D. M., & Wheatley, M. A. (2003). Development of a novel method for synthesis of a polymeric contrast ultrasound agent. [Journal Article]. *Journal of Biomedical materials research, 66A*, 347-355.

Faisant, N., Akiki, J., Siepmann, F., Benoit, J. P., & J., S. (2006). Effects of the type of release medium on drug release from PLGA-based microparticles: experiment and theory. [Journal Article]. *International Journal of Pharmaceutics, 314*, 189-197.

Faisant, N., Akiki, J., Siepmann, F., Benoit, J. P., & Siepmann, J. (2006). Effects of the type of release medium on drug release from PLGA-based microparticles: experiment and theory. [Journal Article]. *International Journal of Pharmaceutics, 314*, 189-197.

Ferrara, K. W., & Merritt, C. R. B. (2000). Evaluation of tumor angiogenesis with US: Imaging, Doppler, and contrast agents. [Journal Article]. *Academic Radiology, 7*, 824-839.

Forsberg, F. (Ed.). (2001). *Physics of ultrasound contrast agents* (1st ed.). London: Martin DunitzLtd.

Forsberg, F., & Goldberg, B. B. (2000). Subharmonic imaging of contrast agents. [Journal Article]. *Ultrasonics, 38*, 93-98.

Forsberg, F., Lathia, J. D., Merton, D. A., Liu, J.-B., Le, N. T., Goldberg, B. B., et al. (2004). Effect of shell type on the in vivo backscatter from polymer-encapsulated microbubbles. *Ultrasound in Medicine & Biology, 30*(10), 1281-1287.

Forsberg, F., Ro, R., Potoczek, M., Liu, J.-B., Merritt, C. R. B., James, K. M., et al. (2004). Assesment of angiogenesis: implications for ultrasound imaging. [Journal Article]. *Ultrasonics, 42*, 325-330.

Forsberg, F., Wu, Y., Makin, I. R. S., Wang, W., & Wheatley, M. A. (1997). Quantitative acoustic characterization of a new surfactant-based ultrasound contrast agent. [Journal Article]. *Ultrasound in Medicine & Biology, 23*(8), 1201-1208.

Foster, Stuart F., Burns, P. N., Simpson, D. H., Wilson, S. R., & Christopher, D. A. (2000). Ultrasound for the visualization and quantification of tumor microcirculation. [Journal Article]. *Cancer and metastasis reviews, 19*, 131-138.

Freiberg, S., & Zhu, X. X. (2004). Polymer microspheres for controlled drug release. *International Journal of Pharmaceutics, 282*(1-2), 1-18.

Gabizon, A., Isacson, R., Rosengarten, O., Tzemach, D., Shmeeda, H., & Sapir, R. (2008). An open-label study to evaluate dose and cycle dependence of the pharmacokinetics of pegylated liposomal doxorubicin. *Cancer Chemother Pharmacol, 61*, 695–702.

Gao, Z., Kennedy, A. M., Christensen, D. A., & Rapoport, N. Y. (2008). Drug-loaded nano/microbubbles for combining ultrasonography and targeted chemotherapy. [Journal Article]. *Ultrasonics, In Press, Corrected Proof*, in press.

Garmiak, R., & Shah, P. M. (1968). Echocardiography of the aortic root. [Journal Article]. *Invest Radiology, 3*, 356-366.

Goldberg, B. B., Merton, D. A., Liu, J.-B., Murphy, G., & Forsberg, F. (2005). Contrast-enhanced sonographic imaging of lymphatic channels and sentinel lymph nodes. [Journal Article]. *Journal of Ultrasound in Medicine, 24*, 953-965.

Goldberg, B. B., Raichlen, J. S., & Forsberg, F. (Eds.). (2001). *Ultrasound contrast agents* (2nd ed.). London: Martin Dunitz Ltd.

Gopferich, A. (1996). Mechanisms of polymer degradation and erosion. [Journal Article]. *Biomaterials, 17*, 103-114.

Hamidi M, Zarei N, Zarrin A, & S, M.-S. (2007). Preparation and validation of carrier human erythrocytes loaded by bovine serum albumin as a model antigen/protein. [Journal Article]. *Drug delivery, 14*(5), 295-300.

Hanauske, A.-R., Cassidy, J., Sastre, J., Bolling, C., Jones, R. J., Rakhit, A., et al. (2007). Phase1bDose Escalation Studyof Erlotinibin Combinationwith Infusional 5-Fluorouracil, Leucovorin, and Oxaliplatin in Patients with Advanced SolidTumors. [Journal Article]. *Clinical Cancer Research, 13*(2), 523-531.

Husseini, G. A., Christensen, D. A., Rapoport, N. Y., & Pitt, W. G. (2002). Ultrasonic release of doxorubicin from Pluronic P105 micelles stabilized with an interpenetrating network of

N,N-diethylacrylamide. [journal Article]. *Journal of Colloid and Interface Science, 83*, 303-305.

Husseini, G. A., Myrup, G. D., Pitt, W. G., Christensen, D. A., & Rapoport, N. Y. (2000). Factors affecting acoustically triggered relese of drugs frompolymeric micelles. [Journal article]. *Journal of Controlled Release, 69*, 43-42.

Ikeda, T., Yoshizawa, S., Tosaki, M., Allen, J. S., Takagi, S., Ohta, N., et al. (2006). Cloud cavitation control for lithotripsy using high intensity focused ultrasound. *Ultrasound in Medicine & Biology, 32*(9), 1383-1397.

Jain, R. A. (2000). The manufacturing techniques of various drug loaded biodegradable poly(lactide-co-glycolide) (PLGA) devices. *Biomaterials, 21*(23), 2475-2490.

Jakobsen, J. A. (2001). Ultrasound contrast agents: clinical applications. *European Journal of Radiology, 11*, 1329-1337.

Jemal, A., Siegel, B., Ward, E., Murray, T., Xu, J., & Thun, M. J. (2007). Cancer statistics 2007. [Journal Article]. *CA: A cancer journal for clinicians, 57*, 43-66.

Jie, P., Venkatraman, S. S., Min, F., Freddy, B. Y. C., & Huat, G. L. (2005). Micelle-like nanoparticles of star-branched PEO-PLA copolymers as chenotherapeutic carrier. [Journal Article]. *Journal of controlled release, 110*, 20-33.

Kamiyama, N. (2004). Update of ultrasound contrast imaging. [Journal Article]. *International Congress series 1274*, 53-56.

Kamiyama, N., Moriyasu, F., Mine, Y., & Goto, Y. (1999). Analysis of flash echo from contrast agent for designing optimal ultrasound diagnostic systems. *Ultrasound in Medicine & Biology, 25*(3), 411-420.

Katayama, N., Tanaka, R., Ohno, Y., Ueda, C., Houjou, t., & Takada, K. (1995). Implantable slow release cyclosporin A (CYA) delivery system to thoracic duct. [Journal Article]. *International Journal of Pharmaceutics, 115*, 87-93.

Kelner, A., & Schacht, E. H. (2005). Tailor-made polymer for local drug delivery: release of macromolecular model drugs from biodegradable hydrogels based on poly(ethylene oxide). [Journal Article]. *Journal of Controlled Release, 101*, 13-20.

Keyhani, K., Guzman, H. R., Parson, A., Lewis, T. N., & Prausnitz, M. R. (2001). Intracellular drug delivery using low-frequency ultrasound: quantification of molecular uptake and cell viability. [Journal Article]. *Pharmaceutical Research, 18*(11), 1514-1520.

Kim, R., Osaki, A., & Toge, T. (2003). Feasibility and therapeutic efficacy of weeekly 1-h low-dose paclitaxel infusion for relapsed breast cancer. [Journal Article]. *Oncology Reports, 10*(1), 145-150.

Kinoshita, M., & Hynynen, K. (2005). Intracellular delivery of Bak BH3 peptide by microbubble-enhanced ultrasound. [Journal Article]. *Pharmaceutical Research, 22*(5), 716-720.

Kinsler, L. E., Frey, A. R., Coppens, A. B., & Sanders, J. V. (Eds.). (2002). *Fundamentals of acoustics* (4th ed.): John Wiely & sons, Inc.

Klaassen, U., Wilke, H., Strumberg, D., Eberhardt, W., Korn, M., & Seeber, S. (1996). Phase I study with a weekly 1 h infusion of paclitaxel in heavily pretreated patients with metastatic breast and ovarian cancer. *European Journal of Cancer, 32*(3), 547-549.

Konan, Y. N., Gurny, R., & Allemann, E. (2002). Preparation and characterization of sterile and freeze-dried sub-200 nm nanoparticles. [Journal Article]. *International Journal of Pharmaceutics, 233*, 239-252.

Kremkau, F. W., Shah, R., & Kramer, D. H. (1969). Ultrasound cardiography contrast studies in anatomy and function. [Journal Article]. *Radiology, 92*, 939-948.

Lanza, G. M., & Wickline, S. A. (2003). Targeted ultrasound contrast agents for molecular imaging and therapy. [Journal Article]. *Current problems in cardiology, 28*(12), 625-653.

Larina, I. V., Esenaliev, R. O., & Evers, M. B. (2005a). Optimal drug and gene delivery in cancer cells by ultrasound-induced cavitation. *Anticancer research, 25*, 149-156.

Larina, I. V., Evers, M. B., Ashitkov, T. V., Bartels, C., Larin, K. V., & Esenaliev, R. O. (2005b). Enhancement of drug delivery in tumors by using interaction of nanoparticles with ultrasound radiation. *Technology in Cancer Research & Treatment, 4*(2), 1-10.

Lathia, J. D., Leodore, L., & Wheatley, M. A. (2004). Polymeric contrast agent with targeting potential. [Journal Article]. *Ultrasonics, 42*, 763-768.

Lawrie, A., Brisken, A. F., Francis, S. E., Tayler, D. I., Chamberlain, J., Crossman, D. C., et al. (1999). Ultrasound Enhances Reporter Gene Expression After Transfection of Vascular Cells In Vitro. [Journal Article]. *Circulation, 99*(20), 2617-2620.

Lewis, D. D. (Ed.). (1990). *Controlled release of bioactive agents from lactide/glycolide polymers*. New York: Marcel Dekker.

Li, S., Hu, j., & Liu, B. (2005). A study on the adsorption behavior of protein onto functional microspheres. [Journal Article]. *Journal of chemical technology and biotechnology, 80*, 531-536.

Lin, R., Shi Ng, L., & Wang, C.-H. (2005). In vitro study of anticancer drug doxorubicin in PLGA-based microparticles. *Biomaterials, 26*(21), 4476-4485.

Lindner, J. R. (2002). [Journal Article]. *American Journal of Cardiology, 90*, 72J-80J.

Lindner, J. R. (2004). Microbubbles in medical imaging: current applications and future directions. [Journal Article]. *Nature reviews, 3*, 527-532.

Liu, J., Li, J., Rosol, T. J., Pan, X., & Voorhees, J. (2007). Biodegradable nanoparticles for targeted ultrasound imaging of breast cancer cells in vitro. [Journal Article]. *Physics in Medicine and Biology, 52*, 4739-4747.

Liu, L., Jin, P., Cheng, M., Zhang, G., & Zhang, F. (2006). 5-Fluorouracil-loaded self-assembled pH-sensitive nanoparticles as novel drug carrier for treatment of malignant tumors. [Journal Article]. *Chinese journal of chemical engineering, 14*(3), 377-382.

Liu, S. Q., Tong, Y. W., & Yang, Y.-Y. (2005). Incorporation and in vitro release of doxorubicin in thermally sensitive micelles made from poly(N-isopropylacrylamide-co-N,N-dimethylacrylamide)-b-poly(D,L-lactide-co-glycolide) with varying compositions. [Journal Article]. *Biomaterials, 26*, 5064-5074.

Maeda, H., Greish, K., & Fang, J. (2006). The EPR effect and polymeric drugs: a paradigm shift for cancer chemotherapy in the 21st century. [Journal Article]. *Advances in polymer science, 193*, 103-121.

Marret, H., Sauget, S., Giraudeau, B., Brewer, M., Ranger-Moore, J., Body, G., et al. (2004). Contrast-enhanced sonography helps in discrimination of benign from malignant adnexal masses. [journal Article]. *Journal of Ultrasound in Medicine, 23*, 1629-1639.

McLoon, L. K., & Wirtschafter, J. D. (1999). Direct Injection of Liposome-Encapsulated Doxorubicin Optimizes Chemomyectomy in Rabbit Eyelid. [Journal Article]. *Investigative Ophthalmology & Visual Science, 11*(40), 2561-2567.

Mathelin, C., Salvador, S., Croce, S., Andriamisandratsoa, N., Huss, D., & Guyonnet, J.-L. (2007). Optimization of sentinel lymph node biopsy in breast cancer using an operative gamma camera. [Journal Article]. *World Journal of Surgical Oncology, 5*(132), 1-6.

Misfeldt, M. L., & Grimm, D. R. (1994). Sinclair miniature swine: an animal model of human melanoma. [Journal Article]. *Vetrinary Immunology and Immunopathology, 43*, 167-175.

Mitragotri, S., Blankschtein, D., & Langer, R. (1995). Ultrasound-mediated transdermal protein delivery [Journal Article]. *Science, 269*(5225), 850-853.

Myhr, G., & Moan, J. (2006). Synergistic and tumor selective effects of chemotherapy and ultrasound treatment. [Journal Article]. *Cancer Letters, 232*, 206-213.

Narayan, P., & Wheatley, M. A. (1999). Preparation and characterization of hollow microcapsules for use as ultrasound contrast agents. [Journal Article]. *Polymer Engineering and Science, 39*(11), 2242-2255.

O'Driscoll, C. M., & Griffin, B. T. (2008). Biopharmaceutical challenges associated with drugs with low aqueous solubility--The potential impact of lipid-based formulations. *Advanced Drug Delivery Reviews, 60*(6), 617-624.

Oeffinger, B. E., & Wheatley, M. A. (2004). Development and characterization of a nano-scale contrast agent. *Ultrasonics, 42*(1-9), 343-347.

Oh, J. E., Nam, Y. S., Lee, K. H., & Park, T. G. (1999). Conjugation of drug to poly(,-lactic-co-glycolic acid) for controlled release from biodegradable microspheres. *Journal of Controlled Release, 57*(3), 269-280.

Omathanu, P., & Panchagnula, R. (2001). Polymers in drug delivery. [Journal Article]. *Current opinion in chemical biology, 5*, 447-451.

Panyam, J., & Labhasetwar, V. (2003). Biodegradable nanoparticles for drug and gene delivery to cells and tissue. [Journal article]. *Advanced Drug Delivery Reviews, 55*, 329-347.

Pareta, R., & Edirisinghe, M. J. (2006). A novel method for the preparation of biodegradable microspheres for protein drug delivery. *Journal of the Royal Society Interface, 3*, 573-582.

Parikh, R. H., Parikh, J. R., Dubey, R. R., Soni, H. N., & Kapadia, k. N. (2003). Poly (D,L-lactide-co-glycolide) microspheres containing 5-fluorouracil: optimization of process parameters. [Journal Article]. *AAPS PharmSciTech, 4*(2), 1-8.

Poole, C. J., Perren, T., Gawande, S., Ridderheim, M., Cook, J., Jenkins, A., et al. (2006). Optimized sequence of drug administration and schedule leads to improved dose delivery for gemcitabine and paclitaxel in combination: a phase I trial in patients with recurrent ovarian cancer. [journal Article]. *International Journal of Gynecological Cancer, 16*, 507-514.

Price, R. J., & Kaul, S. (2002). Contrast ultrasound targeted drug and gene delivery: an update on a new therapeutic modality. [Journal Article]. *Journal of Cardiovascular Pharmacology and Therapeutics, 7*(3), 171-180.

Price, R. J., Skyba, D. M., Kaul, S., & Skalak, T. C. (1998). Delivery of colloidal particles and red blood cells to tissue through microvessel ruptures created by targeted microbubbles destruction with ultrasound. *Circulation, 98*, 1264-1267.

Raisinghani, A., & DeMaria, A. N. (2002). Physical principles of microbubble ultrasound contrast agents. [Journal Article]. *American Journal of Cardiology, 90*, 3J-7J.

Rapoport, N., Gao, Z., & Kennedy, A. (2007). Multifunctional nanoparticles for combining ultrasonic tumor imaging and targeted chemotherapy. [Journal Article]. *Journal of National cancer institute, 99*, 1095-1106.

Rapoport, N., Pitt, W. G., Sun, H., & Nelson, J. L. (2003). Drug delivery in polymeric micelles: from in vitro to in vivo. [Journal Article]. *Journal of Controlled release, 91*, 85-95.

Rembielak, A., Cullen, J., Saleem, A., & Price, P. (2008). Imaging in cancer. *Medicine, 36*(1), 5-8.

Ruan, G., & Feng, S.-S. (2003). Preparation and characterization of poly(lactic acid)-poly(ethylene glycol)-poly(lactic acid) (PLA-PEG-PLA) microspheres for controlled release of paclitaxel. [Journal Article]. *Biomaterials, 24*, 5037-5044.

Ruoslahti, E. (2002). Specialization of tumor vasculature. [Journal Article, review]. *Nature, 2*, 83-90.

Rychak, J. J., Klibanov, A. L., & Hossack, J. A. (2005). Acoustic radiation force enhances targeted delivery of ultrasound contrast microbubbles: in vitro verification. [Journal Article]. *IEEE transactions on ultrasonics, ferroelectrics, and frequency control, 52*(3), 421-433.

Sherertz, E. F., Sloan, K. B., & McTiernan, R. G. (1987). Use of Theoretical Partition Coefficients Determined From Solubility Parameters to Predict Permeability Coefficients for 5-Fluorouracil. [journal Article]. *Journal of Investigative Dermatology, 89*, 147-151.

Sinha, B. K., & Lewis, G. J. (1981). Role of one-electron and two-electron reduction products of adriamycin and daunomycin in deoxyribonucleic acid binding. *Biochemical Pharmacology, 30*(18), 2626-2629.

Stride, E., & Saffari, N. (2003). Microbubble ultrasound contrast agents: a review. [Journal Article]. *Proceedings instn in mechanical Engineering, 217*, 429-447.

Suslick, K. S., & Price, G. J. (1999). Applications of ultrasound to materials chemistry. [Journal Article]. *Annual reviews in Materials Science, 29*, 295-326.

Takalkar, A. M., Klibanov, A. L., Rychak, J. J., Lindner, J. R., & Ley, K. (2004). Binding and detachment dynamics of microbubbles targeted to P-selectin under controlled shear flow. [Journal Article]. *Journal of Controlled release, 96*, 473-482.

Tamber, H., Johansen, P., Merkle, H. P., & Gander, B. (2005). Formulation aspects of biodegradable polymeric microspheres for antigen delivery. *Advanced Drug Delivery Reviews, 57*(3), 357-376.

Tan, E. C., Lin, R., & Wang, C.-H. (2005). Fabrication of double-walled microspheres for the sustained release of doxorubicin. *Journal of Colloid and Interface Science, 291*(1), 135-143.

Tang, H., Wang, C. C. J., Blankschtein, D., & Langer, R. (2002). An investigation of the role of cavitation in low-frequency ultrasound-mediated transdermal drug transport. [Journal Article]. *Pharmaceutical Research, 19*(8), 1160-1169.

Tilcock, C. (1999). Delivery of contrast agents for magnetic resonance imaging, computed tomography, nuclear medicine and ultrasound. [Journal Article]. *Advanced Drug Delivery Reviews, 37*, 33-51.

Tsutsui, J. M., Xie, F., & Porter, R. T. (2004). The use of microbubbles to target drug delivery. [Journal Article]. *Cardiovascular ultrasound, 2*(23), 1-7.

Unger, E., McCreery, T., Sweitzer, R., Caldwell, V. E., & Wu, Y. (1998). Acoustically active lipospheres containing paclitaxel: a new therapeutic ultrasound contrast agent. [Journal Article]. *Invest Radiology, 33*(12), 886-892.

Unger, E. C., McCreery, T. P., & Sweitzer, R. H. (1997). Ultrasound Enhances Gene Expression of Liposomal Transfection. [Journal Article]. *Investigative Radiology, 32*(12), 723-727.

van Wamel, A., Bouakaz, A., Versluis, M., & de Jong, N. (2004). Micromanipulation of endothelial cells: Ultrasound-microbubble-cell interaction. *Ultrasound in Medicine & Biology, 30*(9), 1255-1258.

Wang, B., Siahaan, T., & Soltero, R. (Eds.). (2005). *Drug delivery: principles and applications* (1 ed.): John Wiley & Sons, Inc.

Watanabe, H., Yamamoto, N., Tamura, T., Shimoyama, T., Hotta, K., Inoue, A., et al. (2003). Study of Paclitaxel and Dose Escalation of Cisplatin in Patients with Advanced Non-small Cell Lung Cancer. [Journal Article]. *Japanese journal of clinical Oncology, 33*(12), 626-630.

Wei, W., Zhengzhong, B., Yongjie, W., Lafeng, Y., & Yalin, M. (2004). A novel approach to quantitative ultrasonic naked gene delivery ans its non-incvasivve assessment. [Journal Article]. *Ultrasonics, 43*, 69-77.

Wheatley, M. A. (Ed.). (2001). *Composition of contrast microbubbles: Basic chemistry of encapsulated and surfactant-coated bubbles* (2nd ed.). London: Martin Dunitz Ltd.

Wischke, C., & Borchert, H. H. (2006). Fluorescein isothiocyanate labelled bovine serum albumin (FITC-BSA) as a model protein drug: opportunities and drawbacks. [Journal Article]. *Pharmazie, 61*(9), 770-774.

Wong, H. M., Wang, J. J., & Wang, C.-H. (2001). In vitro release of human immunoglobulin G from biodegradable microspheres. [Journal Article]. *Industrial Engineered chemistry research, 40*, 933-948.

Yang, Y.-Y., Chung, T.-S., & Ping Ng, N. (2001). Morphology, drug distribution, and in vitro release profiles of biodegradable polymeric microspheres containing protein fabricated by double-emulsion solvent extraction/evaporation method. *Biomaterials, 22*(3), 231-241.

Yip, D., Karapetis, C., Strickland, A. H., Steer, C., Holford, C., Knight, S., et al. (2003). A dose-escalating study of oral eniluracil/5-fluorouracil plus oxaliplatin in patients with advanced gastrointestinal malignancies. [Journan Article]. *Annals of Oncology, 14*, 864-866.

Yuh, E. L., Shulman, S. G., Mehta, S. A., Xie, J., Chen, L., Frenkel, V., et al. (2005). Delivery of systemic chemoterapeutic agent to tumors by using focused ultrasound: study is a murine model. *Radiology, 234*(2), 431-437.

Zaman, N. T., Tan, F. E., Joshi, S. M., & Ying, J. Y. (2006). Targeted stimuli-responsive Dextran conjugates for doxorubicin delivery to hepatocytes. [Journal Article].

Zderic, V., Clarck, J. I., Martin, R. W., & Vaezy, S. (2004). Ultrasound-enhanced transcorneal drug delivery. [Journal Article]. *Cornea, 23*(8), 804-811.

8. Appendices

8.1 *Appendix A: Contrast Agent Fabrication By Double Emulsion Method*

Fresh microbubbles are recommended to be used in each experiment; the following procedure is done in sets of three for convenience. Stock solutions to be made one day prior to microbubbles fabrication:

A. **5% Poly vinyl alcohol - PVA (for 0.5L preparation)**:

1. Weigh out 50g of PVA.
2. Heat 0.5L deionized water in a 1L beaker, to about 40-45°C, on a magnetic stir plate.
3. Gradually add the polymer, making sure no big aggregates are formed and that the solution is being well stirred, vortex flow reaches the bottom of the cup. Make sure the temperature isn't going above 50°C.
4. When fully dissolved cool down the polymeric solution.
5. Filter polymer solution using a 0.22μm filter paper, to get rid of un-dissolved polymer chunks.
6. Store in refrigerator until use. Before use make sure no aggregates were formed over the storage time, if so discard the solution and use a fresh one.

B. **1M Ammonium carbonate**:

1. Weigh out 0.40g of Ammonium carbonate
2. Dissolve ammonium carbonate in 10ml of deionized water, placed in a 40ml beaker, stir until fully dissolved. Store the solution in the refrigerator until used.

Microbubbles preparation day:

1. Weigh out the following chemicals: 0.50g polymer, 0.05g camphor.

2. Prepare a 2% mix of isopropyl alcohol (IPA), 100ml needed per sample. Mix 2ml of IPA with 98ml of deionized water (multiply this ratio to make as much IPA as needed).
3. Place 10ml of methylene chloride in a beaker (40ml max volume) on a magnetic stir plate and slowly add the polymer and camphor, when dissolved, cover with wax paper, and keep stirring to get a clear polymer solution.
4. Measure out 50ml of 5% poly vinyl alcohol (PVA) and put it in a beaker (600ml max volume) and place it in the refrigerator.
5. Measure out 100ml of 2% isopropyl alcohol (IPA) and keep it in the graduated cylinder.
6. When the camphor and polymer are dissolved, remove stir bar and complete solvent volume to match the original 10ml. Then put in 1ml of the ammonium carbonate solution and sonicate at 110W for 30 seconds, using sonicator (Ultrasonic Processor XL, Misonix Inc., New Highway Farmingdale, NY), over an ice-water bath (use 3 sec on then 1 sec off).
7. After sonication, pour the solution into the cold PVA and homogenize for 5 minutes at 9,000 rpm, using homogenizer (PT 3100, Polytron Inc., USA).
8. Pour the 100ml of IPA in the solution, add a larger stir bar, and stir on a magnetic stir plate for 1 hour. Make sure the vortex reaches the bottom of the beaker so the solvent can fully evaporate. Cover the beaker with wax paper having 1" slit.
9. Collect the solution in at least 4 centrifuge tubes (50ml max volume) and then centrifuge for 5 minutes at 5,000 rpm (the equivalent of approximately 1500 g).
10. Decant the liquid and combine the microcapsules into 1 tube and re-centrifuge for 5 minutes at 5,000 rpm.
11. Decant the liquid and wash the microcapsules three times with hexane, let hexane evaporate for about 30 minutes in a fume hood.

12. When the microcapsules appear to be thick and pasty, to pup the test tube with deionized water, mix and re-centrifuge for 5 minutes at 5,000 rpm.
13. Decant the water, mix the microcapsules with 3 ml of deionized water, put a kim wipe on top of the tube with a rubber band, and fast freeze the microcapsules in liquid nitrogen
14. Put the frozen microcapsules in a freeze dryer vessel and on the freeze dryer for at least 48 hours.
15. When fully lyophilized, remover the dry microbubbles from the freeze drier, seal their tubes and store in a -80C freezer until used.

Variations on microbubbles fabrication:

Polymer choice: When using PLA the former steps 1-15 should be performed with out any modification. When using any_PLGA polymer the volume of methylene chloride should be doubled to be 20ml (step 3).

Porogen content in the shell: Porogen is a general name for a material that introduces pores into the final structure of material. In this case, the porogen in use is camphor and it is responsible for the porous structure of the microbubble polymer shell. Changing the amount of camphor may affect the shell porosity, hence its stability in water and drug release profile in buffer.

Mannitol protection: In order to minimize the swelling of re-lyophilized microbubbles, that were loaded with drug using the dry adsorption method, the addition of mannitol as a protector was tested. The dry surface adsorption method of drug results in swelled bubbles that degrade faster. Mannitol was used as a lyoprotectant to act as a sugar excipient, thereby reducing the

microbubble swelling and degradation rate. Mannitol was added to deionized water used in step 13, just before freezing in the following ratios (of mannitol: polymer): 0.15:1, 0.25:1, 0.5:1, 1:1.

8.2 *Appendix B: Acoustic Testing - Dose and Time Response*

The following two protocols were established in our lab in order to test the back scattering performance of fabricated contrast agents, and were used in order to compare and estimate the different preparations, using the in vitro set up, Figure 3-1.

Acoustic set up description:

A 12.7 mm diameter, 50.8 mm spherically focused transducer (Panametrics, Inc., Waltham, MA, USA) was used with a center frequency of 5 MHz. The transducer had a -6 dB bandwidth of 91% and a pulse length of 1.2 mm. The transducer was placed in a 25ºC water filled bath with 17.8 MΩ-cm deionized water. The transducer was then focused through an acoustically transparent window in the sample holder at a depth of 14 cm from the top of the surface. A pulser/receiver (5072 PR Panamterics Inc.) was used to generate a pulse repetition frequency of 100 Hz. Received signals were then amplified 40 dB and read in an oscilloscope (LeCroy 9350 A, Chestnut Ridge, NY, USA). Data was then stored and analyzed using LabView 7 Express (National Instruments, Austin, TX, USA). The sample vessel was custom made of HDPE (diameter=4.25mm height=140mm to allow a total volume of 50mL or more. The sample vessel was mounted in a fixed location in the water tank. The water tank was equipped with a submerged titanium heater (AZOO, AZ60052, Taiwan), to keep a fixed water temperature of 37±0.5°C. The sample was stirred throughout the insonation period using a magnetic stir bar to keep the contrast agent suspended and uniformly distributed in the vessel.

Dose Response short cumulative protocol:

This procedure can be done in two different fashions, a short cumulative one and a single-dose one. The short cumulative protocol was used initially to screen samples and evaluate the preparation method and CA stability in warm aqueous solution.

1. Preparations before starting the test: make sure the water tank temperature is set to 37°C.
2. Align the ultrasound beam facing the sample holder. The most common transducer in use was 5MHz, spherically focused.
3. Set the right parameters in the amplifier and oscilloscope, turn on the LabView software and prepare folders for results.
4. Fill the sample holder with a 37°C PBS solution, turn on the magnetic stirring plate, re-check beam alignment.
5. Weight 3mg of dry sample and suspend in 800μL of deionized water.
6. Record a baseline.
7. Add 20μL of suspended sample into the sample holder, wait 5 second for the sample to mix in and record the first dose interval. Continue adding sample till 10 dose points are acquired. Samples are stirred throughout the insonation period to keep the contrast agent suspended and uniformly distributed in the vessel.
8. Rinse the sample vessel three times with DI.
9. Process data including and plot the increase in signal enhancement as a function of increasing sample dose.

Dose Response single-step protocol:

1. Preparations before starting the test: make sure the water tank temperature is set to 37°C.
2. Align the ultrasound beam facing the sample holder. The most common transducer in use was 5MHz, spherically focused.
3. Set the right parameters in the amplifier and oscilloscope, turn on the LabView software and prepare folders for results.
4. Fill the sample holder with a 37°C PBS solution, turn on the magnetic stirring plate, re-check beam alignment.
5. Weight 10 aliquots of 3mg of dry sample and place each in a glass vial, suspend one of them in 800μL of warm 37°C PBS.
6. Record a baseline.

7. Add 20μL of suspended sample into the sample holder, wait 10 second for the sample to mix in and record the first dose interval.
8. Rinse the sample vessel three times with DI, refill with war PBS, place back in the water tank and align the US beam.
9. Suspend the second aliquot with 800L and add 40μL ("dose 2") into the sample vessel. Record.
10. Repeat steps 8-9 for all doses, till "dose 10".
11. Process data including and plot the increase in signal enhancement as a function of increasing sample dose.

Time Response protocol:

Based on the results obtained from Dose response, determine the highest dose of contrast agents giving the highest signal enhancement when the curve was still rising.

1. Repeat steps 1-6 of Dose Response (short cumulative) protocol.
2. Add the right dose according to the dose response curve, usually "dose 5" or "dose 6".
3. Allow 10 sec for stirring and start recording. The LabView program should store data of 60rms measurements once every minute, for 15 minutes.
4. Process data and plot the signal enhancement decay as function of time.

8.3 *Appendix C: In Vivo Qualitative Acoustic Studies*

All In vivo tests were carried out at Thomas Jefferson University Hospital, Philadelphia, PA, USA.

1. **PLA-Sudan tests on rabbit kidney**

Four New Zealand white rabbits (of either sex), within the weight range of 2.5-4.0 kg, were sedated with an intramuscular injection of 0.65mg/ml of Ketamine hydrochloride (Ketaset, Aveco, Fort Dodge, IA, USA) and xylazine hydrochloride (Gemini; Rugby Laboratory,

Rockville Centre, NY, USA). A facemask with Isoflurane 0.5 to 2 % (Iso-thesia; Abbott Labs, N.Chicago, IL) was used for maintaining the anesthetic effect. After each experiment the rabbit was sacrificed by a lethal dose of pentobarbital (Beuthanasia; Schering-Plough Animal Health, Kenilworth, NJ, USA).

CA was weighed and suspended in saline prior to injection. The agent was injected through a catheterized ear vein with an 18-gauge needle. Immediately after injection, the injection port was flushed with 5mL of saline. Power Doppler imaging of the kidney was performed using an abdominal scan. The following equation was used to calculate the CA dose that was injected in each injection, for a 3kg rabbit:

0.35mL/kg * 3kg * 0.04g/mL = 0.042 g CA

Power Doppler (PDI) and pulse inversion harmonic (PIHI) imaging were done with SB loaded PLA in two different concentration, 2% and 4%. The rabbit (average weight 2.8 kg) kidneys were imaged transabdonimaly using an HDI 5000 scanner with an L7-4 linear array (Philips Medical Systems, Bothell, WA). Power Doppler imaging was done with a broad bandwidth L12-5 transducer (5-12 MHz), a PRF of 700 kHz and a mechanical index (MI) of 0.33. Pulse inversion harmonic imaging was performed with an L7-4 broad bandwidth transducer and an MI of 0.26. Digital clips were stored for off-line review.

2. **PLA-Sudan and FITC-BSA on tumor model in mice**

This experiment was done on a tumor model induced in mice.

Tumor induction: Thirty, 6 week old, female, athymic nude mice (NCR nu/nu) weighing 20 to 25 g were purchased from Taconic Inc. (Hudson, NY). The human melanoma cell line DB-1 was provided by Dr. David Berd (Thomas Jefferson University, Philadelphia, PA). Localized melanoma xenografts were established by injection of 2×10^6 DB-1 tumor cells (a 0.2 ml tumor cell suspension) in the lower right flank of each mouse using a 27 gauge needle (Becton Dickinson Co., Franklin Lakes, NJ). The mice were then placed back in their cages, where they

remained until the time of their study. They were observed daily for tumor growth and abnormal clinical signs.

The animal studies were carried out in an ethical and humane fashion under supervision of a veterinarian, and Thomas Jefferson University's Institutional Animal Care and Use Committee approved all protocols.

Preparations: Contrast enhanced ultrasound evaluations of the melanoma xenografts were performed 7 weeks after tumor implantation. The mice were anesthetized by intraperitoneal injections of a mixture of 20 μL acepromazine (Henry Schein Inc., Melville, NY),10 mg/ml and 5 μL ketamine (Henry Schein Inc., Melville, NY) at a concentration of 100 mg/ml. A 24 gauge catheter (BD Insyte; Becton Dickinson Co., Franklin Lakes, NJ) was inserted into a tail vein for injections of CA.

Imaging: All mice in this study were imaged using a Sonoline Elegra scanner (Siemens Medical Solutions, Issaquah, WA) and a 7.5 MHz linear array transducer. Three ultrasound imaging techniques were performed on each mouse: power Doppler imaging (PDI), grayscale pulse inversion harmonic imaging (PIHI) and intermittent grayscale PIHI (22, 26). Frame-rates of 30 or 1 Hz (for intermittent imaging) were used for PIHI with a 3.6/7.2 MHz transmission/reception frequency pair. All imaging parameters were kept constant before and after contrast administration (in particular a Mechanical Index below 0.5 was used to limit the amount of bubble destruction). The time between injections was at least 10 minutes to allow the CA to clear the blood pool.

A total of three injections of contrast were administered per mouse. PDI was performed first, followed by PIHI and then intermittent PIHI—with dosages of 10 μl, 15 μl and 15 μl, respectively. Digital ultrasound clips were recorded.

Ultrasound coupling gel was applied liberally on the site of the tumor, thereby creating a standoff pad, which minimized pressure on the tumor from the ensuing placement of the transducer.

Upon completion of the study, the mice were euthanized with an intracardiac injection of sodium pentobarbital (Euthasol; Delmarva Laboratories Inc., Midlothian, VA) at a concentration of 20 to 30 mg/ml.

3. **Sudan black B for sentinel lymph nodes**

All rabbit experiments were done using the same protocol for in vivo studies, details and animal information including preparation, anesthesia and handling are available in Appendix C, above. This study was set to test ultrasound CA, PLA loaded with 4% SB by incorporation, for evaluating intra-abdominal organs via intravenous injection. The purpose was to see if these CA can enhance sentinel lymph nodes (SLNs) on ultrasound imaging by subcutaneous injection, and test the ability of drug loaded CA to travel along lymph channel reaching to their lymph nodes. For this purpose SB loaded CA are most suitable since their color is visibly detectable and can be matched with ultrasound imaging.

Injections Procedure: Each injection ranged between 0.5 to 1.0 ml of a PLA-based CA into the right foot pad of the hind leg and same amount of saline was injected as control into the left foot pad. Four rabbits were used for this pilot study. After contrast injection, the area was massaged for up to 5 minutes to stimulate contrast movement into the lymphatic channels (LCs) and SLNs. Soon after contrast administration, contrast lymphosonography was used to identify the location of the draining LCs and ultimately the SLN(s). The locations, sizes and sonographic appearances of the SLNs detected with contrast enhancement were determined and recorded. Before sacrifice a surgical dissection of the LCs and SLNs was performed and the SLNs were excised. The lymphosonography findings were compared to the surgical specimens.

Ultrasound Imaging: The 4 rabbits were imaged using a Sonoline Elegra scanner (Siemens Medical Solutions, Issaquah, WA) and a 7.5 MHz linear array transducer. Grayscale pulse inversion harmonic imaging (PIHI) with a 3.6/7.2 MHz transmission/reception frequency pair. All imaging parameters were kept constant before and after contrast administration (in

particular a Mechanical Index below 0.5 was used to limit the amount of bubble destruction). The time between injections was at least 10 minutes to allow the CA to clear the blood pool. The normal popiteal lymph nodes and the lymphatic channels leading to the nodes.

8.4 *Appendix D: Size Distribution and Zeta Potential Measurements*

Both size distribution analysis and zeta potential measurements were done using a dynamic light scattering instrument with a Malvern Nano ZS Particle Sizer, (Malvern Instruments, Worcestershire, United Kingdom).

Particle size distribution measurement:

1. Make a 1 mg sample/mL suspension, and put it in a cuvette, and insert into the sample chamber. Repeat this step at least three times for each sample.
2. After measurement plot particle size as numbered percent distribution.

Zeta potential measurement:

1. Repeat step 1 of size distribution measurement but place the sample in a zeta potential cuvette.
2. Place in the sample chamber.
3. Read.

8.5 *Appendix E: Morphology by ESEM*

In order to obtain ESEM pictures, non-conductive samples must first be coated with metal layer.

Platinum Coating procedure:

1. Tape metal stubs with double sided carbon tape, covering most of the stub surface area.
2. Place a small amount of dry sample on the adhesive surface, blow away un-attached sample chunks using air.
3. Place stubs on stage of sputter coater (Cressington, 208 HR, Watford, England).
4. Close the sputter chamber and follow the manual instructions.
5. Set the instrument for 30 seconds.
6. Once coated the samples are ready to use.

ESEM picture taking:

1. Place samples on sample holder, screw well, seal the chamber and operate vacuum system.
2. Start with a 10kV acceleration voltage, spot size 3, and magnification of x1000, x3000, x6000 and if possible x9000.

8.6 *Appendix F: Drug Loading – Shell Incorporation*

Shell incorporation should be done as part of microbubbles preparation, the following protocol is used for hydrophilic drugs:

1. Weigh out the following chemicals: 0.50g polymer, 0.05g camphor.
2. Weigh out the drug in desired amounts. For example: in order to prepare 1% (W/W) of drug to be loaded, weight out 5mg (for 500mg polymer). Add the drug to 1ml of ammonium carbonate solution, keep in a micro-test tube.
3. Prepare a 2% mix of isopropyl alcohol (IPA), 100ml needed per sample. Mix 2ml of IPA with 98ml of deionized water (multiply this ratio to make as much IPA as needed).
4. Place 10ml of methylene chloride in a beaker (40ml max volume) on a magnetic stir plate and slowly add the polymer and camphor, when dissolved, cover with wax paper, and keep stirring to get a clear polymer solution.
5. Measure out 50ml of 5% poly vinyl alcohol (PVA) and put it in a beaker (600ml max volume) and place it in the refrigerator.
6. Measure out 100ml of 2% isopropyl alcohol (IPA) and keep it in the graduated cylinder.
7. When the camphor and polymer are dissolved, remove stir bar and complete solvent volume to match the original 10ml. Then put in 1ml of the ammonium carbonate solution including drug and sonicate at 110W for 30 seconds, using sonicator (Ultrasonic Processor XL, Misonix, Inc., New Highway Farmingdale, NY), over an ice-water bath (use 3 sec on then 1 sec off).
8. After sonication, pour the solution into the cold PVA and homogenize for 5 minutes at 9,000 rpm, using homogenizer (PT 3100, Polytron Inc., USA).

9. Pour the 100ml of IPA in the solution, add a larger stir bar, and stir on a magnetic stir plate for 1 hour. Make sure the vortex reaches the bottom of the beaker so the solvent can fully evaporate. Cover the beaker with wax paper having 1" slit.
10. Collect the solution in at least 4 centrifuge tubes (50ml max volume) and then centrifuge for 5 minutes at 5,000 rpm (the equivalent of approximately 1500 g).
11. Decant the liquid and combine the microcapsules into 1 tube and re-centrifuge for 5 minutes at 5,000 rpm.
12. Decant the liquid and wash the microcapsules three times with hexane, let hexane evaporate for about 30 minutes in a fume hood.
13. When the microcapsules appear to be thick and pasty, to pup the test tube with deionized water, mix and re-centrifuge for 5 minutes at 5,000 rpm.
14. Decant the water, mix the microcapsules with 3 ml of deionized water, put a kim wipe on top of the tube with a rubber band, and fast freeze the microcapsules in liquid nitrogen
15. Put the frozen microcapsules in a freeze dryer vessel and on the freeze dryer for at least 48 hours.
16. When fully lyophilized, remover the dry microbubbles from the freeze drier, seal their tubes and store in a -80C freezer until used.

Variations on drug shell incorporation:

Hydrophobic drug:

1. Steps 1-3 no change.
2. Step 4: Place 10ml of methylene chloride in a beaker (40ml max volume) on a magnetic stir plate and slowly add the polymer, camphor, and drug. When dissolved, cover with wax paper, and keep stirring to get a clear polymer solution.
3. Continue steps 4-15 according to microbubbles preparation protocol (appendix A).

Appendix G: Drug Loading – Surface Adsorption

Wet surface adsorption should be done as part of microbubbles preparation:

1. Weigh out the following chemicals: 0.50g polymer, 0.05g camphor.
2. Weigh out the drug in desired amounts. For example: in order to prepare 1% (W/W) of drug to be loaded, weight out 5mg (for 500mg polymer). Add the drug to 1ml of ammonium carbonate solution, keep in a micro-test tube.
3. Prepare a 2% mix of isopropyl alcohol (IPA), 100ml needed per sample. Mix 2ml of IPA with 98ml of deionized water (multiply this ratio to make as much IPA as needed).
4. Place 10ml of methylene chloride in a beaker (40ml max volume) on a magnetic stir plate and slowly add the polymer and camphor, when dissolved, cover with wax paper, and keep stirring to get a clear polymer solution.
5. Measure out 50ml of 5% poly vinyl alcohol (PVA) and put it in a beaker (600ml max volume) and place it in the refrigerator.
6. Measure out 100ml of 2% isopropyl alcohol (IPA) and keep it in the graduated cylinder.
7. When the camphor and polymer are dissolved, remove stir bar and complete solvent volume to match the original 10ml. Then put in 1ml of the ammonium carbonate solution including drug and sonicate at 110W for 30 seconds, using sonicator (Ultrasonic processor XL, Misonix Inc. New Highway Farmingdale, NY), over an ice-water bath (use 3 sec on then 1 sec off).
8. After sonication, pour the solution into the cold PVA and homogenize for 5 minutes at 9,000 rpm, using homogenizer (PT 3100, Polytron Inc. USA).
9. Pour the 100ml of IPA in the solution, add a larger stir bar, and stir on a magnetic stir plate for 1 hour. Make sure the vortex reaches the bottom of the beaker so the solvent can fully evaporate. Cover the beaker with wax paper having 1” slit.

10. Collect the solution in at least 4 centrifuge tubes (50ml max volume) and then centrifuge for 5 minutes at 5,000 rpm (the equivalent of approximately 1500 g).
11. Decant the liquid and combine the microcapsules into 1 tube and re-centrifuge for 5 minutes at 5,000 rpm. Decant the liquid and gently still in the dry drug.
12. Decant the liquid and wash the microcapsules three times with hexane, and let hexane evaporate for about 30 minutes in a fume hood.
13. When the microcapsules appear to be thick and pasty, to pup the test tube with deionized water, mix and re-centrifuge for 5 minutes at 5,000 rpm.
14. Decant the water, mix the microcapsules with 3 ml of deionized water, put a kim wipe on top of the tube with a rubber band, and fast freeze the microcapsules in liquid nitrogen
15. Put the frozen microcapsules in a freeze dryer vessel and on the freeze dryer for at least 48 hours.
16. When fully lyophilized, remover the dry microbubbles from the freeze drier, seal their tubes and store in a -80C freezer until used.

Dry surface adsorption is addition of drug to dry microbubbles:

1. Weigh out 100mg of dry microbubbles, and desired amount of drug. For example: in order to prepare 1% (W/W) of drug to be loaded, weight out 1mg (for 100mg dry CA).
2. Incubate the dry CA in 2ml of desired buffer (depending on the drug, PBS, NaAc or DI water) in a scintillation vial and stir-in the drug, make sure there are no chunks of CA left.
3. Place the vials on a rotating device, moderate speed, for desired time period, in a cold room. Loading temperature experiment was done placing the samples in room temperature (22°C) and in an incubator (37°C).

4. Collect the samples and wash three times with DI, centrifuge 5 minutes at 5,000 rpm (the equivalent of approximately 1500 g).
5. Freeze dry the remaining drug loaded microbubbles for another 48 hours.
6. Keep frozen until used.

8.7 *Appendix H: Drug Quantification and Encapsulation Efficiency*

This protocol is used to dissolved drug loaded microbubbles and quantify the amount of drug that was loaded.

1. Weigh out 4mg of dry loaded microbubbles, and place in a clean 10ml test tube.
2. Add 2ml of DMSO, and gently vortex for 10 sec.
3. Let it stay for 10 minutes in room temperature.
4. Before reading the absorbance/fluorescence make sure the sample is properly dissolved and that no chunks of visible particles of CA are present.
5. Pippett out 200µL of sample from each tube into a well in a 96-well-plate. Black plates were used for fluorescence readings and clear plates for absorbance. In case of 5FU special clear UV plates were used.
6. Add a free drug calibration curve set of samples using DMSO as a solvent. The highest concentration of each calibration curve was used for fluorescence/absorbance scan, determining the exact wavelength at which a peak of absorbance/fluorescence exists.
7. Read the plate using a micro-plate reader (M200, Tecan, Austria) in the appropriate wave-length. FITC-BSA was read at 450ex./530em., DOX was read at 450ex./580em., Sudan Black was read at 634nm and 5FU at 266nm.

Calculations:

Drug loading percent:

$$Drug[\%] = \frac{Drug_{tube}[mg]}{(CA_{tube}[mg] - Drug_{tube}[mg])} \cdot 100$$

Drug encapsulation Efficiency (EE):

$$EE[\%] = \frac{Drug_{tube}[mg]}{(CA_{tube}[mg] - Drug_{tube}[mg]) \cdot C_i[\%]} \cdot 100$$

Where:

$Drug_{tube}$ is the drug amount found in the test tube after CA was dissolved

CA_{tube} is the weight of CA that was dissolved by DMSO

C_i is the initial concentration of drug to be loaded on the CA, resembles the maximal possible loading.

8.8 *Appendix I: Drug Release*

This protocol was performed using the ultrasound set up shown in Figure 3-2, for both ultrasound activated release and control (no ultrasound).

1. Weigh out 10mg of drug loaded microbubbles, and add 1ml of warm (37°C) PBS.
2. Fill the sample vessel with 50ml of warm PBS, make sure magnetic stirring is on, and take out the first sample of 700µL.
3. Add the CA suspension into the sample vessel and immediately turn on the ultrasound transducer and take out the next sample.
4. Centrifuge both samples in a table top centrifuge (Centrifuge 5415D, Eppendorf, Hamburg, Germany), 5 minutes, 5000rpm, then pipette out the supernatant into 3 wells, having 200µL in each well.
5. Samples of 700µL are taken each 5minutes for a period of 30 minutes, centrifuged immediately and plated.
6. Calibration curve is added to each plate.

Variations for this method:

Sampling intervals: in some experiments the sampling interval was 2minutes.

CA concentration: in some experiments 20mg of CA were suspended in 1ml PBS.

Ultrasound frequency: four transducer were used, 2.25, 5, 10 and 15 MHz.

Ultrasound energy: two levels of energy were used 1 and 4.

8.9 *Appendix J: Statistical Analysis*

Statistical analysis was performed using GraphPad Prism software, version 5.01 (San Diego, CA, USA), and some statistical tools from Microsoft Excel (mean, linear regression).

- Linear Regression: a method of fitting a straight line to data points, determining the slope and intercept by equaling the change in Y for each unit change in X.
- Standard Deviation: quantifies the scattering of data point form each other, it is the square root of the sum of all square distances between data and mean divided by the number of data less one.
- Standard Error Mean: is the standard deviation of the sampling distribution of the mean, calculated as the standard deviation divided by the square root of the number of specimens in the group.
- One way ANOVA: compares the means of three or more unmatched groups, assuming their variance is similar.
- Two way ANOVA: compares the means of three or more unmatched groups, assuming their variance is similar, for two factors at once.
- P-value: The P value answers the question: If all the populations really have the same mean (the treatments are ineffective), what is the chance that random sampling would result in means as far apart (or more so) as observed in this experiment?
- If the overall P value is small, then it is unlikely that the observed differences are due to random sampling, rejecting the idea that all the populations have identical means.
- Tukey test for multiple comparisons: a post test comparing pairs of group means that may follow a one-way ANOVA when there are more than three groups of data. This test is also suitable for unequal sample sizes.

8.10 *Appendix K: List of abbreviations*

BSA	Bovine serum albumin
CA	contrast agents
DI	deionized
DLS	dynamic light scattering
DOX	doxorubicin
EE	encapsulation efficiency
FITC-BSA	fluorescein isothiocyanate labeled bovine serum albumin
LCs	lymph channels
MI	mechanical index
MtCl	methylene chloride
MW	molecular weight
NaAc	sodium acetate buffer
PBS	phosphate buffer saline
PDI	power Doppler imaging
PI	iso-electric point
PIHI	pulse inversion harmonic imaging
pKa	first dissociation constant
PLA	poly-lactic acid
PLGA	poly-lactic-co-glycolic acid
PMMA	poly methyl methacrylate
PRF	pulse repetition frequency
PVA	poly vinyl alcohol
RMS	root mean square
SB	sudan black B

SLNs	sentinel lymph nodes
Tg	glass transition temperature
5FU	5-fluorouracil

9. Vita

Odelia Mualem-Burstein has received her B.Sc. in Biology from Tel Aviv University in 1993. After a 27 months service as an officer in the IDF, she obtained her M.Sc. in Biomedical Engineering in 2000, at the Technion (Israel's Institute of Technology), focusing in biomaterials. While at the Technion, Odelia performed extra-curricular activities, including, among others, Treasurer of the Graduate Students Organization. She started her way in the biomedical engineering industry in 1998 at Carmel Biosensors, Haifa, Israel, as R&D staff member, developing glucose sensor for artificial pancreas, joining Levram, Haifa, Israel, later on during 2001, as research staff member, developing a left ventricle assist device. After five years in the industry, she decided to pursue her Ph.D. at the School of Biomedical Engineering Science and Health Systems at Drexel University. While at Drexel, she tutored several classes and mentored students. Odelia presented her work in various conferences, winning two awards. She is co-author of a patent on methods of drug loading onto polymeric ultrasound contrast agents.